2017

FORMATION OF THE ETHER BRIDGE IN THE LOLINE ALKALOID BIOSYNTHETIC PATHWAY

Minakshi Bhardwaj
University of Kentucky, mbh222@g.uky.edu
Digital Object Identifier: https://doi.org/10.13023/ETD.2017.188

STUDENT AGREEMENT:

I represent that my thesis or dissertation and abstract are my original work. Proper attribution has been given to all outside sources. I understand that I am solely responsible for obtaining any needed copyright permissions. I have obtained needed written permission statement(s) from the owner(s) of each third-party copyrighted matter to be included in my work, allowing electronic distribution (if such use is not permitted by the fair use doctrine) which will be submitted to UKnowledge as Additional File.

I hereby grant to The University of Kentucky and its agents the irrevocable, non-exclusive, and royalty-free license to archive and make accessible my work in whole or in part in all forms of media, now or hereafter known. I agree that the document mentioned above may be made available immediately for worldwide access unless an embargo applies.

I retain all other ownership rights to the copyright of my work. I also retain the right to use in future works (such as articles or books) all or part of my work. I understand that I am free to register the copyright to my work.

REVIEW, APPROVAL AND ACCEPTANCE

The document mentioned above has been reviewed and accepted by the student's advisor, on behalf of the advisory committee, and by the Director of Graduate Studies (DGS), on behalf of the program; we verify that this is the final, approved version of the student's thesis including all changes required by the advisory committee. The undersigned agree to abide by the statements above.

Minakshi Bhardwaj, Student

Dr. Robert B. Grossman, Major Professor

Dr. Mark A. Lovell, Director of Graduate Studies

FORMATION OF THE ETHER BRIDGE IN THE LOLINE ALKALOID BIOSYNTHETIC PATHWAY

DISSERTATION

A dissertation submitted in partial fulfillment of the requirements for the degree of Doctor of Philosophy in the College of Arts and Sciences at the University of Kentucky

By
Minakshi Bhardwaj
Lexington, Kentucky

Director: Dr. Robert B. Grossman, Professor of Chemistry
Lexington, Kentucky
2017

ABSTRACT OF DISSERTATION

FORMATION OF THE ETHER BRIDGE IN THE LOLINE ALKALOID BIOSYNTHETIC PATHWAY

Lolines are specialized metabolites produced by endophytic fungi, such as *Neotyphodium* and *Epichloë* species, that are in symbiotic relationships with cool-season grasses. Lolines are vital for the survival of the grasses because their insecticidal and antifeedant properties protect the plant from insect herbivory. Although lolines have various bioactivities, they do not have any concomitant antimammalian activities.

Lolines have complex structures that are unique among naturally occurring pyrrolizidine alkaloids. Lolines have four contiguous stereocenters, and they contain an ether bridge connecting C(2) and C(7) of the pyrrolizidine ring. An ether bridge connecting bridgehead C atoms is unusual in natural products and leads to interesting questions about the biosynthesis of lolines in fungal endophytes.

Dr. Pan, who was a graduate student in Dr. Schardl Lab at University of Kentucky, isolated a novel metabolite, 1-*exo*-acetamidopyrrolizidine (AcAP). She observed that AcAP was accumulating in naturally occurring and artificial *lolO* mutants. I synthesized an authentic sample of (±)-AcAP and compared it spectroscopically with AcAP isolated from a *lolO* mutant to determine the structure and stereochemistry of the natural product. I was also able to grow crystals of synthetic (±)-AcAP, X-ray analysis of which further supported our structure assignment.

There were two possible explanations for the fact that a missing or nonfunctional LolO led to the accumulation of AcAP: that AcAP was the actual substrate of LolO, or that it was a shunt product derived from the real substrate of LolO, 1-*exo*-aminopyrrolizidine (AP), and that was produced only when LolO was not available to oxidize AP. To distinguish between the two hypotheses, I synthesized 2´,2´,2´,3-[$^{2}H_{4}$]-AcAP. Dr. Pan used this material to confirm that AcAP was an intermediate in loline alkaloid biosynthesis, not a shunt product.

To determine the product of LolO acting on AcAP, Dr. Pan expressed LolO in yeast (*Saccharomyces cerevisiae*). When Dr. Pan fed AcAP (synthesized by me) to the modified organism, it produced NANL, suggesting that LolO catalyzed *two* C–H activations of AcAP and the formation of *both* C–O bonds of the ether bridge in NANL, a highly unusual transformation. Dr. Chang then cloned, expressed, and purified LolO and incubated it with (±)-AcAP, 2-oxoglutarate, and O_2. He observed the production of NANL, further confirming the function of LolO. Dr. Chang also observed an intermediate, which we tentatively identified as 2-hydroxy-AcAP.

In order to determine whether the initial hydroxylation of AcAP catalyzed by LolO occurred at C(2) or C(7), I prepared (±)-7,7-[$^{2}H_{2}$]- and (±)-2,2,8-[$^{2}H_{3}$]-AcAP. When Dr. Pan measured the rate of LolO-catalyzed hydroxylation of these substrates under conditions under which only one C–H activation would occur, she observed a very large kinetic isotope effect when C(2) was deuterated, but not when C(7) was deuterated, establishing that the initial hydroxylation of AcAP occurred at the C(2) position.

In order to determine the stereochemical course of C–H bond oxidation by LolO at C(2) and C(7) of AcAP, I synthesized *trans*- and *cis*-3-[^{2}H]-Pro and (2*S*,3*R*)-3-[^{2}H]- and (2*S*,3*S*)-2,3-[$^{2}H_{2}$]-Asp. Feeding experiments with these substrates carried out by both Dr. Pan (Pro) and me (Asp) showed that at both the C(2) and C(7) positions of AcAP, LolO abstracted the *endo* H atoms during ether bridge formation.

In summary, feeding experiments with deuterated (±)-AcAP derivatives and its amino acid precursors have shown that AcAP is an intermediate in loline biosynthesis. We have shown that LolO catalyzes the four-electron oxidation of AcAP at the endo C(2) position first and then the endo C(7) position to give NANL.

KEYWORDS: Loline, biosynthesis, pyrrolizidine, LolO, C–H activation

Minakshi Bhardwaj

4/28/2017

FORMATION OF THE ETHER BRIDGE IN THE LOLINE ALKALOID BIOSYNTHETIC PATHWAY

By

Minakshi Bhardwaj

Dr. Robert B. Grossman

Director of Dissertation

Dr. Mark A. Lovell

Director of Graduate Studies

4/28/2017

Date

To My Parents
(Rekha Rani and
Ravi Dutt Bhardwaj)

ACKNOWLEDGEMENTS

I would like to express my gratitude to all the people who helped me to reach this stage in my academic career. Without them, it would not be possible to complete my dissertation.

I would like to express my heartfelt gratitude to my supervisor, Dr. Robert B. Grossman, who accepted me in his group and gave me the opportunity to work on the loline biosynthesis project that was of great interest to me. His expertise in the field of organic synthesis was incomparable. His perseverance, enthusiasm, valuable supervision, and encouragements in every step helped me to accomplish the goals of my project.

I am grateful to my committee member, Dr. Christopher L. Schardl, for his patience and guidance during the progress of this project. He was generous to let me learn fungal culture and related experiments in his lab. Dr. Padmaja Nagabhyru in his lab was very kind and supportive during the process of learning. She was always there to help me to understand and solve any problem I had.

I would like to thank my other committee member, Dr. Edith C. Glazer, for her constant support and helpful feedback to achieve the goals of my project. She was generous for approving one of her graduate students (Catherine Denning) to teach me enzyme purification. This skill was very important for completing an important part of my project. I would like to thank Catherine for her time and kindness.

I would like to extend my thanks to my other committee member, Dr. Arthur Cammers, for being supportive of my research work and providing constructive criticism

to understand the project better. I would like to thank my external examiner, Dr. David Watt, during my final defense for his time and patience.

I want to acknowledge the help provided by Dr. Anne-Frances Miller in the learning of 2D NMR. Apart from this, I enjoyed my time with her in all the educational outreaches to different schools.

I am particularly grateful for the assistance provided by Mr. W. John Layton in the process of learning NMR skills. He was nice to help me in my NMR experiments even after hours. This skill helped me to analyze structures of organic compounds all through my academic life in the University of Kentucky.

It was my pleasure to have Dr. Juan Pan as my collaborator at all steps of my project. I really appreciated her patience all this time as she waited for me to synthesize compounds. She was there for me as a great friend and resource to understand biochemistry better. I would also like to acknowledge Dr. Wei-chen Chang from Dr. Bollinger lab for the initial work of cloning, expressing, and purifying LolO. This work helped us to identify the previously unknown metabolite.

I would like to thank Dr. Robert B. Grossman, Dr. Christopher L. Schardl, Dr. J. Martin Bolinger, and the UK Department of Chemistry for supporting me financially during the course of my PhD.

I want to acknowledge the help provided by Dr. Sean Parkin with X-ray crystallography. I would like to thank Mr. Jeff Babbitt for repairing all the broken glassware and building new creative glassware for me. I would also like to thank Mr. Art Sebesta for all the timely help he provided to fix broken instruments such as the glovebox,

vacuum pump, GC-MS, etc. I am greatful to John May at the ERTL of the University of Kentucky for GC-MS analysis

I also like to acknowledge my fiancé, Faruk H. Moonschi, for his patience and encouragement during the preparation of my dissertation. He is one of the supporting pillars in my life. Without him, it would have been difficult to complete this important chapter of my life. Apart from this, he helped me to learn enzyme chemistry and basic biochemistry skills.

I like to thank my laboratory member, Shubhankar Dutta, for helping me understand basic organic chemistry synthetic skills. Without his help, I would not have been able to conduct any experiments efficiently. He was there my entire time in the Grossman lab as an elder brother to guide me. I also like to thank my other lab member Setareh Saryazdi for her help in the lab. I like to acknowledge my friends Soledad G. Yao, Dr. April N. French, Bidhya L. Maharjan, and Deepshika Gupta for their support.

Last, but not least, I would like to express my gratitude to my parents, Rekha Rani and Ravi Dutt Bhardwaj for being there for me and being supportive in all the decisions I made in my life. I would like to thank my sisters Monika, Geeta, and Reetu for filling my life with lots of love and fun.

Table of Contents

LIST OF TABLES

LIST OF FIGURES

LIST OF SCHEMES

LIST OF ABBREVIATIONS

1D	One Dimensional
2D	Two Dimensional
2-OG	2-Oxoglutarate
AcAP	1-*exo*-Acetamidopyrrolizidine
AP	1-exo-Aminopyrrolizidine
CAS	Clavaminic acid synthase
Cbz	Carboxybenzyl
^{13}C NMR	Carbon-13 Nuclear Magnetic Resonance
conc.	Concentration
COSY	Correlation spectroscopy
DEAD	Diethyl azodicarboxylate
DMAP	4-Dimethylaminopyridine
DMSO	Dimethyl sulfoxide
FAD	Flavin Adenine Dinucleotide
GC-MS	Gas Chromatography-Mass Spectrometer
H6H	Hyoscyamine 6β-hydroxylase
^{1}H NMR	Proton Nuclear Magnetic Resonance
^{2}H NMR	Deuterium Nuclear Magnetic Resonance
HMBC	Heteronuclear Multiple-Quantum Coherence
HPLC	High Performance Liquid Chromatography
HRMS	High Resolution Mass Spectrometry
HSQC	Heteronuclear Single Quantum Coherence
IPNS	Isopenicillin *N*-synthase
IR	Infrared
LB	Luria-Bertani
LC-MS	Liquid Chromatography Mass Spectrometry
LDA	Lithium Diisopropyl Amide
MOPS	3-(*N*-morpholino)propanesulfonic acid

MS	Mass Spectrometry
MsCl	Methanesulfonyl chloride
NANL	*N*-Acetylnorololine
NFL	*N*-Formylloline
NL	Norololine
NOE	Nuclear Overhauser Effect
NOESY	Nuclear Overhauser SpectroscopY
PDA	Potato Dextrose Agar
PLP	Pyridoxal-5´-Phosphate
RNAi	RNA interference
RT	Room Temperature
THF	Tetrahydrofuran
TLC	Thin Layer Chromatography
UV/Vis	Ultraviolet-Visible

Chapter 1. Introduction

1.1. Aim and scope of this study

As part of a study to establish the intermediates and elucidate the role of LolO enzyme in the loline alkaloid biosynthetic pathway.

In this report, I describe the isolation of a previously unknown metabolite from naturally occurring and artificial *lolO* mutants. To determine the structure and stereochemistry of this compound, I synthesized an authentic sample of (±)-AcAP, demonstrated its stereochemistry, and showed its spectroscopic identity with the metabolite isolated from the endophyte. I describe the synthesis of deuterium-labeled AcAP isotopologues, which was then used to confirm that AcAP was an intermediate in loline alkaloid biosynthesis, not a shunt product (Scheme *1.1*).

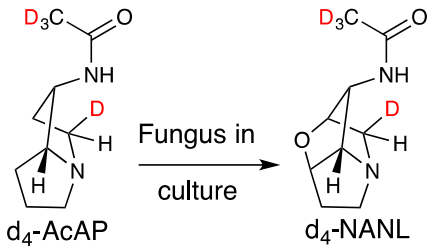

Scheme 1.1. AcAP as an intermediate in loline biosynthesis. Showing incorporation of D atom in NANL from d_4-AcAP.

In this report, I also describe our investigation to determine what is the product of LolO acting on AcAP. The experiments involved feeding AcAP to yeast that was genetically modified with LolO and also to cloned, expressed, and purified LolO. Both experiments resulted in the production of NANL. The feeding to purified LolO revealed a

new intermediate between AcAP and NANL, which we tentatively identify as hydroxy-AcAP (Scheme *1.2*).

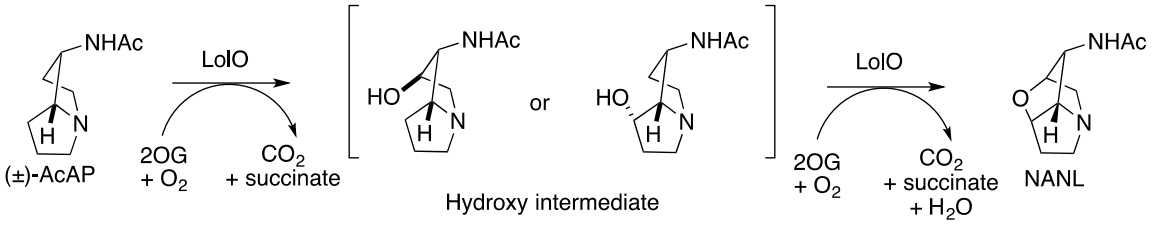

Scheme 1.2. Presence of hydroxy intermediate produce during the oxidation of AcAP to NANL by LolO.

In this report, I describe an independent confirmation of the sequence of C–H activation events. In order to determine whether the initial hydroxylation of AcAP catalyzed by LolO occurred at C(2) or C(7), I prepared (±)-7,7-[$^{2}H_2$]- and (±)-2,2,8-[$^{2}H_3$]-AcAP. Stop-flow kinetics experiments by Dr. Juan Pan with 2,2,8-[$^{2}H_3$]- and 7,7-[$^{2}H_2$]-AcAP under single-oxidation conditions revealed a very large kinetic isotope effect in the former case, but not in the latter, establishing that the initial hydroxylation of AcAP occurred at the C(2) position. Dr. Juan Pan was able to isolate 2-hydroxy AcAP from unreacted ACAP and the product NANL. With the help of ^{1}H NMR, ^{1}H-^{1}H COSY and NOE experiments, I was able to establish the structure and stereochemistry of isolated compound as 2-*endo*-2-hydroxy AcAP (Scheme *1.3*).

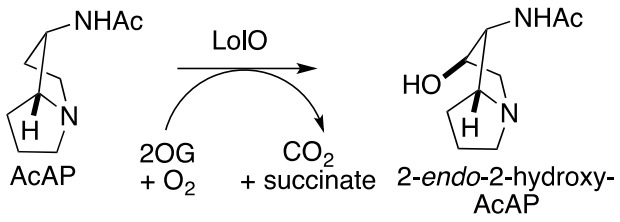

Scheme 1.3. Initial Hydroxylation of AcAP at C(2) position on endo face.

In this report, I describes the investigation of the stereochemical course of C–H bond activation by LolO at C(2) and C(7) of AcAP. I synthesized *trans*- and *cis*-3-[^{2}H]-Pro and (3*R*)-3-[^{2}H]- and (3*S*)-2,3-[$^2H_2$]-Asp. Feeding experiments with these substrates carried out by both Dr. Pan (Pro) and me (Asp) showed that at both the C(2) and C(7) positions of AcAP, LolO abstracted the *endo* H atoms during ether bridge formation (Scheme *1.4*).

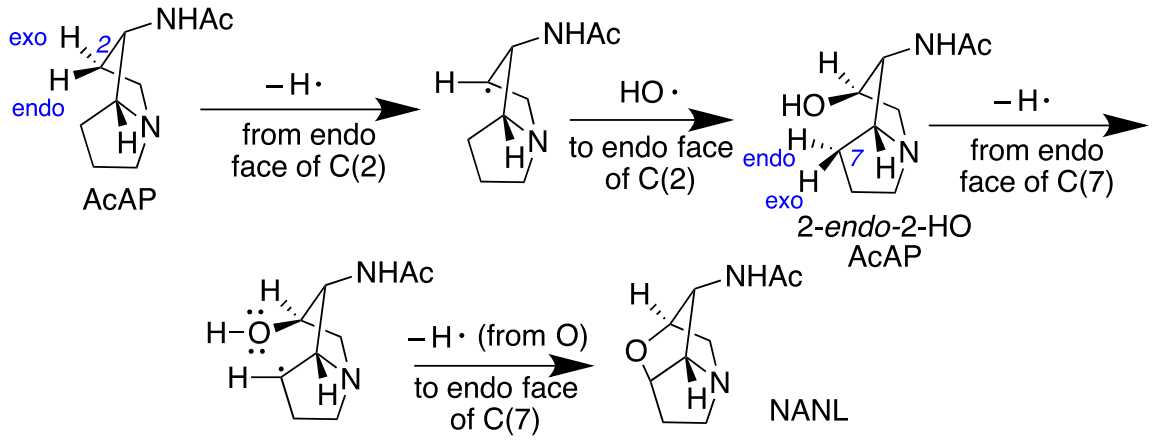

Scheme 1.4. Abstraction of endo H atoms from C(2) and C(7) of AcAP by LolO.

1.2. Endophytes and their interaction with host plants

Endophytes are organisms that flourish intercellularly in host plants, with asymptomatic infections for some parts or all of their life cycle. The host plants usually provide all of the essential nutrients (such as sucrose, amino acids, etc.,) to endophytes for

their survival.[1] Endophytes are omnipresent across the plant kingdom (trees, plants, grasses, algae, etc.) and are commonly fungi and bacteria. Endophytes produce a range of biologically active compounds that may provide survival benefits to the host plants, such as protection against its natural enemies.[2] Some strains of endophytic fungi only produce biologically active compounds in symbiosis, while others produce in both symbiosis and culture. The reasons for this dichotomy are still not understood.

There needs to be a balanced interaction between the endophytes and host plants, and the interaction is usually maintained by the plant defense system. There are generally two balanced interactions: commensalism and mutualism. In commensalism, endophytes survive within the host on the nutrient supply, neither harming nor benefiting the host. On the contrary, mutualism is an interaction in which both of the organisms provide survival benefits to the other.[3] Under certain conditions, the interaction may become parasitic, i.e., harmful for the host plant.[4]

Table 1.1. Summary of *Epichloë* spp. mediated resistances to multiple biotic and abiotic stresses.

Stress	Endophyte-mediated response
Drought tolerance	Increase root growth; altered stomatal behavior and osmotic adjustments
Nematode resistance	Reduced nematode reproduction.
Growth responses	Phytohormones and synthetic growth hormones, increased phosphorous and mineral uptake, growth tolerance to low soil pH or high aluminum concentration, nitrogen use efficiency
Interspecific competition	Increased clonal growth and lateral spread; production of alleochemicals; increased seedling vigor and seed yield
Disease resistance	Increased, decreased or no effect, depending on the system.
Insect resistance	Peramine, lolines, ergot alkaloids
Anti-herbivory of mammals	Ergot alkaloids and indole-diterpenes
Heat or low light intensity	Enhance tolerance.

An increase in host plant resistance by the endophytes toward other enemies in a mutualistic relationship is called "acquired plant defense."[5] The host acquires defense against insects, herbivores, and a wide range of environmental conditions, such as drought and heat. A summary of *Epichloë* spp. mediated resistances to multiple biotic and abiotic stresses is given in *Table 1.1*.[6]

Plants cannot protect themselves by moving away from an attack of their foe, nor are they blessed with immune systems like animals are. To cope with these problems, plants have developed defenses such as bark, thorns, etc. They also evolved to synthesize certain compounds or acquire them from an organism with which they have a symbiotic relationship. These compounds may act as antifeedants or precursors to physical defense tools. These compounds are called "secondary" or "specialized" metabolites.[7]

This interaction between endophytes and host plants has been studied for a long time for its importance to agriculture. Some specialized metabolites produced by endophytes may cause problems to grazing livestock but can also possess anti-insect properties. It has been of great interest for the pastoral farming sector to find the endophyte strains that can synthesize compounds that have anti-insect activity but lack concomitant antimammalian activity.[6]

Many types of specialized metabolites are produced by grass-associated endophytes. They help the grass to cope with numerous stress conditions such as drought, protection against vertebrates and invertebrates, and survival in poor soil conditions. The specialized metabolites discussed in this report are alkaloids that are produced by *Epichloë* species, which are groups of filamentous fungi that live as grass endophytes. Alkaloids produced by *Epichloë* spp. provide many benefits for the host grass. Some specialized metabolites produced by endophytes are ergovaline, aminopyrrolizidine, pyrolopyrazines, the indole-diterpenoids, and 11,12-epoxyjanthitrems (Figure *1.1*) may be toxic to cattle and other livestock. The alkaloids are produced by different species of grasses infected with endophytes, but not every endophyte-grass association produces alkaloids.[6] In this dissertation, I discuss the loline alkaloids that are produced by endophytic fungi of grasses.

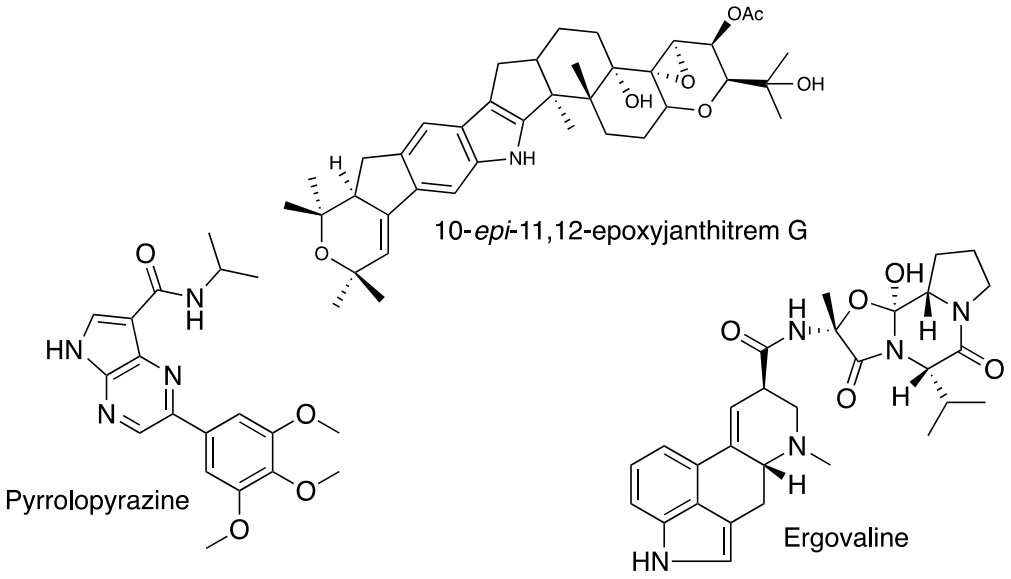

Figure 1.1. Structure of ergovaline, pyrrolopyrazine, and 10-*epi*-11,12-epoxyjanthitrem.

1.3. Loline background

In 1892, Hofmeister recognized an alkaloid with the elemental formula $C_7H_{12}N_2O$ and called it temuline.[8] In 1955, Yunusov and Akramov isolated a related alkaloid from the *Lolium temulentum* (darnel) seeds and named it loline.[9] In addition to loline and temuline, they also isolated other alkaloids, which they named *N*-acetylloline. In 1960, Yunusov and Akramov proposed the structure of loline with an exocyclic nitrogen and an oxygen attached to the same carbon (**A**) (Figure *1.2*).

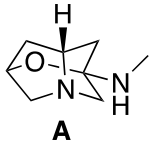

A

Figure 1.2. Proposed structure of loline by Yunusov and Akramov in 1960.

In 1966, they proposed a new structure, *N*-methyl-1-*endo*-aminopyrrolizidine (**B**) (Figure *1.3*).[9]

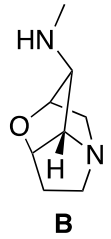

B

Figure 1.3. Revised proposed structure of loline by Yunusov and Akramov in 1966.

In 1965, Yates and Tookey proposed a structure for festucine that was the same as loline, but the *N*-methyl group was on the exo face (**C**) (Figure *1.4*).

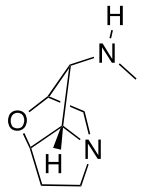

C

Figure 1.4. Revised proposed structure of loline by Yates and Tookey in 1965.

In 1969, Aasen and Culvenor showed that the structure of loline was identical to festucine. In 1972, Bates and Morehead established the absolute configuration of loline dihydrochloride by X-ray crystallographic analysis. The structure of loline is now regarded as having a pyrrolizidine nucleus with an ether linkage and containing both endocyclic and exocyclic nitrogen (**C**).[9] In 1985, Dannhardt and Steindl reported that temuline and norloline were the same alkaloid.[10]

Later on, various research groups isolated numerous types of lolines with different types of substituents (methyl, formyl, acetyl, propionyl, butyryl, isobutyryl, isovaleryl, and senecioyl) on the amino group. Some of the common lolines are shown in Figure *1.5*.[9] In

our work, the most relevant lolines have been norloline (NL), *N*-acetylnorloline (NANL), and *N*-formylloline (NFL). Until now, all evidence has suggested that these alkaloids are produced by fungal endophytes, not by the host plants.[11]

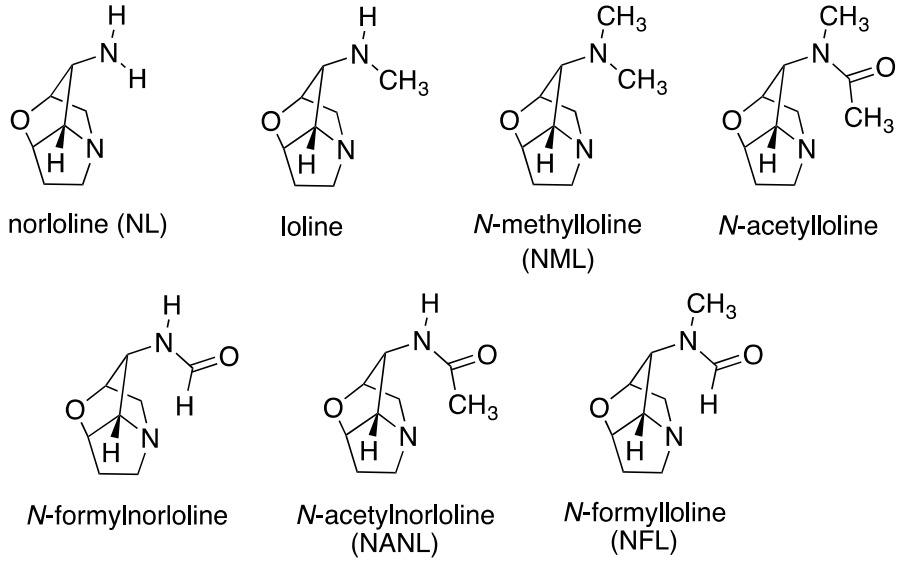

Figure 1.5. Various naturally occurring loline alkaloids

1.4. Unusual features in loline structure

Lolines have unusual molecular architectures for pyrrolizidine natural products. They have a tricyclic structure containing at least one heteroatom in every ring, and they have four contiguous stereocenters. The molecule is strained due to the presence of the ether bridge, which links two bridgehead C atoms, a very unusual context for a natural product. All but one of the carbon atoms in the pyrrolizidine ring are attached to a heteroatom. These features have caused scientists in detail to study the biosynthetic pathway leading to lolines.

1.5. What have we learned in the past about the biosynthetic pathway of loline?

Working together, our group and Dr. Schardl's group were able to identify precursors and intermediates in loline alkaloid biosynthesis by feeding isotopically labeled substrates to a loline-producing culture of *Epicoloë. uncinata* and analyzing by GC-MS the isotopic content of the produced loline alkaloids (Scheme *1.5*).[12-13] These experiments showed that L-proline (Pro) and L-homoserine, likely in the form of *O*-acetylhomoserine (**1**),[12] were the precursors whose carbon and nitrogen atoms were incorporated into the pyrrolizidine core, whereas L-methionine contributed the carbon atoms of the *N*-formyl and *N*-methyl substituents.[12] The experiments also showed that compounds **2** and AP were likely intermediates in the biosynthetic pathway.[13]

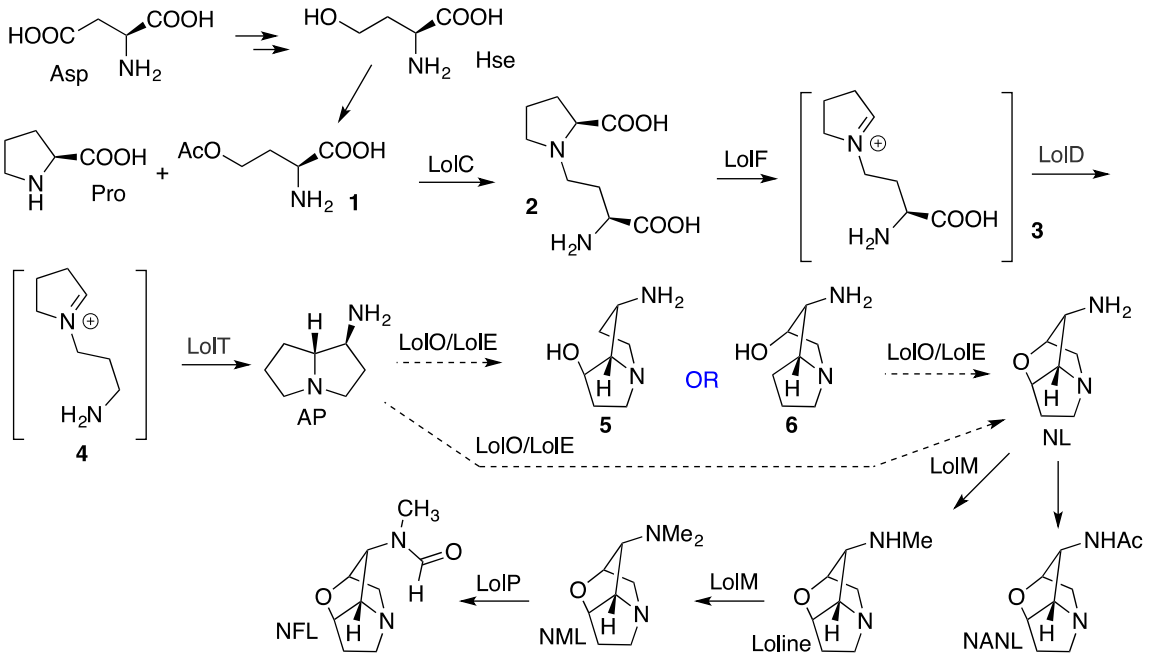

Scheme 1.5. Proposed biosynthetic pathway to lolines.

We hypothesize that an enzyme encoded by the *lolC* gene catalyzes the γ-substitution reaction between Pro and **1**.[12] LolC's inferred amino acid sequence suggests

that is a γ-type pyridoxal-5´-phosphate (PLP) enzyme that is similar to the *O*-acetyl-homoserine(thiol)-lyase encoded by the *cysD* gene of *Aspergillus nidulans.*[14-15] *O*-acetylhomoserine(thiol)-lyase catalyzes the γ-substitution of *O*-acetylhomoserine with H_2S in methionine biosynthesis (Scheme 1.6).[16,13]

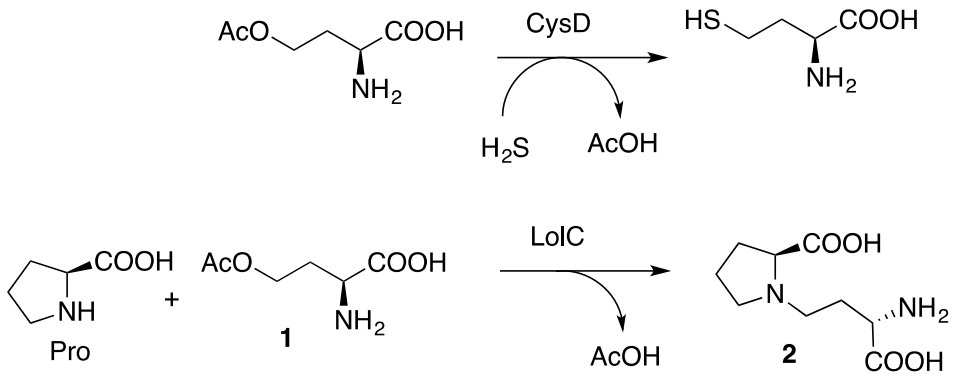

Scheme 1.6. Comparison of reactions catalyzed by CysD and LolC.

We hypothesize that the likely FAD-containing monooxygenase encoded by the *lolF* gene catalyzes the next step, oxidative decarboxylation of the pyrrolidine ring of **2** to give iminium ion **3**.[15] LolF is most closely similar to 1,2-cyclopentanone monooxygenase.[15, 17]

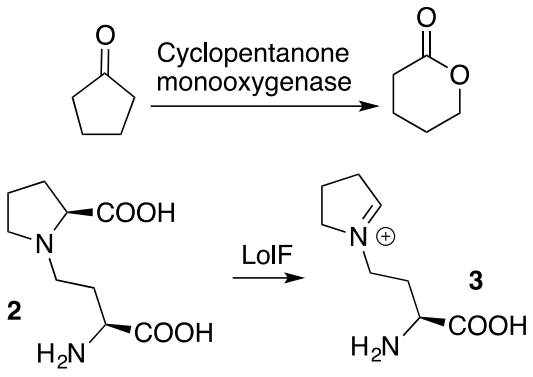

Scheme 1.7. Comparison of reactions catalyzed by cyclopentanone monooxygenase and LolF.

We further hypothesize that amino acid **3** undergoes decarboxylation catalyzed by the PLP enzyme encoded by the *lolD* gene to give amine **4** (Scheme *1.8*).[15] LolD's amino acid sequence suggests that it is related to ornithine decarboxylase.[15-16]

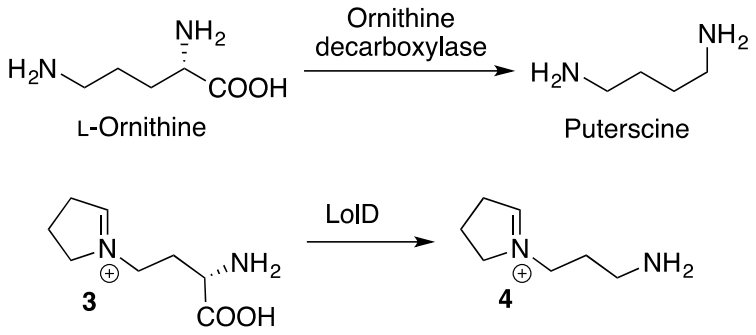

Scheme 1.8. Comparison of reaction catalyzed by ornithine decarboxylase and proposed to be catalyzed by LolD.

We hypothesize that the PLP enzyme encoded by the *lolT* gene catalyzes cyclization of **4** to the known intermediate AP (Scheme 1.4).[13, 15] LolT's amino acid sequence suggests that it is closely related to isopenicillin N epimerase.[15, 18]

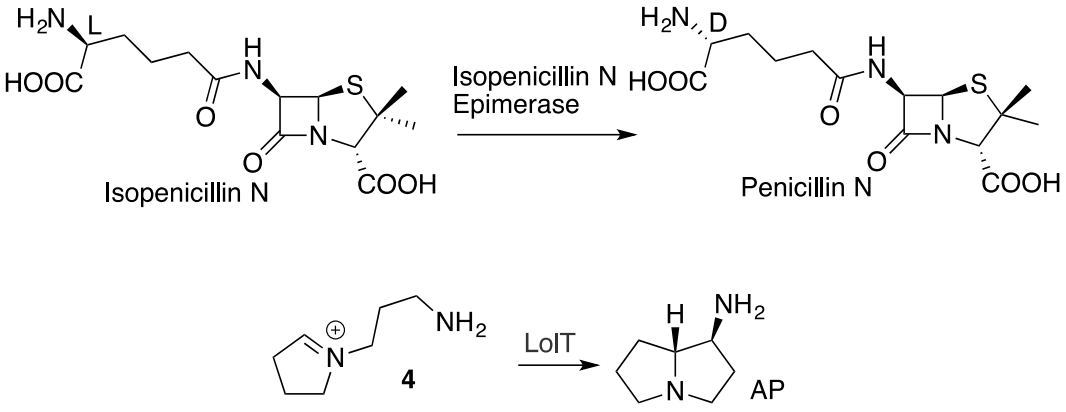

Scheme 1.9. Comparison of reactions catalyzed by isopenicillin N epimerase and proposed to be catalyzed by LolT.

There are several different ways that the ether bridge could be introduced into AP (Scheme *1.5*). Either C(2) or C(7) of AP could be hydroxylated to give intermediate **5** or **6**, respectively, and either intermediate **5** or **6** could then undergo cyclization to NL by C–H activation of C(7) or C(2), respectively, followed by ring closure. Either a single or multiple enzymes could catalyze the hydroxylation and the cyclization.[13] We previously hypothesized that these steps are catalyzed by the dioxygenase and oxidoreductase encoded by the *lolO* and *lolE* genes.[15]

1.6. Synthesis of pyrrolizidine core

1.6.1. Christine et al. approach

In 2000, Christine et al, published a racemic synthesis of AP.[19] They initiated the synthesis by converting L-Pro to ethyl prolinate (**7**). *N*-Alkylation of **7** with ethyl acrylate formed the diester **8**, which underwent Dieckmann cyclization, hydrolysis, and decarboxylation to produce ketone **9**, presumably in racemic form due to epimerization under the decarboxylation conditions. This compound was converted to oxime **10** and then subjected to Raney Ni reduction to form two separable diastereomers, (±)-AP and (±)-1-*epi*-AP (Scheme *1.10*).

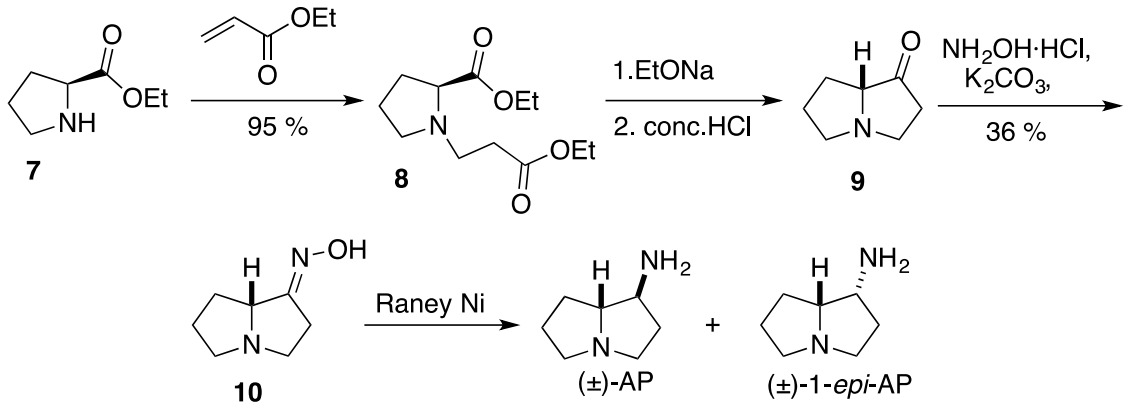

Scheme 1.10. Christine et al synthesis of (±)-AP.

1.6.2. Giri et al. approach

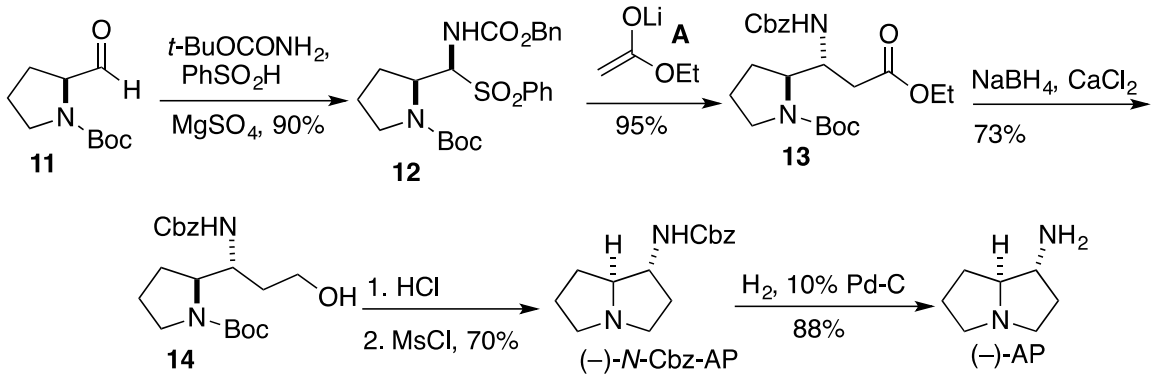

Scheme 1.11. Giri et al. synthesis of (–)-AP.

In 2004, Giri et al. synthesized (–)-AP starting from prolinal **11**.[20] They converted **11** to the sulfone **12** using the usual procedure, and reaction of **12** with enolate **A** formed amino ester **13** with *syn*:*anti* = 10:90. Selective reduction of the ester function in **13** with $NaBH_4$ and $CaCl_2$ produced alcohol **14**. Removal of the Boc group in **14** and formation of a mesylate, which underwent intramolecular S_N2 displacement in situ, resulted in the formation of bicyclic compound (–)-*N*-Cbz-AP. Removal of the Cbz group then gave enantiopure (–)-AP (Scheme *1.11*).

1.6.3. Tang et al. approach

In 2004, Tang et al. synthesized (+)-AP during the total synthesis of the natural product, (1*S*,8*R*)-(+)-absouline.[21] Their synthesis began with chemoselective reduction of **15** to give alcohol **16**, which was subsequently treated with thiophenol to form sulfide **17**. Nucleophilic reaction by allyl iodide produced **18**. Treatment of **18** with $BH_3 \cdot SMe_2$ and subsequent oxidation with H_2O_2 under basic conditions resulted in the formation of alcohol **19**. Mesylation, acidification, and basification of **19** produced (+)-*N*-Cbz-AP. Compound (+)-*N*-Cbz-AP then underwent hydrogenolysis to form enantiopure (+)-AP·2HCl (Scheme *1.12*).

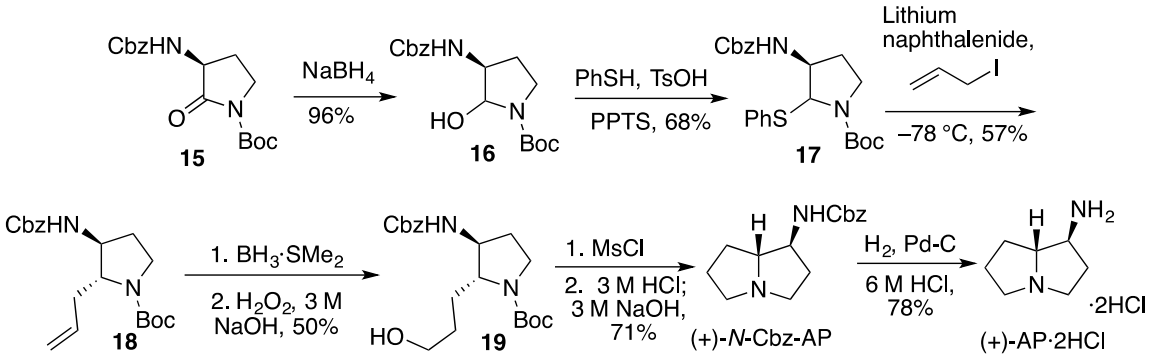

Scheme 1.12. Tang et al synthesis of (+)-AP.

1.6.4. Eklund et al. approach

In 2012, Eklund et al. synthesized (–)-AP during the synthesis of (–)-absouline.[22] They started their synthesis with the reduction of **20** to give the corresponding aldehyde, which was subjected to Horner–Wadsworth–Emmons reaction to give **21a** and **21b** in 2:1 ratio. Compound **21a** underwent conjugate addition of an amine to give an inseparable mixture of **22a** and **22b**. The mixture of **22a** and **22b** was then converted into pyrrolizidines

23a and **23b**, which were easily separated by chromatography. The compound **23b** was then reduced with $BH_3 \cdot SMe_2$ and hydrogenolyzed to form (–)-AP·2HCl (Scheme *1.13*).

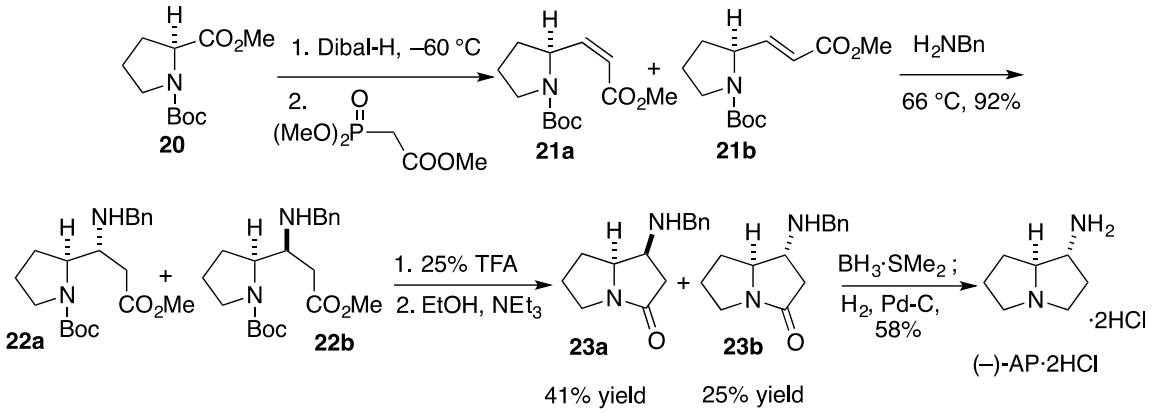

Scheme 1.13. Eklund et al approach to make pyrrolizidine ring.

Chapter 2. What happens if LolO expression is knocked down?

(This chapter has been published as part of "Ether bridge formation in loline alkaloid biosynthesis" by Juan Pan, Minakshi Bhardwaj, Jerome R. Faulkner, Padmaja Nagabhyru, Nikki D. Charlton, Richard M. Higashi, Anne-Frances Miller, Carolyn A. Young, Robert B. Grossman, Christopher L. Schardl.[23] This chapter's experimental section reports only the work done by me.)

2.1. Introduction:

In 2008, Dr. Jerome Faulkner observed the accumulation of an unknown metabolite in the culture of *E. uncinata* after he used RNAi to knock down expression of the *lolO* gene.[16] Dr. Juan Pan later isolated the metabolite and tentatively identified it as AcAP (Figure *2.1*).[23] Dr. Pan also observed that several *Epichloë* species (such as *Epichloë. amarillans* strains E721, E722 and E862, *Epichloë. brachyelytri* E4804, and *Epichloë. canadensis* e4814)[23] with *lolO* mutations accumulated the same compound but did not produce loline alkaloids. These observations suggested that the compound was an intermediate in the biosynthetic pathway leading to loline alkaloids.

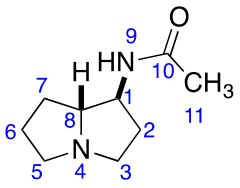

Figure 2.1. (±)-1-*exo*-Acetamidopyrrolizidine (AcAP) and its numbering scheme.

Dr. Juan Pan isolated enough of the new metabolite, which I used to determine its formula and connectivity by MS and NMR, but NMR experiments to assign its

stereochemistry gave ambiguous results. I decided to prepare AcAP synthetically in order to compare its structure with that of the new metabolite and establish the structure of the latter, including its stereochemistry, with certainty.

2.2. Results and discussion

2.2.1. Synthesis of (±)-AcAP and (±)-1-*epi*-AcAP

To make AcAP, I adapted (Scheme *2.1*) the procedure for synthesis of AP developed by Christine et al. (Scheme *1.10*).[19] Christine et al. used NaOMe as a base for Dieckmann cyclization to cyclize diester **8**, but I found that when I used LDA as a base, our yield was higher than the reported yield.[19] Hydrolysis, decarboxylation, and oxime formation then gave (±)-**10**. I reduced (±)-**10** with Raney Ni in THF to give AP along with some 1-*epi*-AP, and allowed this mixture to react with Ac_2O and DMAP to afford (±)-AcAP in 8% yield over the two steps. The 1-*epi*-AP was not observed to react with Ac_2O under these conditions. By contrast, when I reduced (±)-**10** with Pd/C/H_2, I observed (±)-1-*epi*-AcAP only.

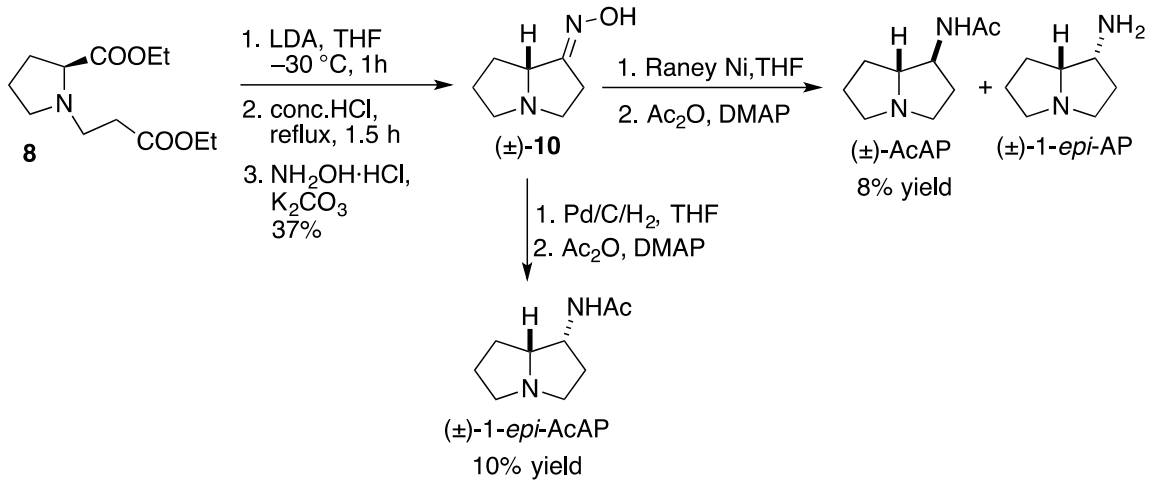

Scheme 2.1. Synthetic scheme to make (±)-AcAP and (±)-1-*epi*-AcAP.

2.2.2. HRMS and NMR analysis of synthetic (±)-AcAP

The fact that only one of the diastereomers obtained from the Raney Ni reduction reacted further with Ac_2O made us confident that our AcAP had exo stereochemistry, but I wanted to establish the stereochemistry of our presumed (±)-AcAP with absolute certainty. Therefore, I analyzed its structure and stereochemistry with NMR and HRMS.

HRMS (Figure A.1) revealed that synthetic (±)-AcAP showed an [M + H] peak with the molecular formula $C_9H_{17}N_2O$. The HSQC spectrum (Figure *2.2*) confirmed the presence of 15 H atoms: two methine groups, five pairs of methylene groups, and one methyl group.

The HSQC spectrum (Figure 2.2) showed that the two most downfield protons, at 4.12 and 3.26 ppm, were due to the methine H atoms at C(1) and C(8). Due to the greater electronegativity of the amido functional group, I assigned the most downfield resonance to the C(1) H atom. The HMBC spectrum (Figure A.2) supported this assignment, as there was a correlation between the ^{1}H NMR resonance at 4.12 ppm and the ^{13}C NMR resonance

due to C(10), a three-bond coupling (Figure 2.3). By contrast, there was no correlation in the HMBC spectrum between the ^{1}H NMR resonance at 3.26 ppm and the ^{13}C NMR resonance due to C(10).

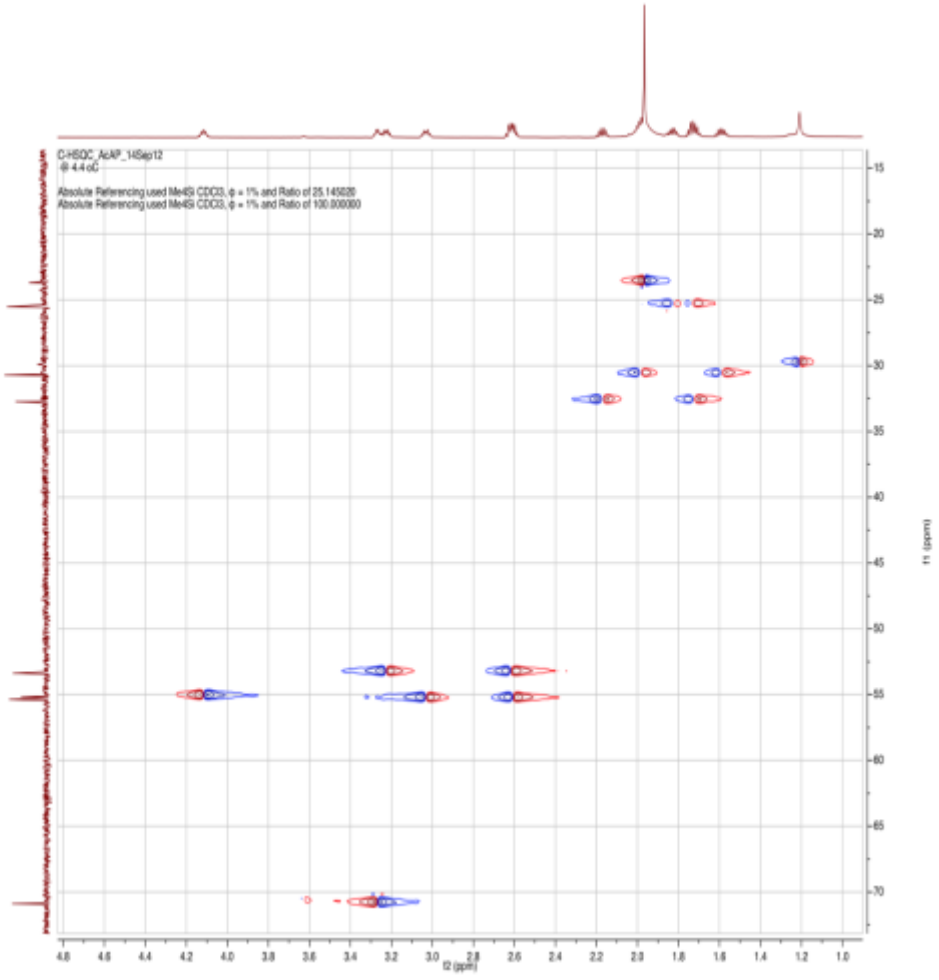

Figure 2.2. 600 MHz ^{1}H–^{13}C HSQC NMR spectrum of (±)-AcAP.

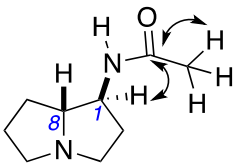

Figure 2.3. HMBC correlations between H atom at C(1) and acetyl group of AcAP.

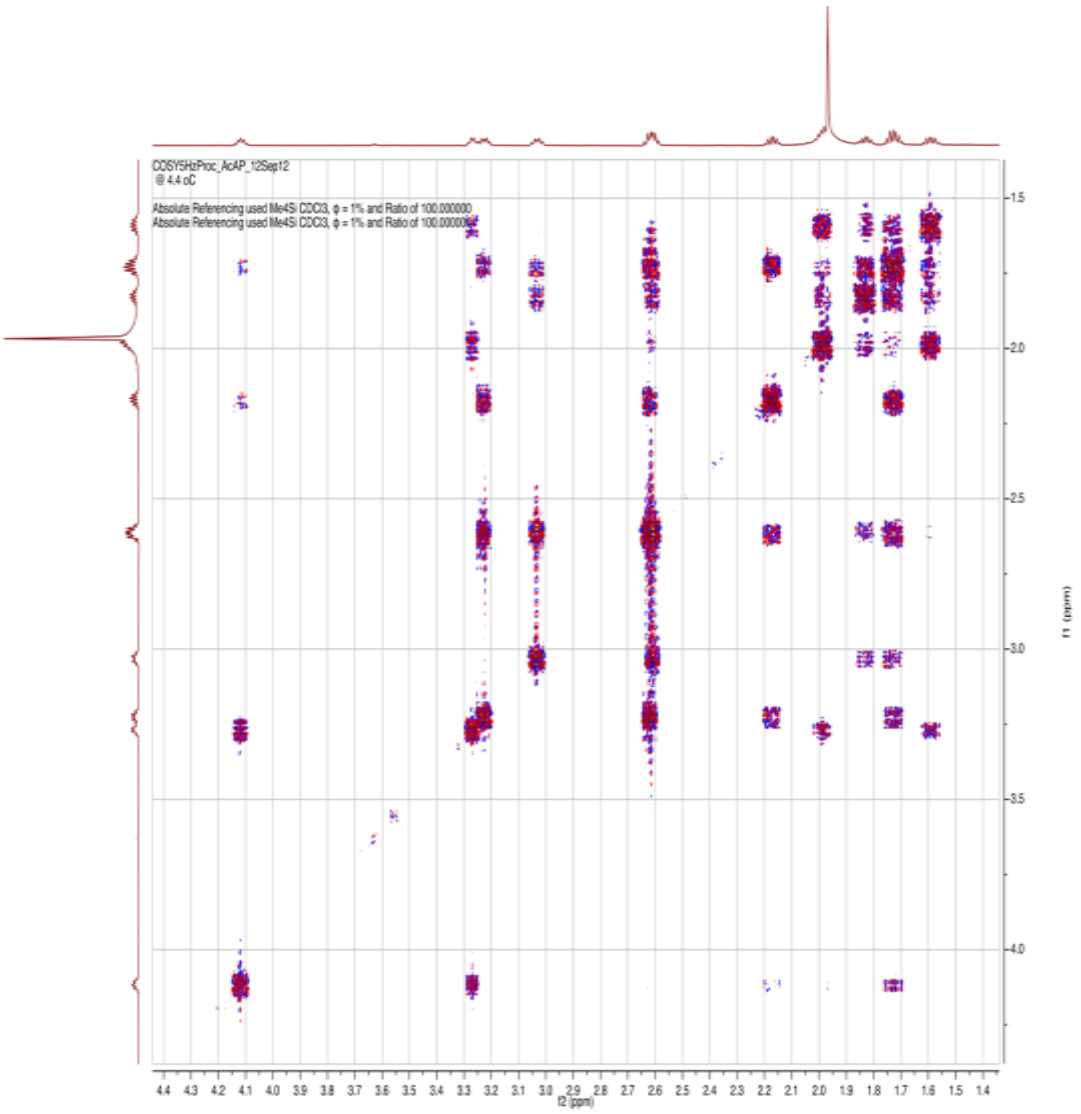

Figure 2.4. 600 MHz ^{1}H–^{1}H COSY NMR spectrum of (±)-AcAP.

I assigned the remainder of the resonances to H atoms on the basis of chemical shifts and ^{1}H-^{1}H COSY correlations (Figure *2.4*). The next most downfield resonance after the C(1) proton was at 3.22 ppm, which could have been one of the C(3) protons, as it was nearer to two N atoms as compared to others. I inferred from the HSQC spectrum that the H atom resonating at 3.22 ppm was geminal to the H atom resonating at 2.61 ppm, suggesting that these two resonances were due to the two H atoms at C(3). The resonance

at 3.03 ppm could have been due to an H atom at C(5), as it was near to a N atom, and HSQC showed that it was geminal to the H atom resonating at 2.61 ppm. COSY showed the strongest correlation between the C(1) and C(8) H atoms and strong correlation between the C(1) H atom and H atoms resonating at 1.73 ppm and 2.16 ppm, which HSQC showed were a geminal pair (Figure *2.5*). These data suggested that the H atoms resonating at 1.73 ppm and 2.16 ppm were at C(2). There was also a strong correlation in the COSY spectrum between the C(2) resonances and those assigned to C(3), which supported the initial assignment of the latter resonances.

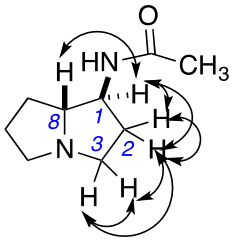

Figure 2.5. COSY correlations between H atoms at C(1), C(2), C(3) and C(8) of AcAP.

In the COSY spectrum of AcAP, there was a strong correlation between the resonance arising from the C(8) H atom and the resonances at 2.16 ppm and 1.60 ppm, which HSQC showed were a geminal pair, suggesting that they could be assigned to the H atoms at C(7) (Figure *2.6*).

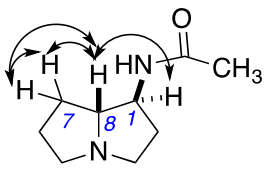

Figure 2.6. COSY correlations between H atoms at C(1), C(7) and C(8) of AcAP.

The remaining resonances at 1.73 ppm and 1.83 ppm, which HSQC showed were

a geminal pair, showed strong correlations in the COSY spectrum with the resonances arising from the C(7) and C(5) H atoms. These data suggested that these last two resonances could be assigned to the H atoms at C(6) (Figure *2.7*). The resonances at C(6) also showed a strong correlation with the resonances that had previously been assigned to the C(5) H atoms, further supporting our initial assignments.

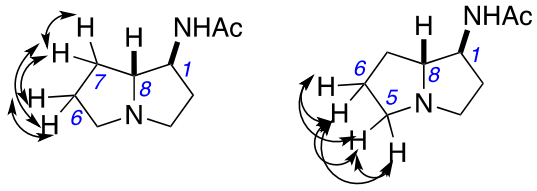

Figure 2.7. COSY correlations between H atoms at C(6) and C(7) and between H atoms at C(5) and C(6) of AcAP.

2.2.3. HRMS and NMR analysis of (±)-1-*epi*-AcAP

Meanwhile, I was able to synthesize (±)-1-*epi*-AcAP through the reduction of (±)-**10** with Pd/C/H_2 (Scheme *2.1*). The HRMS spectrum of (±)-1-*epi*-AcAP (Figure A.*3*) was similar to (±)-AcAP, as expected for these diastereomers. The HSQC spectrum of (±)-1-*epi*-AcAP (Figure *2.8*) showed the presence of the same numbers of methine groups (two), methylene groups (five), and methyl groups (one) as its diastereomer.

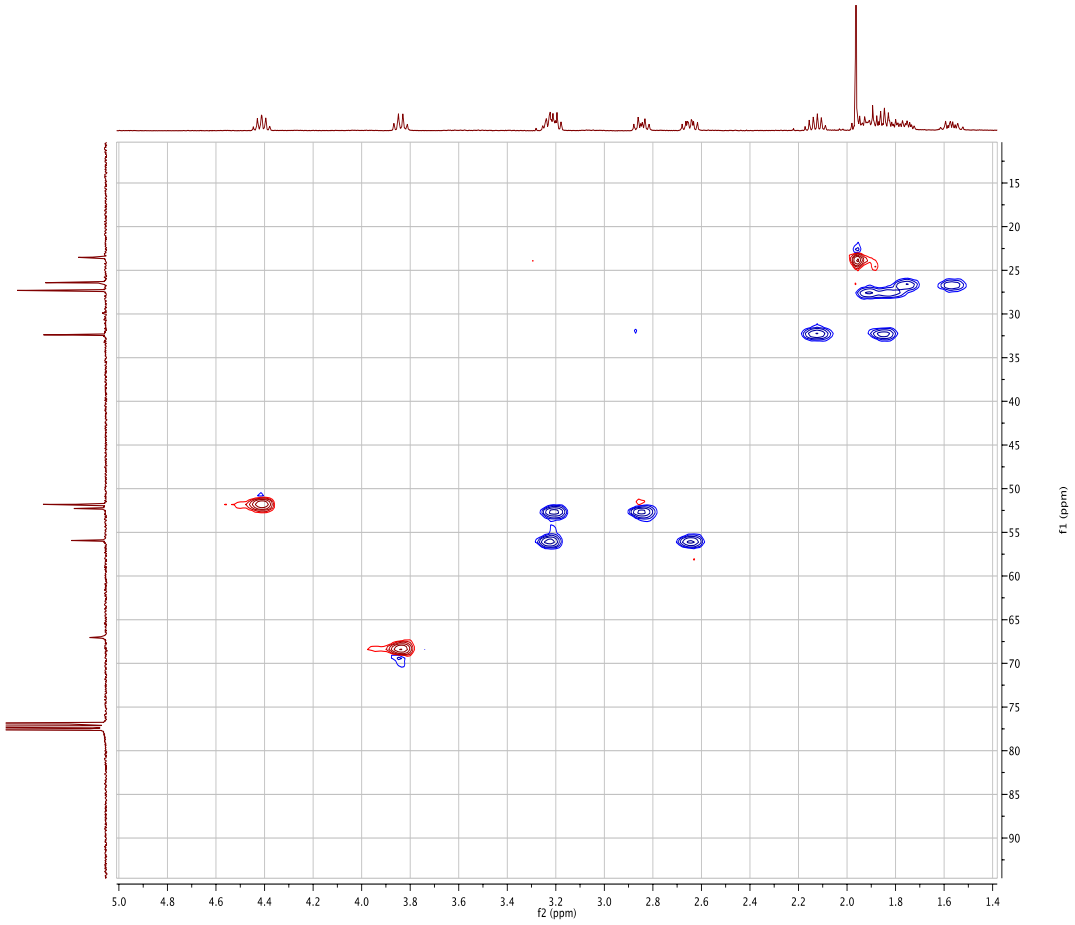

Figure 2.8. 400 MHz ^{1}H–^{13}C HSQC NMR spectrum of (±)-1-*epi*-AcAP.

The two downfield resonances in the HSQC spectrum of compound (±)-1-*epi*-AcAP were methine H atoms, one at 4.41 ppm and the other at 3.84 ppm. I assigned the 4.41 ppm resonance to the H atom at C(1) due to its close proximity to an amido group. The only remaining methine H atom in the structure was at C(8), allowing us to assign the resonance at 3.84 ppm to it. I allotted the chemical shifts of the remaining protons with the help of the COSY spectrum (Figure *2.9*).

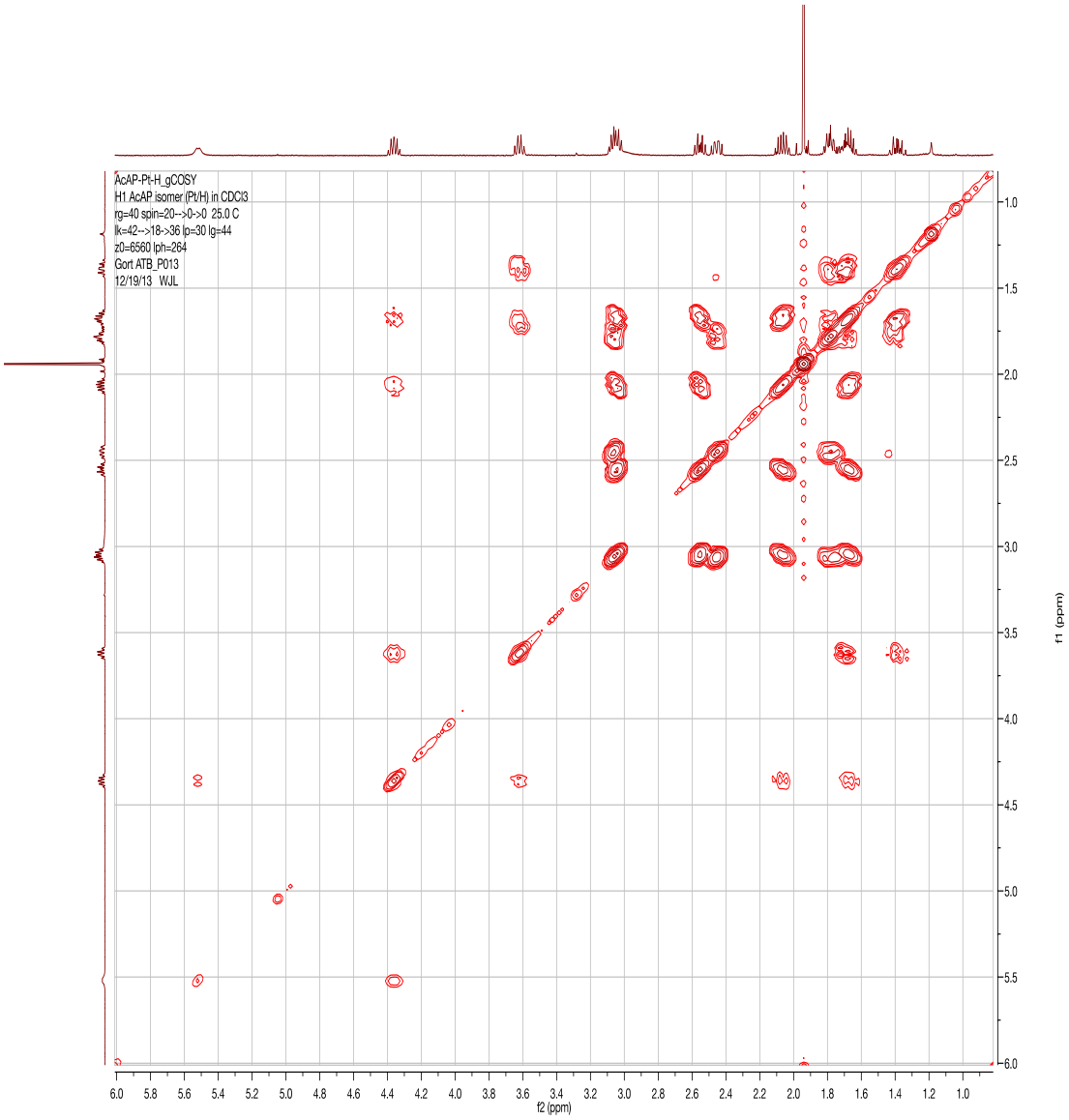

Figure 2.9. 400 MHz ^{1}H–^{1}H COSY NMR spectrum of (±)-1-*epi*-AcAP.

The resonances that I attributed to the H atoms at C(1) and N(9) showed a strong correlation in the COSY spectrum (Figure *2.10*), which further supported our assignment of the C(1) H atom. The COSY spectrum showed no correlation between the resonances that I attributed to the H atoms at C(8) and N(9).

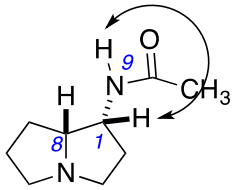

Figure 2.10. COSY correlation between H atoms at C(1) and N(9) of 1-*epi*-AcAP.

There was a strong correlation in the COSY spectrum between the resonance due to the H atom at C(1) and resonances at 2.07 ppm and 1.69 ppm (Figure *2.11*), which the HSQC spectrum showed arose from a geminal pair. These data suggested that these resonances were due to the two H atoms at C(2).

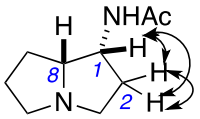

Figure 2.11. COSY correlations between H atoms at C(1) and C(2) of 1-*epi*-AcAP.

The resonance due to the H atom at C(8) showed a correlation in the COSY spectrum with resonances at 1.69 ppm and 1.38 ppm (Figure *2.12*), which the HSQC spectrum showed arose from a geminal pair. These data suggested that these resonances were due to the two H atoms at C(7).

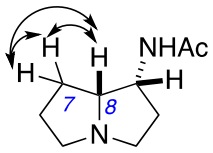

Figure 2.12. COSY correlations between H atoms at C(7) and C(8) of 1-epi-AcAP.

After the resonances due to the H atoms at C(1) and C(8), the next most downfield resonance in the ^{1}H NMR spectrum of (±)-1-*epi*-AcAP was at 3.22 ppm. This resonance

could have arisen from an H atom at C(3) or one at C(5), as these H atoms were closest to N as compared to the rest of the unassigned H atoms. In the HSQC spectrum, the resonance at 2.85 ppm showed a geminal relationship with the resonance at 3.22 ppm. I assigned these two resonances to the H atoms at C(3) due to their greater proximity to two electronegative N atoms. This assignment then suggested that the remaining resonances at 3.22 ppm and 2.64 ppm, which the HSQC spectrum showed arose from geminal H atoms, should arise from the H atoms at C(5).

The only unassigned H atoms left in (±)-1-*epi*-AcAP were those at C(6). In the COSY spectrum, the resonances that arose from the H atoms at C(5) and C(7) showed a strong correlation with overlapping resonances at 1.79 ppm (Figure *2.13*), which the HSQC spectrum showed arose from a geminal pair. These data suggested that these resonances arose from the H atoms at C(6).

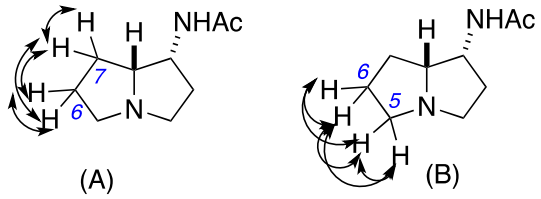

Figure 2.13. COSY correlations between protons at, (A) C(6) and C(7); and (B) C(6) and C(5) of 1-*epi*-AcAP.

2.2.4. NMR analysis of stereochemistry of (±)-AcAP and (±)-1-*epi*-AcAP

The COSY and HSQC NMR spectra helped us to assign the structures of both diastereomers (±)-AcAP and 1-*epi*-AcAP, but the relative stereochemistry of the H atoms at C(1) and C(8) in the two diastereomers could not be determined until I considered NOESY correlations (Figures 2.14 and 2.15).

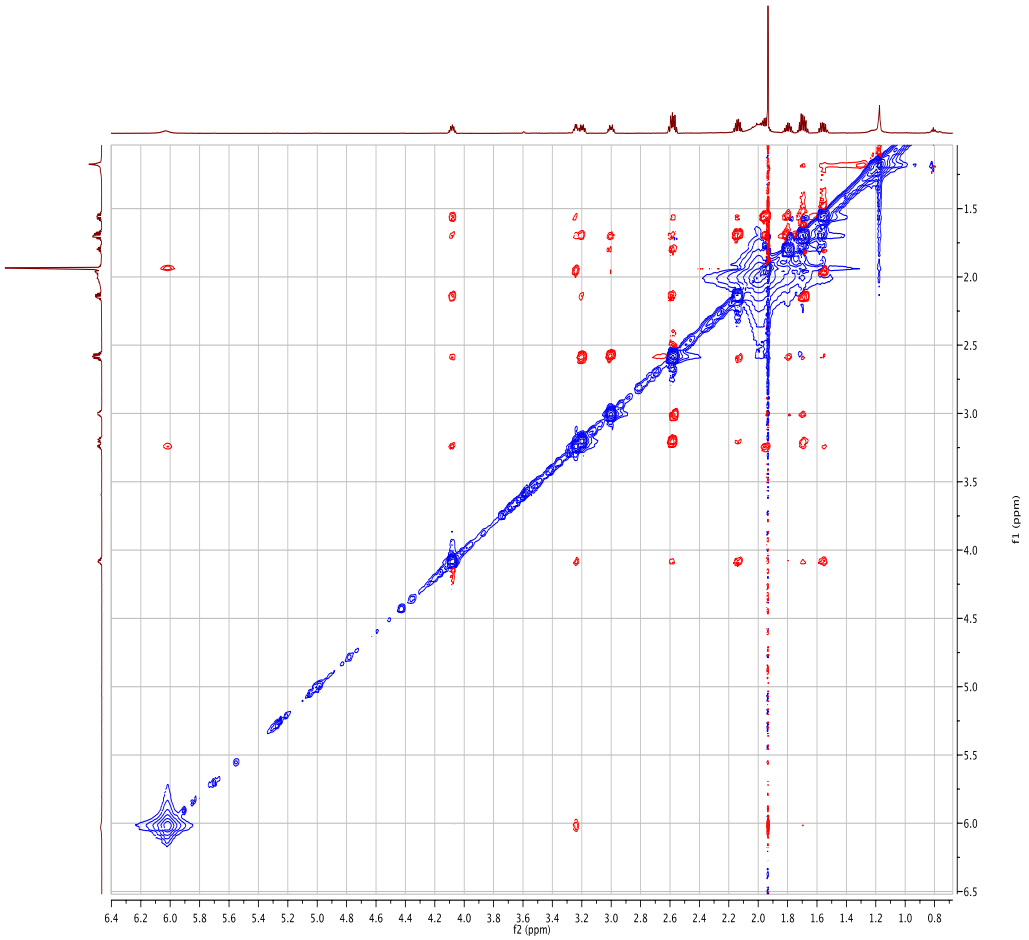

Figure 2.14. 400 MHz ^{1}H–^{1}H NOESY NMR spectrum of (±)-AcAP.

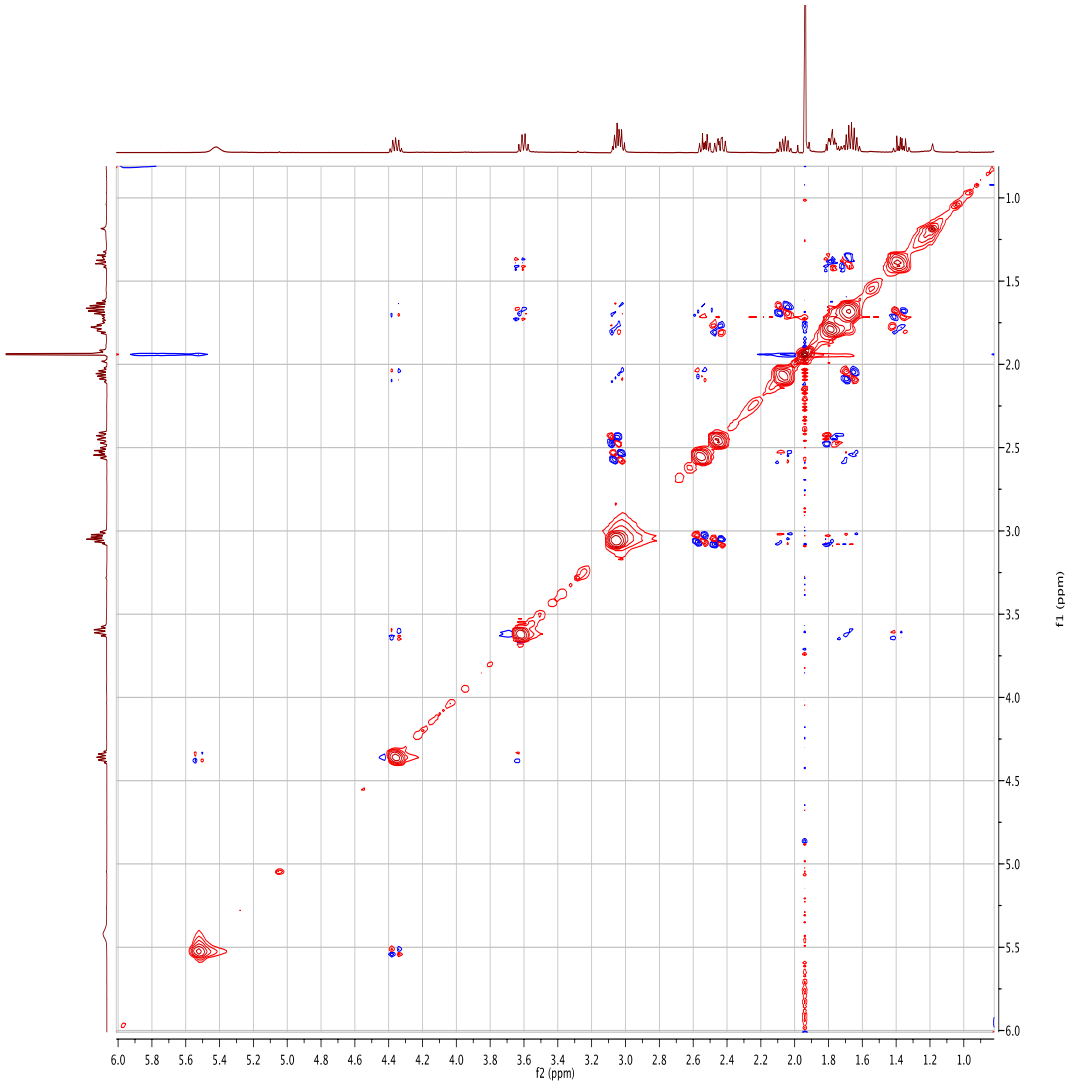

Figure 2.15. 400 MHz ^{1}H–^{1}H NOESY NMR spectrum of (±)-1-*epi*-AcAP.

To unambiguously establish the stereochemistry of C(1) relative to C(8) in (±)-AcAP and (±)-1-*epi*-AcAP, I looked for NOE interactions between the H atoms at N(9) and C(1); N(9) and C(8); C(1) and C(7); and C(1) and C(8). In the NOESY spectrum of (±)-AcAP, I observed correlations between one of the H atoms at C(7) and the H atom at C(1), and between the H atoms at N(9) and C(8) (Figure *2.16*). These correlations were

only possible in (±)-AcAP if the H atom at C(1) was trans with respect to the ring fusion H atom at C(8). I did not observe these interactions in the NOESY spectrum of (±)-1-*epi*-AcAP, but I did observe correlations between the H atoms at C(1) and C(8), and between the H atoms at C(1) and N(9) (Figure *2.17*). These data strongly suggested that (±)-AcAP was the exo isomer, and (±)-1-*epi*-AcAP was the endo isomer.

However, I found a correlation in the NOESY spectrum of (±)-AcAP that was difficult to explain with our assignment. The correlation was between the resonances due to the H atom at C(1) and the resonance due to H atoms at C(8) and C(3). If the correlation was to the H atom at C(8), it could be rationalized as being due to hopping (transfer of energy from one atom to another) or COSY leakage. If the correlation was to the H atom at C(3), it could be a transannular NOE. It was hard to distinguish between these possibilities.

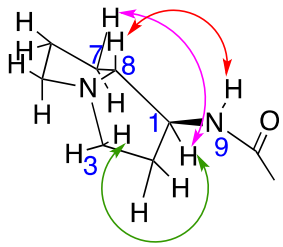

Figure 2.16. ^{1}H–^{1}H NOESY correlations between H atoms at C(1) and C(7), and C(8) and N(9) in (±)-AcAP.

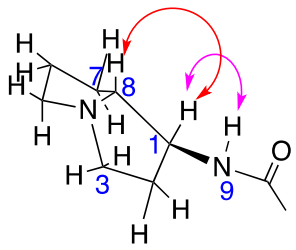

Figure 2.17. ^{1}H–^{1}H NOESY correlations between H atoms at C(1) and C(8), and C(1) and N(9) in (±)-1-*epi*-AcAP.

2.2.5. Crystal structure of synthetic (±)-AcAP

I was able to grow crystals of (±)-AcAP from $CHCl_3$ that were suitable for analysis by X-ray crystallography, which allowed me to assign its stereochemistry unequivocally. The crystals that I obtained were centrosymmetric, with each unit cell containing a single complex consisting of a 2:1 ratio of (±)-AcAP to HCl (Figure *2.18*). In this complex, the ring N atoms of the two molecules of (±)-AcAP formed a linear N–H^+–N arrangement, and the two amide N-H groups coordinated to Cl^-. There was a very short intramolecular N-H-N bond (2.632 Å) in the crystal, which is rare but not unique for this type of compound.[24-26] In any case, the crystal structure clearly showed that the stereochemistry of the amido group at C(1) of (±)-AcAP was exo with respect to the C(8) H atom, further supporting the structure determined by NMR.

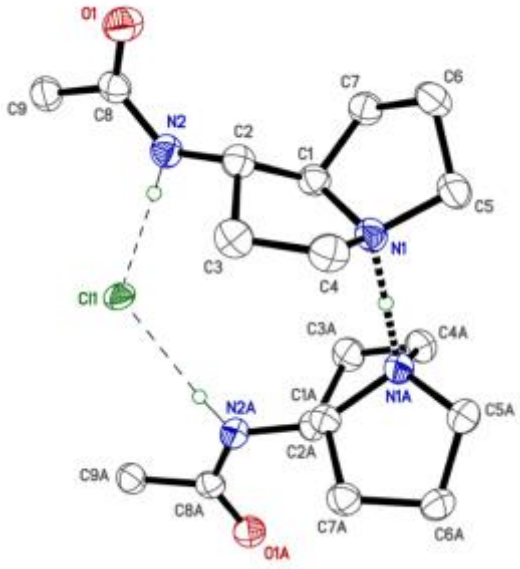

Figure 2.18 ORTEP diagram of 2AcAP·HCl.

2.2.6. NMR and MS spectra of mixture of synthetic (±)-AcAP and isolated metabolite were identical to those of individual samples

In order to determine whether synthetic (±)-AcAP was identical to putative isolated AcAP, I mixed equimolar samples of the two materials in $CDCl_3$, and I analyzed the mixture by ^{1}H NMR (Figure A.*4*) and ^{13}C NMR (Figure A.*5*). There were no changes from the NMR spectra of isolated and synthetic (±)-AcAP to the NMR spectra of the mixed material. The GC–MS spectrum of the equimolar mixture was also indistinguishable from the GC–MS spectra of the individual compounds (Figure A.*6*). These analyses established that the new metabolite had a structure and stereochemistry identical to synthetic (±)-AcAP, with the caveat, of course, that the isolated AcAP was almost certainly enantiomerically pure.

2.3. Conclusion

I have shown that AcAP is a novel metabolite that can be isolated from fungi that have a mutated *lolO* gene. The natural conclusion is that AcAP is the substrate for LolO in the loline biosynthetic pathway. However, there is also the possibility that AP, a known intermediate, is the actual substrate of LolO, and that AcAP forms by reaction of AP with an endogenous acetylase only when AP begins to accumulate because functional LolO is absent. In other words, AcAP could be a shunt product, and may not be involved in the biosynthesis of loline at all. In the following chapter, I will investigate whether AcAP is a real intermediate or a shunt product.

2.4. Experimental Section

Ethyl (2*S*)-*N*-(3-ethoxy-3-oxopropyl)prolinate (8)

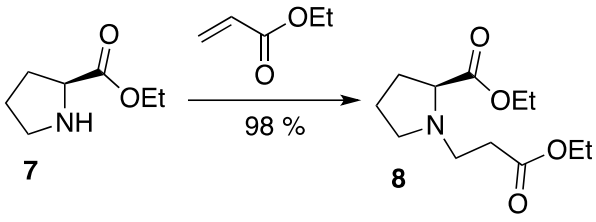

Ethyl L-prolinate (**7)** (10.0 g, 69.8 mmol) and ethyl acrylate (34.9 g, 349 mmol) were added to the reaction vessel and were heated to reflux under nitrogen for 24 h. The reaction mixture was allowed to come to RT, and excess ethyl acrylate was evaporated. It was poured onto a silica column, then eluted with ethyl acetate:petroleum ether (4:6). The solvent was evaporated to yield 16.9 g (98%, 69.5 mmol) of **8**. ^{1}H NMR (400 MHz, $CDCl_3$): δ 4.14 (q, 7.2 Hz, 2H), 4.09 (q, 7.2 Hz, 2H), 3.12 (ddt, J_d = 19.8 Hz, J_d = 8.1 Hz, J_t = 4.2 Hz, 2H), 2.99 (dt, J_d = 12.2 Hz, J_t = 7.7 Hz, 1H), 2.70 (dt, J_d =12.2 Hz, J_t = 7.5 Hz, 1H), 2.48 (t, 7.6 Hz, 2H), 2.37 (q, 8.0 Hz, 1H), 2.12-1.97 (m, 1H), 1.96-1.68 (m, 3H),

1.23 (t, 7.1 Hz, 3H), 1.20 (t, 7.2 Hz, 3 H). ^{13}C NMR (100 MHz, $CDCl_3$): δ 14.3, 14.4, 23.3, 29.5, 34.0, 50.0, 53.4, 60.5, 60.7, 65.9, 172.4, 174.2. IR (ATR): 1729 cm^{-1}.

(±)-1-Oximinopyrrolizidine ((±)-10)

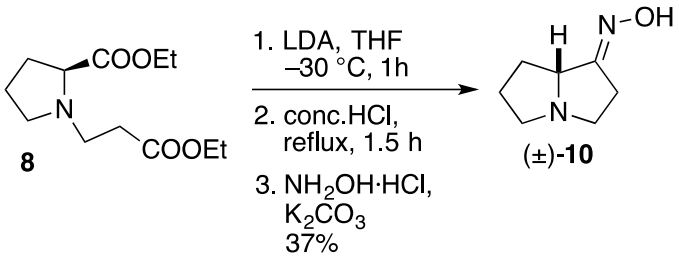

A solution of *n*-BuLi (18.1 mL, 2.27 M) in hexane was added to a solution of diisopropylamine (6.81 mL) in dry THF (225 mL) at –78 °C. The reaction mixture was stirred for 1 h. A solution of **8** (5.00 g, 20.6 mmol) in THF was prepared and added to the above reaction mixture. The reaction mixture was stirred at –78 °C for 2 h and then brought to RT. Water (30.0 mL) was added to it, and the mixture was concentrated by evaporation of THF. The reaction mixture was cooled to 0 °C. Conc. HCl (30 mL) was added to it drop-by-drop, and the mixture was heated to reflux for 1.5 h. The reaction mixture was adjusted to pH 9 by adding a saturated solution of K_2CO_3 at 0 °C. $NH_4OH{\cdot}HCl$ (1.43 g, 20.6 mmol) was added, and the mixture was heated to reflux for 2 h. The mixture was then left to stir for 24 h. The crude compound was extracted with continuous extraction for 3 days with CH_2Cl_2. The solvent was concentrated and poured onto a silica column, and then eluted with CH_2Cl_2:CH_3OH:NH_4OH (8:2:0.2). Solvent was evaporated to yield 1.07 g (37%, 7.6 mmol) of (±)-**10** as a light brown powder that consisted of an inseparable mixture of diastereomers. ^{1}H NMR (400 MHz, CD_3OD): δ 4.09 (t, 7.7 Hz, 1H, minor), 3.82 (dd, 8.2

Hz, 3.6 Hz, 1H, major), 3.19-2.85 (m, 6H, minor), 2.84-2.47 (m, 6H, major), 2.37-2.23 (m, 1H, major), 2.21-2.05 (m, 1H, minor), 2.00-1.70 (m, 3H). ^{13}C NMR (100 MHz, CD_3OD): δ (major) 25.9, 30.3, 30.9, 51.0, 54.13, 62.8, 161.2; δ (minor) 25.9, 30.2, 30.9, 51.6, 54.1, 66.5, 165.9. IR (ATR): 3201, 1738, 1676 cm^{-1}.

(±)-1-*exo*-Acetamidopyrrolizidine ((±)-AcAP)

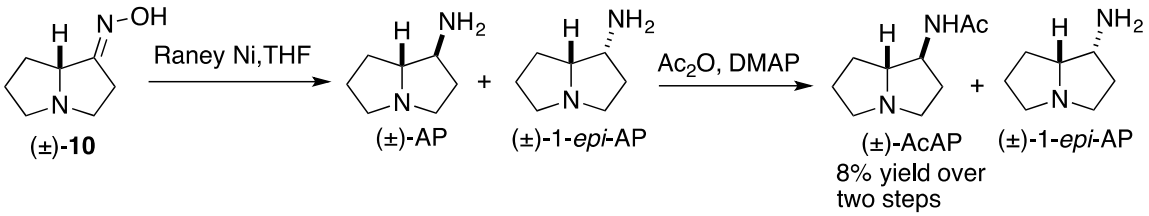

Compound (±)-**10** (0.29 g, 2.09 mmol) was dissolved in THF, and Raney Ni (in excess) was added to it. The mixture was stirred for 13 h at RT as indicated by TLC for completion of reduction to amine. Acetic anhydride (0.196 mL, 2.08 mmol) and DMAP (0.254 g, 2.08 mmol) were added to the reaction mixture, which was stirred at RT for 2 h. It was filtered through a short bed of Celite, followed by dilution with $CHCl_3$. The pH of the solution was adjusted to 12 by adding 1 M NaOH, followed by an addition of saturated $NaHCO_3$ and brine. The phases were allowed to separate for 30 min, and the aqueous layer was extracted with $CHCl_3$ twice. The organic layers were combined and dried over $MgSO_4$, filtered, and concentrated. The residue was poured onto a silica column, then eluted with CH_2Cl_2:CH_3OH:NH_4OH (6:4:1.5). Solvent was evaporated to yield 29 mg (8%, 0.17 mmol) of (±)-AcAP as white crystalline solid, mp 72-74 °C. ^{1}H NMR (400 MHz, $CDCl_3$): δ 1.63 (dq, J_d = 6.8 Hz, J_q = 13.2 Hz, 1H), 1.68-1.78 (m, 2H), 1.79-1.85 (m, 1H), 1.93 (s, 3H), 1.99 (dq, J_d = 7.0 Hz, J_q = 13.0 Hz, 1H), 2.16 (dq, J_d = 6.4 Hz, J_q = 12.6 Hz, 1H),

2.62 (dq, J_d = 10.7 Hz, J_q = 7.0 Hz, 2H), 3.07 (dt, J_d = 10.7 Hz, J_t = 6.4 Hz, 1H), 3.29 (dt, J_d = 11.3 Hz, J_t = 6.4 Hz, 1H), 3.35 (dt, J_d = 12.6 Hz, J_t = 6.4 Hz, 1H) 4.2 (app. quint., 6.4 Hz, 1H), 6.64 (broad d, 5.9 Hz, 1H). ^{13}C NMR (100 MHz, $CDCl_3$): δ 23.6, 25.6, 30.8, 33.0, 53.5, 55.4, 55.5, 71.0, 170.1. IR (ATR): 3272, 1649, 1554 cm^{-1}. HRMS: *m/z* calcd for $C_9H_{17}ON_2$ (M + H): 169.1341; found: 169.1336.

(±)-1-*endo*-Acetamidopyrrolizidine ((±)-1-*epi*-AcAP)

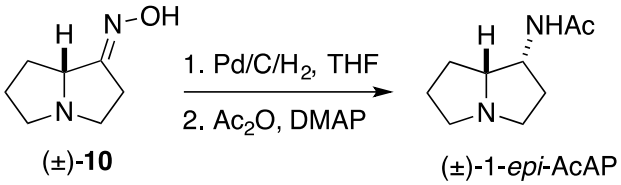

(±)-**10** (±)-1-*epi*-AcAP

Compound **10** (0.10 g, 0.73 mmol) was dissolved in THF and palladium charcoal (0.22 g) was added to it and hydrogenated with a H_2 balloon. The reaction mixture was stirred overnight at RT as indicated by TLC for completion of reduction to amine. Acetic anhydride (0.06 mL, 0.73 mmol) was added and stirred at RT for 2 h. The reaction mixture was filtered through a short bed of Celite, followed by dilution with $CHCl_3$. The pH of the solution was adjusted to 12 by adding 1 M NaOH, followed by addition of saturated $NaHCO_3$ and brine. The phases were allowed to separate for 30 min and aqueous layer was extracted with $CHCl_3$ twice. The organic layers were combined and dried over $MgSO_4$. It was filtered and concentrated. The residue was poured onto a silica column and eluted with CH_2Cl_2:CH_3OH:NH_4OH (6:4:1.5). Solvent was evaporated to yield 12.7 mg (10%, 0.08 mmol) of (±)-1-*epi*-AcAP as yellow solid. ^{1}H NMR (400 MHz, $CDCl_3$): δ 5.51 (s, 1H),

4.36 (dddd, 7.6 Hz, 6.6 Hz, 6.4 Hz, 6.3 Hz, 1H), 3.62 (q, 7.3 Hz, 1H), 3.05 (dt, J_d = 10.9 Hz, J_t = 6.4 Hz, 2H), 2.55 (dt, J_d = 10.8 Hz, J_t =6.9 Hz, 1H), 2.45 (ddd, 10.0 Hz, 8.2 Hz, 6.6 Hz, 1H), 2.07 (dq, J_d = 13.4 Hz, J_q = 6.8 Hz, 1H), 1.94 (s, 3H), 1.85-1.60 (m, 4H), 1.39 (dq, J_d = 12.5 Hz, J_q = 8.3 Hz, 1H); ^{13}C NMR (100 MHz, $CDCl_3$): δ 23.6, 25.6, 30.5, 32.6, 53.5, 54.8, 55.4, 71.6, 170.2; IR (ATR): 3258, 1667, 1547 cm^{-1}. HRMS: *m/z* calcd for $C_9H_{17}ON_2$ (M + H): 169.1341; found: 169.1333

Chapter 3. Is AcAP a shunt product or a substrate for LolO?

(This chapter has been published as part of "Enzymes from Fungal and Plant Origin Required for Chemical Diversification of Insecticidal Loline Alkaloids in Grass-Epichloë Symbiota" by Juan Pan, Minakshi Bhardwaj, Padmaja Nagabhyru, Robert B. Grossman, Christopher L. Schardl.[27] This chapter's experimental section reports only the work done by me.)

3.1. Introduction

The *lolO* gene belongs to the genome of loline-producing fungi.[23] A homology search of the genome sequence of various enzymes shows that LolO is a mononuclear non-heme iron oxygenase enzyme.[27] LolO belongs to the superfamily of alpha-ketoglutarate dependent enzymes.[27] Enzymes of this family are known to catalyze a wide variety of reactions, such as halogenation, hydroxylation, H-atom abstraction via C–H bond activation, oxidative ring closure, desaturation, oxidative aromatic ring cleavage, and C=C double bond epoxidation.[28-29] Such enzymes play an important role in the biosynthesis of antibacterial agents, neurotransmitters, and other metabolites.[30]

I discussed the new metabolite, AcAP in chapter 2, where I was able to establish the structure and stereochemistry of AcAP by comparing it with synthetic (±)-AcAP. In the present chapter, I will explore whether AcAP is a shunt product or a natural substrate of LolO.[23]

There were two possible explanations (Scheme *3.1*) for the accumulation of AcAP when *lolO* was either mutated or subjected to RNAi. Our favored explanation was that AcAP was an intermediate in the loline biosynthesis pathway, and that *lolO* catalyzed

oxidative ether bridge formation on AcAP to make NANL (Scheme *3.1*, Pathway **A**). The hypothesis that AcAP was the intermediate could be explained by the reason that the oxidative C–H bond activations catalyzed by LolO might go more smoothly in the presence of the amide group of AcAP as compared to the more easily oxidized primary amino group of AP. The other explanation was that AP was the intermediate and *lolO* catalyzed the oxidative ether bridge formation on AP, resulting in the formation of NL as the first tricyclic loline in the biosynthetic pathway. NL would then undergo acetylation to make NANL (Scheme *3.1*, Pathway **B**). If the latter hypothesis were true, then AcAP would be only a shunt product, the result of an endogenous enzyme acting on AP accumulating in the absence of LolO.[23]

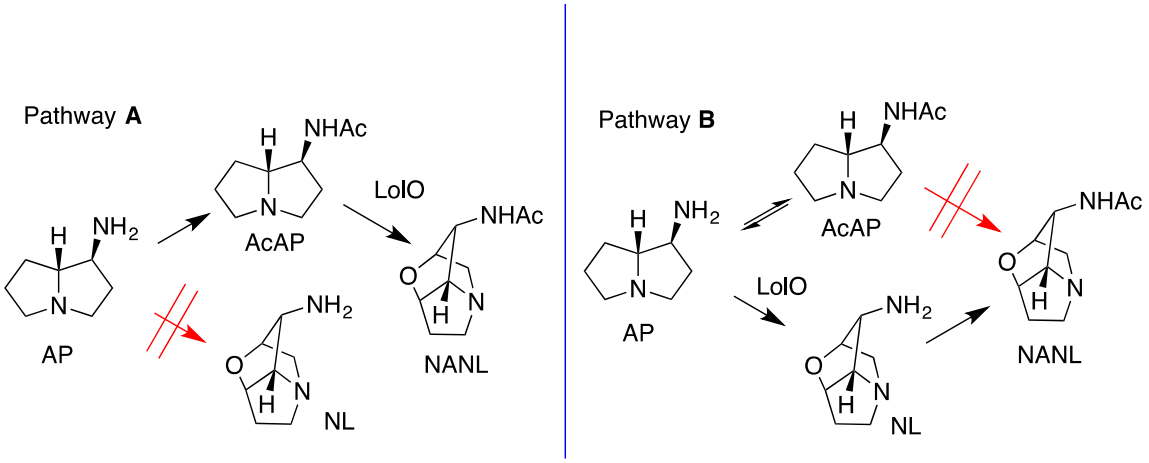

Scheme 3.1. Alternative pathways that might explain accumulation of AcAP. Pathway **A**: AcAP is an intermediate in loline biosynthesis. Pathway **B**: AcAP is a shunt product.

In order to determine which hypothesis was correct, we decided to feed (±)-AcAP that had a D atom in both the ring and the acetyl group to loline-producing culture. This experiment would allow us to determine which pathway the loline biosynthesis took. If AcAP were the intermediate (Scheme *3.1*, Pathway **A**), then the product NANL would

retained all of the D. However, if AcAP were a shunt product (Scheme *3.1*, Pathway **B**), then any AcAP that converted to NANL would first have to be hydrolyzed to AP by removal of the deuterated acetyl group, and hence the NANL would retain only D from the ring.[23]

3.2. Results and discussion

3.2.1. Synthesis of 2′,2′,2′,3-[$^2H_4$]-AcAP

To distinguish which of the two pathways (Scheme *3.1*, **A** and **B**) was operative, I decided to synthesis (±)-AcAP that was labeled both in the pyrrolizidine ring and on the acetyl group, which could be feed to loline-producing fungus in culture. My predecessor, Dr. Hussaini, had previously prepared (±)-3,3-[$^2H_2$]-AP by replacing ethyl acrylate with ethyl 3,3-[$^2H_2$]-acrylate in the Christine et al. procedure (Scheme *1.10*).[13] Adapting this protocol, I prepared (+)-3,3-[$^2H_2$]-**10**, reduced it with Raney Ni in THF, and allowed the product to react with acetic anhydride-d_6 (Scheme 3.2). Sadly, the MS analysis of the resulting AcAP showed that it consisted of about 85% tetradeuterated AcAP, 13% trideuterated AcAP, and only trace amounts of desired pentadeuterated AcAP. The ^{1}H NMR spectrum of the material showed the presence of H atoms at the C(3) position, rather than being fully deuterated as hoped. These results implied that Raney Ni must have catalyzed the substitution of D with H. It may have been that Dr. Hussaini did not see as much scrambling of D with H in our past syntheses of AP because he ran the reduction in isopropanol, whereas I used THF. It is also possible that the Raney Ni that he used in his reactions was less active than what I used.

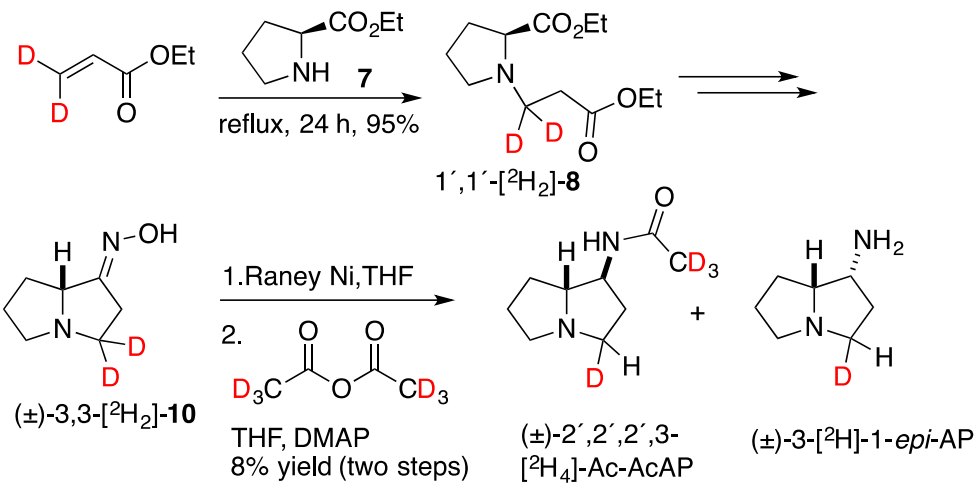

Scheme 3.2. Synthesis of 2´,2´,2´,3-[$^2H_4$]-AcAP.

Even though I lost one of the two D atoms from the pyrrolizidine ring, the fact that one D atom was still present there in 85% of the material allowed us to move forward with the feeding experiment with loline-producing culture.

3.2.2. Production of [$^2H_4$]-NANL upon feeding (±)-2´,2´,2´,3-[$^2H_4$]-AcAP to loline-producing culture

Dr. Juan Pan fed synthetic (±)-2´,2´,2´,3-[$^2H_4$]-AcAP to loline-producing culture of *E. uncinata*, e167. The GC-MS of the NANL that was produced showed peaks at *m/z* = 183 and *m/z* = 187 (Figure *3.1*C). We knew that the 183 peak was due to NANL that was produced from naturally produced AcAP (Figure 3.2b), so it seemed likely that the 187 peak was due to [$^2H_4$]-NANL that was produced from the added [$^2H_4$]-AcAP. We concluded that AcAP was indeed an intermediate in loline alkaloid biosynthesis, acting as the substrate for LolO.[27]

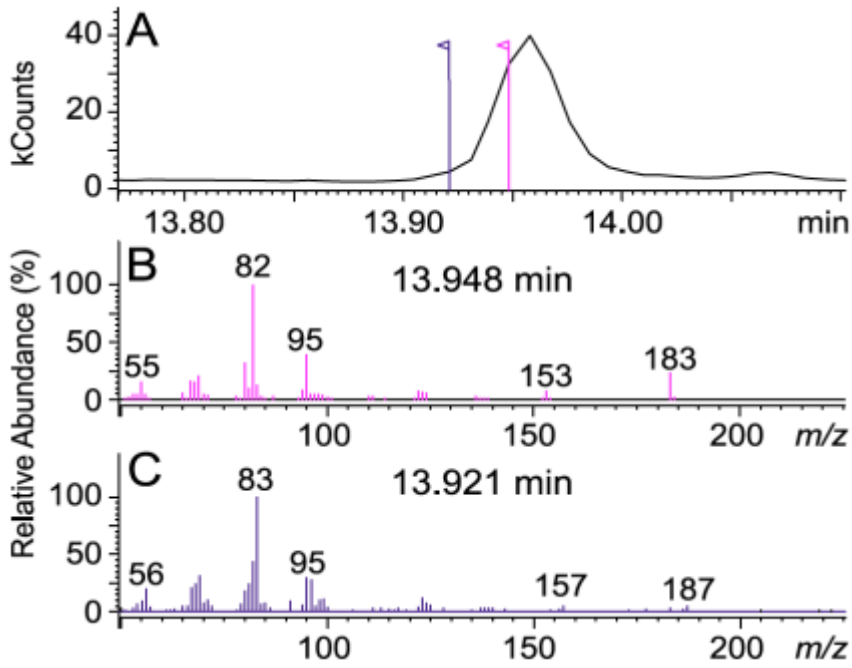

Figure 3.1. (A) GC-MS total ion chromatogram of feeding of 2´,2´,2´,3-[$^2H_4$]-AcAP to loline-producing culture; (B) mass spectrum showing undeuterated NANL at retention time of 13.948 min; (C) mass spectrum showing incorporation of deuterium in NANL at retention time of 13.921 min.[27] (Figure by Dr. Juan Pan.)

3.3. Conclusion

We have established that acetylation occurs before ether bridge formation (Scheme *3.1*, Pathway **A**), that AcAP is the substrate of LolO, and that NANL is the first loline alkaloid in the biosynthetic pathway. It follows that all the loline alkaloids thereafter are derived from NANL through various modifications of substituents on the exocyclic N atom in NANL. However, these data do not tell us what is the product of LolO acting on AcAP. I will investigate this interesting question in more detail in Chapter 4.

3.4. Experimental Section

Ethyl (2*S*)-*N*-(3-ethoxy-3-oxo-1,1-dideuteropropyl)prolinate (1´,1´-[$^2H_2$]-8)

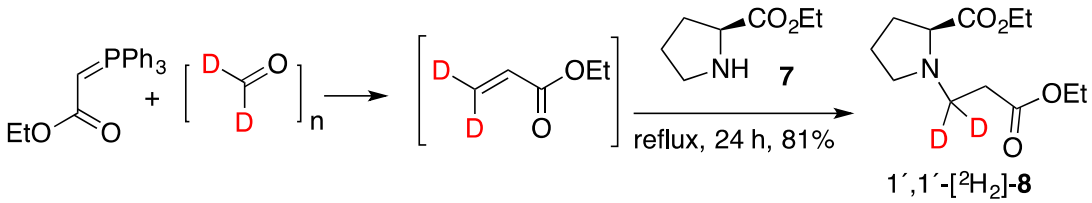

A solution of ethyl triphenylphosphonoacetate (25.0 g, 71.8 mmol) in dry acetonitrile (126 mL) was warmed to 50 °C under nitrogen. Paraformaldehyde-d_2 (2.29 g, 71.8 mmol) was added to it, and the mixture was stirred for 16 h at 50 °C. The reaction mixture was allowed to come to RT, PPh_3 (2.26 g, 8.61 mmol, 12 mol %) and **7** (10.3 g, 71.8 mmol) were added, and the mixture was heated to reflux under nitrogen for 24 h. The reaction mixture was allowed to come to RT and stirred for 48 h. The reaction mixture was concentrated and poured onto a silica column and eluted with ethyl acetate:petroleum ether (4:6). The solvents were evaporated to yield 14.3 g (81%, 58.3 mmol) of 1´,1´-[$^2H_2$]-**8** as a yellow oil . ^1H NMR (400 MHz, $CDCl_3$): δ 4.22-4.00 (m, 4H), 3.23-3.03 (m, 2H), 2.45 (s, 2H), 2.38 (q, 8.0 Hz, 1H), 2.19-2.03 (m, 1H), 1.97-1.69 (m, 3H), 1.33-1.16 (m, 6H). ^2H NMR (61.5 MHz, $CDCl_3$): δ 2.96 (broad s, 1H), 2.68 (broad s, 1H). ^{13}C NMR (100 MHz, $CDCl_3$): δ 14.3, 14.4, 21.3, 23.3, 49.2 (quintet, 21.1 Hz), 53.3, 60.5, 60.8, 65.9, 172.4, 174.1.

(±)-3,3-Dideutero-1-oximinopyrrolizidine ((±)-3,3-[$^2H_2$]-10)

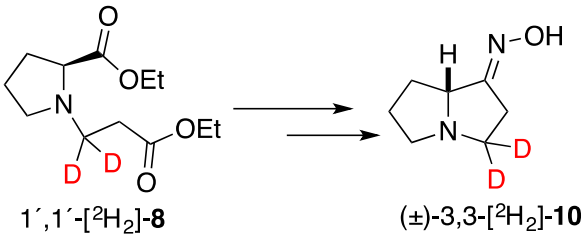

1´,1´-[$^2H_2$]-**8** (±)-3,3-[$^2H_2$]-**10**

This procedure was same as for the synthesis of (±)-**10**. We obtained (±)-3,3-[$^2H_2$]-**10** (900 mg g, 6.36 mmol, 31%) as a mixture of inseparable diastereomers and as a light brown powder. ^{1}H NMR (400 MHz, CD_3OD): δ 4.08 (t, 7.6 Hz, 1H, minor), 3.81 (dd, 8.1 Hz, 3.5 Hz, 1H, major), 2.99 (dq, J_d = 7.9 Hz, J_q = 4.7 Hz, 1H), 2.84-2.40 (m, 3H), 2.38-2.06 (m, 1H), 1.99-1.65 (m, 4H). ^{2}H NMR (61.5 MHz, $CDCl_3$ with CD_3OD as impurity): δ 3.04 (broad s, 1H), 2.75 (broad s, 1H). ^{13}C NMR (100 MHz, CD_3OD): δ (major) 26.1, 26.3, 31.1, 54.2, 64.5, 166.2, NCD_2 not observed. δ (minor) 26.4, 29.1, 30.3, 54.5, 63.0, 166.3, NCD_2 not observed, IR (ATR): 3206, 2207-2106, 1673 cm^{-1}.

(±)-1-*exo*-(2,2,2-Trideuteroacetamido)-3-deuteropyrrolizidine ((±)-2´,2´,2´,3-[$^2H_4$]-AcAP)

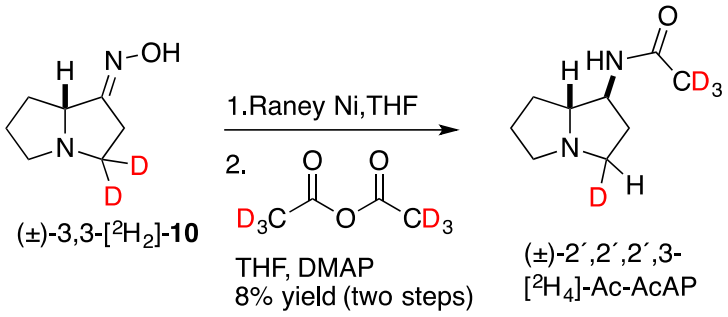

(±)-3,3-[$^2H_2$]-**10** (±)-2´,2´,2´,3-[$^2H_4$]-Ac-AcAP

The procedure was same as for the synthesis of (±)-AcAP, but instead of acetic anhydride, acetic anhydride-d_6 was used, affording 31.1 mg (8%, 0.18 mmol) of mostly (±)-2´,2´,2´,3-[$^2H_4$]-AcAP as a yellow solid, with the major impurity being (±)-2´,2´,2´-[$^2H_3$]-AcAP. ^{1}H NMR (400 MHz, $CDCl_3$): δ 1.61 (dq, J_d = 12.9 Hz, J_q = 6.9 Hz, 1H), 1.71 (dq, J_d = 12.9 Hz, J_q = 6.9 Hz, 2H), 1.81 (m, 1H), 1.95 (dq, J_d = 12.9 Hz, J_q = 6.9 Hz, 1H), 2.14 (~quintet, 5.9 Hz, 1H), 2.59 (broad s, 1H), 3.00 (broad s, 1H), 3.22 (broad d, 2H), 4.08 (~quintet, 6.9 Hz, 1H), 6.52 (broad d, 5.2 Hz, 1H). ^{2}H NMR (61.5 MHz, $CDCl_3$): δ 1.89 (broad s, 6H), 2.60 (broad s, 1H); ^{13}C NMR (100 MHz, $CDCl_3$): δ 22.8 (m), 25.5, 30.8, 32.8, 53.2 (m), 55.3, 55.4, 70.8, 170.3. IR (ATR): 3438, 2254, 1652 cm^{-1}. HRMS: *m/z* calcd for $C_9H_{13}D_4N_2O$ (M+H): 173.1594; found: 173.1586.

Chapter 4. What is the product of LolO acting on AcAP?

(Experiments for this chapter is reported in chapter 2)

4.1. Introduction

We have established that AcAP is the substrate acted upon by LolO, but we do not know whether LolO oxidizes AcAP alone or with the help of other oxidizing enzymes produced by the fungus. Four oxygenase enzymes (LolF, LolP, LolO and LolE) are encoded in the *LOL* gene cluster. Previous studies have established that LolP catalyzes oxidation of NML to NFL (Scheme *1.5*) and is not involved in the biosynthetic pathway of loline until after the formation of the first tricyclic loline.[23] LolF, identified as an FAD monooxygenase, has been proposed to catalyze the oxidative decarboxylation of pyrrolidine ring to iminium ion **5** (discussed in Chapter 1, Scheme *1.5*)[27] because the FAD cofactor does not have enough oxidative potential to catalyze one of the C–H oxidations necessary for ether bridge formation in AcAP. Therefore, LolE and LolO are the only strong candidates for the installation of the ether bridge into AcAP.[23] Moreover, it is possible that LolO is catalyzing the hydroxylation of AcAP and that LolE is catalyzing the subsequent ether bridge formation to make NANL, but it is also possible that LolO is catalyzing both the oxidizing steps to make NANL, and LolE is not involved at all in the process.[23]

To clarify the roles of LolO and LolE in ether bridge formation, we can feed (±)-AcAP to a medium that contains LolO but not LolE. Two experiments that would accomplish this goal are: (1) feeding synthetic AcAP to yeast into which *lolO* has been cloned; and (2) feeding synthetic AcAP to purified LolO in vitro.

Formation of ether bridge by single Fe/2-OG oxygenase (2-OG is 2-oxoglutarate) through activations of two C–H bonds are rare but precedented. Only three enzymes, clavaminic acid synthase (CAS), hyoscyamine 6β-hydroxylase (H6H), and AurH, a cytochrome P450 monooxygenase are known to perform two C–H bond activations and form a new oxacycle.

CAS, a 2-OG-dependent enzyme, catalyzes the key bond-forming step in the clavulanic acid biosynthesis (Scheme *4.1*). Clavulanic acid is a β-lactam drug and is widely used to inhibit serine β-lactamases.[31] CAS performs hydroxylation, oxidative bicyclization, and desaturation.[31-32] It is highly unusual for a single enzyme to do three transformations, with two of those being C–H bond oxidations.

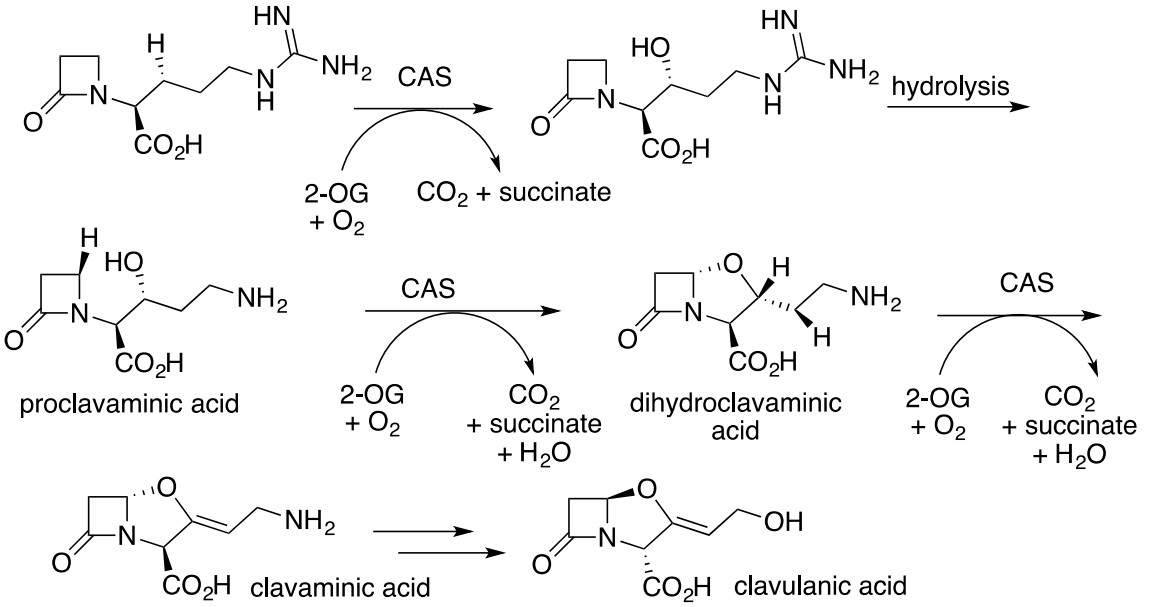

Scheme 4.1. C–H bond activation in clavunic acid biosynthesis.

H6H, another 2-OG-dependent enzyme, catalyzes the epoxidation of hyoscyamine in scopolamine biosynthesis through two C–H bond activations (Scheme *4.2*).

Scopolamine is widely used for the treatment of motion sickness, Parkinson's disease, and eye inflammation.[32-33]

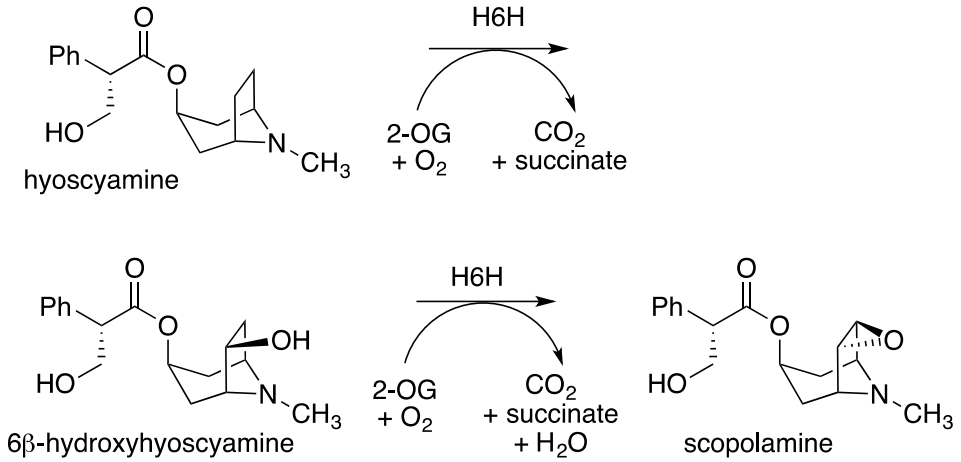

Scheme 4.2. C–H bond activations in scopolamine biosynthesis.

AurH, a cytochrome P450 monooxygenase, links two allylic C atoms with an O atom to form an unstrained tetrahydrofuran in aureothin biosynthesis (Scheme *4.3*).[34-36]

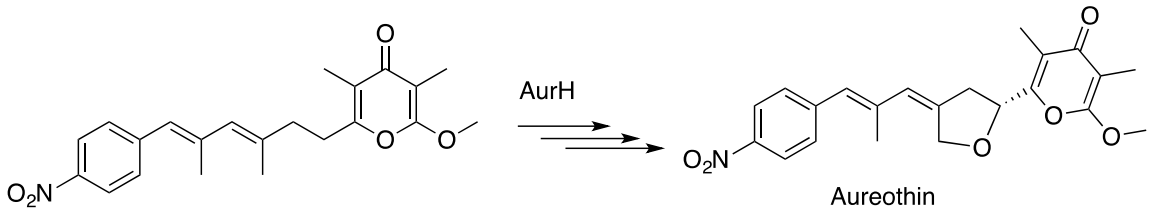

Scheme 4.3. C–H bond activation in aureothin biosynthesis.

4.2. Results and discussion

4.2.1. Production of NANL upon feeding synthetic (±)-AcAP to yeast with *lolO* expression

Scientists have long used yeast (*Saccharomyces cerevisiae*) as a host in studies that require in vivo conditions to test the function of an enzyme. Dr. Juan Pan cloned *lolO* into yeast and added (±)-AcAP (I synthesized in chapter 2) to the modified organism**.** Upon

GC-MS analysis of an extract, she observed a new peak (compare Figure *4.1*b to Figure *4.1*c) whose MS showed *m/z* = 183 (Figure *4.1*a), consistent with NANL. The natural conclusion was that LolO alone was sufficient to catalyze *both* C–H oxidations of AcAP and formation of *both* C–O bonds of the ether bridge, a nearly unprecedented transformation. However, it remained possible, though unlikely, that LolO catalyzed only one hydroxylation, and that some other, endogenous enzyme in the yeast was catalyzing the remaining C–O bond formation to give NANL.[37]

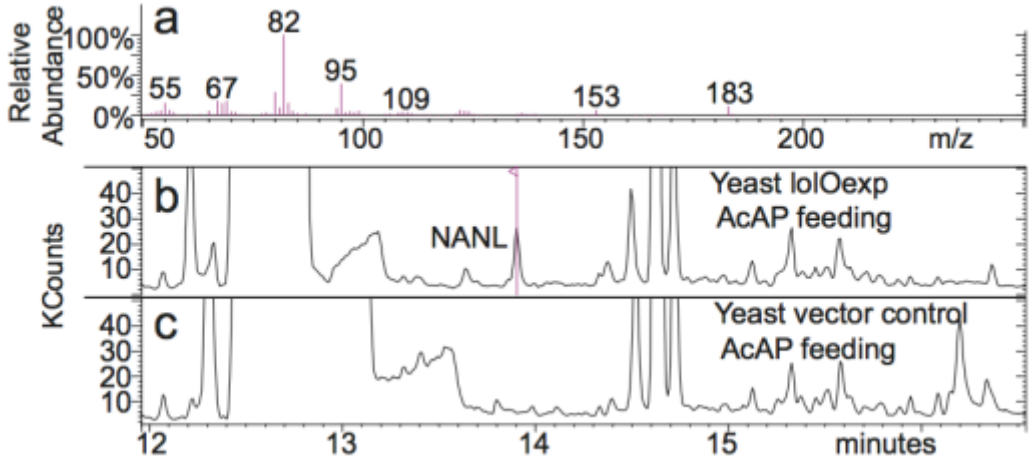

Figure 4.1. (a) Mass spectrum of NANL; (b) GC-MS total ion chromatogram of extract from feeding of (±)-AcAP to yeast expressing LolO; (c) GC-MS total ion chromatogram of extract from feeding of (±)-AcAP to yeast with vector-only (plasmid without *lolO*) transformation.[37] (Figure created by Dr. Juan Pan.)

4.2.2. Purified LolO enzyme catalyzes conversion of (±)-AcAP to NANL

To further support our hypothesis that AcAP was a substrate of LolO and that LolO alone catalyzed formation of the ether bridge, Dr. Chang, who was a post-doctoral scholar

in Dr. Bollinger lab at Penn State University constructed a plasmid to overexpress an N-terminally His_6-affinity-tagged LolO in *E. coli*. He then purified the LolO produced by the transformed *E. coli* with nickel column chromatography. He incubated the purified LolO with 4 equivalents of synthetic (±)-AcAP (I synthesized in chapter 2) in the presence of the two cosubstrates, 2-OG and O_2, and he analyzed the reaction mixture by LC-MS. He observed the consumption of AcAP and production of NANL. This result proved that LolO was the only enzyme needed to convert AcAP to NANL (Scheme *4.4*).

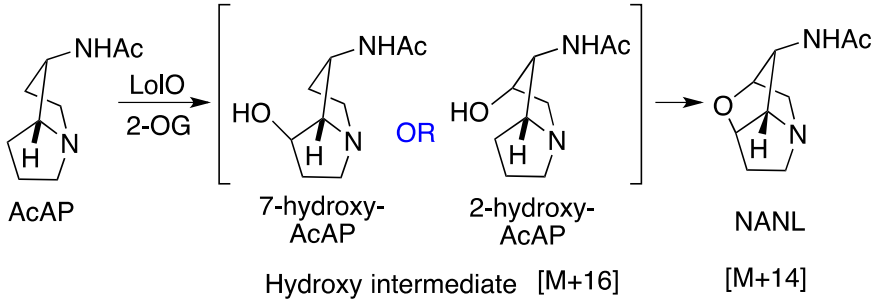

Scheme 4.4 LolO catalyzes the oxidation of AcAP and 2-OG to NANL.

Dr. Chang also observed the production of a compound of mass 16 amu more than AcAP (Figure *4.2*). When the ratio of 2-OG to the natural enantiomer of AcAP was 0.5 (same as 2-OG:enzyme = 1), he observed the maximum amount of this compound. As he increased the ratio of 2-OG to the natural enantiomer of AcAP to 2 (2-OG:enzyme = 4), the amount of the novel compound decreased, and the amount of NANL increased, until the ratio of AcAP to the novel compound to product NANL was approximately 1:0:1, as one would expect if all of the natural enantiomer of AcAP, and none of the unnatural enantiomer, had been converted to NANL. On the basis of its MS and its concentration's gradual increase, and then decrease, with increasing amounts of 2-OG, we tentatively identified the compound as the presumed intermediate in oxacycle formation, 2- or 7-

hydroxy-AcAP (Scheme *4.4*). To our surprise, when Dr. Chang further increased the ratio of 2-OG to the natural enantiomer of AcAP to 4, it appeared that the amount of AcAP continued to decrease, and the amount of NANL appeared to continue to increase. Enzymes usually prefer the natural enantiomer of their substrate and do not react with the unnatural one. However, LolO seemed to be consuming its unnatural substrate in the presence of an excess of 2-OG. We hypothesized that LolO might be converting the unnatural enantiomer of AcAP not to NANL, but to a species with the same *m/z* as NANL, perhaps a ketone. However, if unnatural enantiomer of AcAP was converting to NANL then LolO is promiscuous.

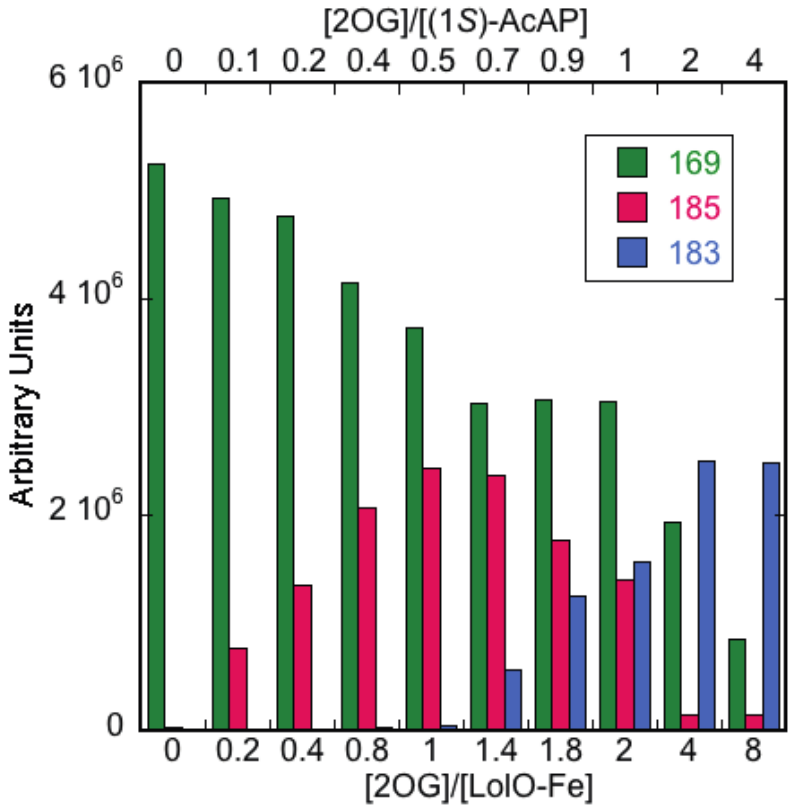

Figure 4.2 LCMS of LolO incubation with various concentrations of (±)-AcAP (4:1 with respect to enzyme) and cosubstrates 2-OG and O_2.

4.3. Conclusion

We have shown that LolO alone catalyzes ether bridge formation in AcAP and that NANL is the product of the reaction of LolO with AcAP. We have observed a new compound of mass 16 amu more than AcAP and that appears to be an intermediate in the oxidation reaction, and we have tentatively identified it as either 2- or 7-hydroxy-AcAP (Scheme *4.4*); the evidence obtained thus far does not allow us to determine which is more likely. In the next chapter, we will investigate the regiochemistry of this previously unknown intermediate in more detail.

Chapter 5. What is the sequence of C-O bond formation events catalyzed by LolO?

5.1. Introduction

In the experiment where we subjected (±)-AcAP to purified LolO and varying concentrations of 2-OG (Scheme *4.4*), we observed a novel compound that reached its maximum concentration at low concentrations of 2-OG and nearly disappeared when the concentration of 2-OG reached twice that of the natural enantiomer of AcAP (Figure *4.2*) The MS data showed that the unidentified compound had a mass 16 amu more than (±)-AcAP and 2 amu more than NANL. These observations suggested that this compound was an alcohol intermediate along the pathway from AcAP to NANL. What remained unclear, however, was whether this alcohol was installed at the C(2) or C(7) position of AcAP (Scheme *4.4*).

The active site of LolO catalysis is not known yet. However, the active sites of 2-OG-dependent enzymes such as LolO are generally conserved.[38] The LolO active site consists of a 2-His-1-carboxylate facial triad,[29] which is formed by two histidine residues and either aspartic acid coordinated to the octahedral mononuclear ferrous ion center (Figure *5.1*). The other remaining sites around the iron center are available for binding with O_2, 2-OG and substrate during enzyme catalysis but are typically occupied by water molecules.[39] The substrate coordinates the enzyme near the active site while O_2 and 2-OG coordinate directly to the metal center (Scheme *5.1*).[40-41] Generally, 2-OG-dependent enzymes couple the oxidation of their primary substrate with a four-electron reduction of O_2. Two electrons are provided by the oxidation of the primary substrate, and the remaining two electrons are provided by the oxidation of 2-OG (cosubstrate) in order to completely reduce O_2.[42]

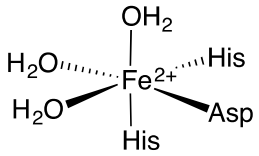

Figure 5.1. Active site of 2-OG dependent enzyme.

As shown in Scheme *5.1*, the commonly accepted mechanism for 2-oxoglutarate-dependent enzymes starts with binary complex **A**.[39] Coordination of 2-OG with displacement of two molecules of H_2O gives ternary complex **(B)**. Complex **B** absorbs at 530 nm due to a metal-to-ligand charge transfer transition. Coordination of substrate with the displacement of another molecule of H_2O results in the formation of quaternary complex **C**. One of the O atoms in O_2 coordinates directly to the iron(II) center, while the uncoordinated O atom attacks the 2-OG carbonyl C atom to give an Fe(IV)=O intermediate complex **F** with the formation of CO_2 and succinate. Complex **F** absorbs at 318 nm due to the loss of the metal-to-ligand charge transfer. The highly reactive **F** begins the oxidation of the substrate by abstraction of an H atom from an unactivated C atom of the substrate, resulting in the formation of substrate radical and Fe(III)-OH intermediate complex **G**. The hydroxylation of the substrate results from a rebounding of OH from **G** to the substrate radical. The hydroxylated product dissociates, resulting in initial binary complex **A**, which restarts the catalytic cycle.

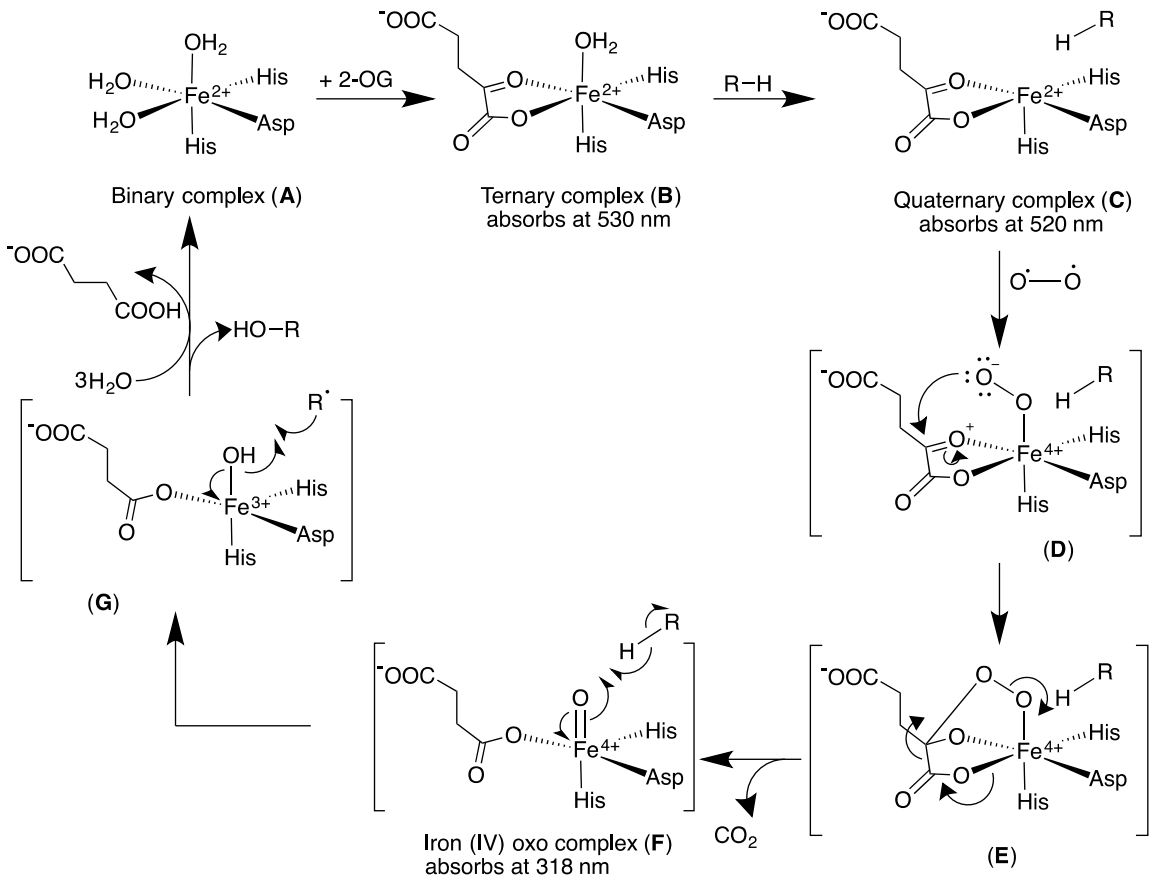

Scheme 5.1. General mechanism for 2-OG-dependent enzymes.

The substitution of an H atom with a D atom on the target C atom of the substrate causes the rate of decay of the Fe(IV)=O intermediate complex (Scheme *5.1*, complex **F**) to decrease due to a kinetic isotope effect. It follows that if replacement of H with D in a substrate causes **F** to accumulate, then the C atom bearing D must be involved in the C–H bond-cleaving step.[43] To determine which carbon atom of AcAP is hydroxylated first, we could introduce D into the C(2) or C(7) position of AcAP. We could then subject these isotopomers to the LolO oxidation reaction in conditions under which only the first C–H activation event was expected to occur. If oxidation at C(2) occurred first, we would expect

to see accumulation of **F** in the case of the C(2) isotopomer, but not the C(7) isotopomer. By contrast, if oxidation at C(7) occurred first, we would expect to see the opposite.

The oxidation reaction that LolO catalyzes proceeds on the time scale of a few milliseconds. A technique that can measure the kinetics of reactions that take place on the time scale of a few milliseconds would help us to determine at which site in AcAP the hydroxylation reaction occurs. One of these techniques is stop-flow absorption, which monitors the reaction by measuring changes in the UV/Vis region of the electromagnetic spectrum.[30] As shown in Figure *5.2*, in the experimental apparatus used for stop-flow absorption, we usually have a reagent and a sample in two different syringes, which a syringe drive pushes into the mixing chamber. The syringe drive keeps pushing the reagent and the sample continuously through the observation cell into the stopping syringe until the stopping block is reached. Thereafter, reaction kinetics are measured spectrophotometrically by measuring UV/Vis spectra, circular dichroism, refractive index, NMR spectra, etc. The time between the end of mixing and the start of measurement is dead time, which is usually a few milliseconds for stop-flow absorption.[44] We can use stop-flow absorption to resolve the two steps of oxidation of AcAP without altering the rate and other kinetic measurements.

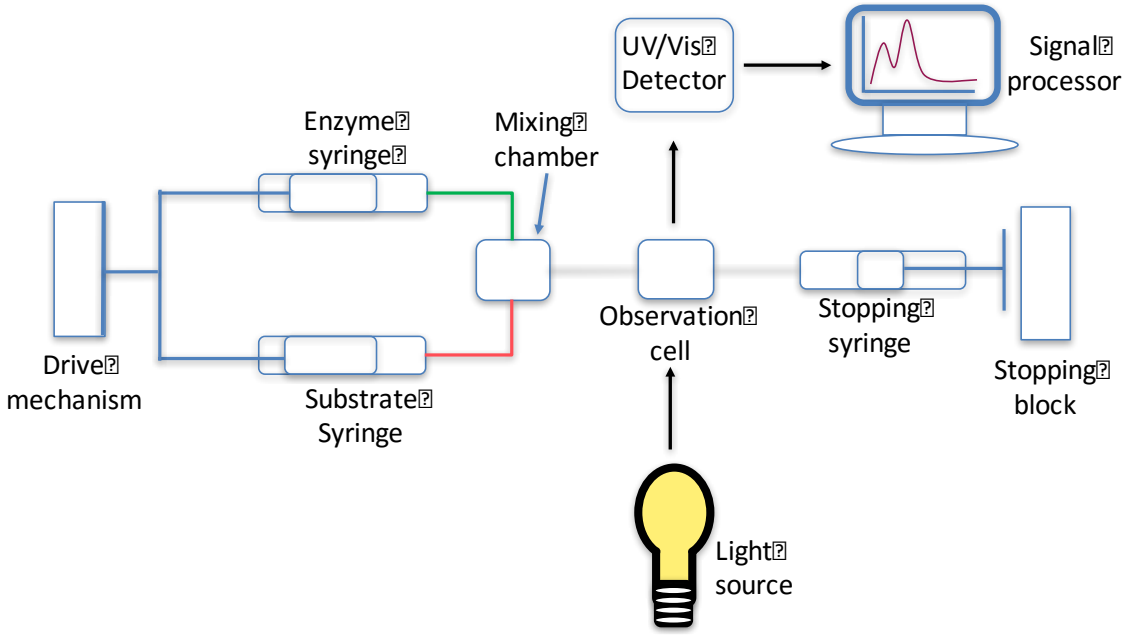

Figure 5.2. Schematic diagram of a stopped-flow analyzer.

5.2. Results and discussion

In order to carry out the stop-flow absorption experiments, I needed to prepare AcAP isotopomers that were deuterated separately at C(2) and C(7). Because I did not know whether LolO was abstracting the exo or endo H atoms of C(2) and C(7), I decided to make substrates that were fully deuterated at these positions. This decision also made my synthetic work much simpler, because I did not need to prepare diastereomerically pure compounds.

5.2.1. Synthesis of (±)-7,7-[$^2H_2$]-AcAP

To place two D atoms at the C(7) position of (±)-AcAP, I synthesized **24** (Scheme *5.2*) by literature procedure[45], then reduced **24** with $NaBD_4$ to give **25**[13]. Compound **25** was then tosylated, reduced again with $NaBD_4$, and deprotected with 6 M HCl to make the

racemic dideuterated proline, (±)-3,3-[$^2H_2$]-Pro·HCl. This compound was further esterified and subjected to a conjugate addition to make diester (±)-3,3-[$^2H_2$]-**8**. The diester (±)-3,3-[$^2H_2$]-**8** was then subjected to Dieckmann condensation, hydrolysis, decarboxylation, and NH_4OH·HCl addition to give oxime (±)-7,7-[$^2H_2$]-**10**.

Previously, I had used Raney nickel to reduce 3,3-[$^2H_2$]-**10** to (±)-2′,2′,2′,3-[$^2H_4$]-AcAP (Scheme 3.2).[27] Apart from giving low yields, Raney Ni also caused a large amount of H/D exchange, resulting in retention of only one D atom in the ring. The scrambling of D with H was even more thorough during the reduction of (±)-7,7-[$^2H_2$]-**10**. Consequently, I had a great need to find a reducing agent which could give an acceptable yield of AcAP without any observable H/D exchange. After an extensive literature search and much experimentation with various widely used reducing agents, I found that when Back et al. used nickel boride (generated *in situ*) for the reductive cleavage of deuterated selenides, they did not observe any H/D exchange.[46] Therefore, I subjected (±)-7,7-[$^2H_2$]-**10** to nickel boride (generated *in situ*) followed by Ac_2O. To our delight, I obtained (±)-7,7-[$^2H_2$]-AcAP (97% d_2 by HRMS) with no observable loss of D enrichment during the reduction.

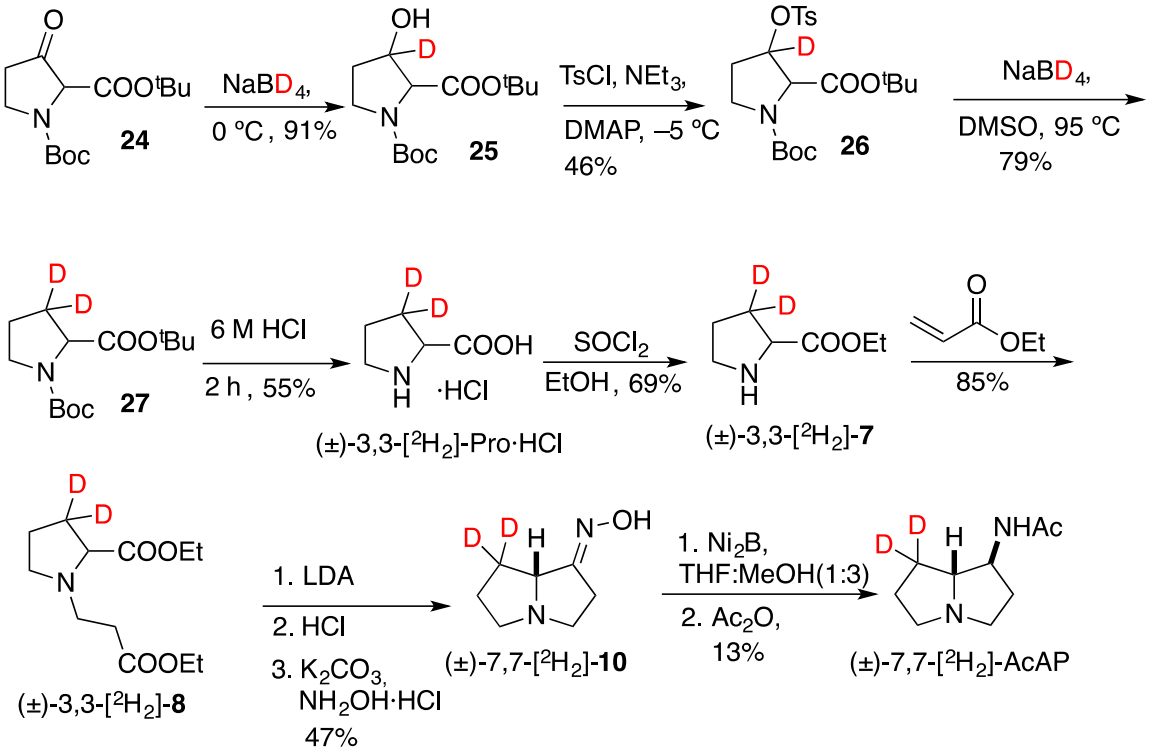

Scheme 5.2. Synthesis of (±)-7,7-[^{2}H$_2$]-AcAP.

5.2.2. Synthesis of (±)-2,2,8-[^{2}H$_3$]-AcAP

To place D at the C(2) position, I synthesized diester **8** following the previously described procedure (Scheme *2.1*).[13] I then subjected **8** to Dieckmann condensation, using DCl in D_2O instead of aqueous HCl for hydrolysis and decarboxylation, and added $NH_2OH{\cdot}HCl$ to give (±)-2,2,8-[^{2}H$_3$]-1**0 (**Scheme *5.3***)**. Nickel boride reduction of (±)-2,2,8-[^{2}H$_3$]-**10** again proceeded well without any loss in D enrichment, and subsequent acetylation gave (±)-2,2,8-[^{2}H$_3$]-AcAP (88% d_3 by HRMS).

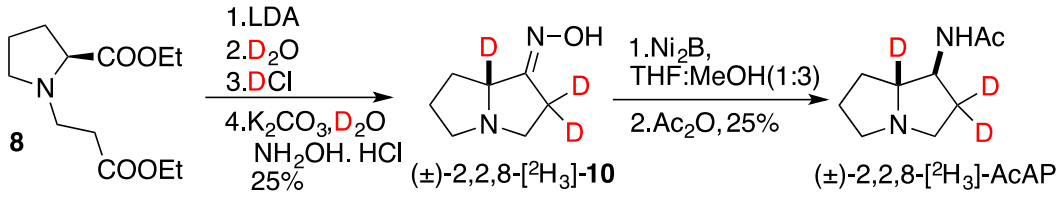

Scheme 5.3 Synthesis of (±)-2,2,8-[$^2H_3$]-AcAP.

5.2.3. Results of incubation of LolO with deuterated derivatives of (±)-AcAP

Dr. Juan Pan incubated (±)-AcAP, (±)-7,7-[$^2H_2$]-AcAP, and 2,2,8-[$^2H_3$]-AcAP with LolO separately under limiting amounts of O_2 and 2-OG. She observed that the quaternary LolO iron(II) complex absorbed at 520 nm in all three substrates. She also observed that, upon the addition of air-saturated buffer, all three substrates caused a temporary increase in absorption at 318 nm, but the increase was much larger and lasted much longer when (±)-2,2,8-[$^2H_3$]-AcAP was the substrate (Figure *5.3*). The much larger and longer-lasting increase in absorption at 318 nm in the case of (±)-2,2,8-[$^2H_3$]-AcAP showed that the LolO ferryl complex **F** (Scheme *5.1*) was accumulating to a much greater extent due to a decrease in its rate of decay (K_{decay} = 1.83 x 10^{-3} s^{-1}) resulting from a deuterium kinetic isotope effect of k_H/k_D = 25.96. The data showed that hydroxylation was much slower when the C(2) position was deuterated than was the case when the C(7) position was deuterated. We concluded that LolO oxidized (±)-AcAP at the C(2) position first, resulting in the formation of the intermediate 2-hydroxy-AcAP before the ether bridge was completed.

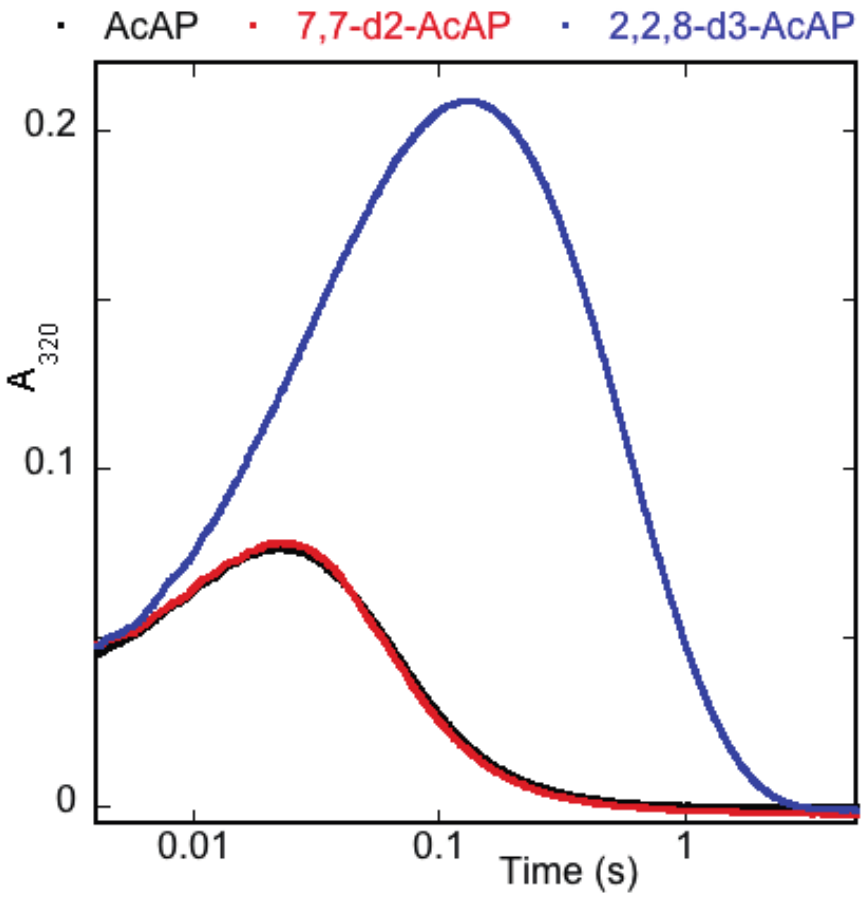

$k_{formation}$ (s^{-1})	k_{decay} (10^{-3} s^{-1})	k_H/k_D
63.8 ± 0.79	47.5 ± 0.47	
69.7 ± 0.85	49.9 ± 0.48	1.05 ± 0.04
69.1 ± 0.48	1.83 ± 0.01	25.96 ± 0.03

Figure 5.3. Stop-flow absorption showing accumulation of C–D cleaving LolO ferryl complex **F** with (±)-2,2,8-[$^2H_3$]-AcAP, and not in the cases of (±)-AcAP and (±)-7,7-[$^2H_2$]-AcAP. (Figure by Dr. Juan Pan.)

5.3. Characterization of hydroxylated intermediate by NMR

Further support for the hypothesis that hydroxylation of AcAP occurred first at C(2) was provided by Dr. Juan Pan. She oxidized AcAP with LolO under conditions of limited

2-OG, and she used prep HPLC to separate the observed intermediate from unreacted AcAP and product NANL, although the sample of intermediate that she obtained contained large amounts of NH_4OAc and one or two other unidentified compounds. Despite the large amounts of impurities, I was able to confirm by ^1H NMR that the structure of the hydroxylated intermediate was 2-hydroxy-AcAP (Figure 5.*4*). The NMR spectrum featured doublets of doublets at 3.15 ppm (J = 12.6 Hz and 6.6 Hz) and 3.80 ppm (J = 12.7 Hz and 5.7 Hz). In the ^1H NMR spectrum of 2-hydroxy-AcAP, I would expect to see a doublet of doublets for the H atoms at C(3), but I would not expect to see such a pattern in the ^1H NMR spectrum of 7-hydroxy-AcAP. This evidence provided independent support for the conclusion from the stop-flow experiment that the observed intermediate was 2-hydroxy-AcAP, the product of hydroxylation of AcAP at C(2).

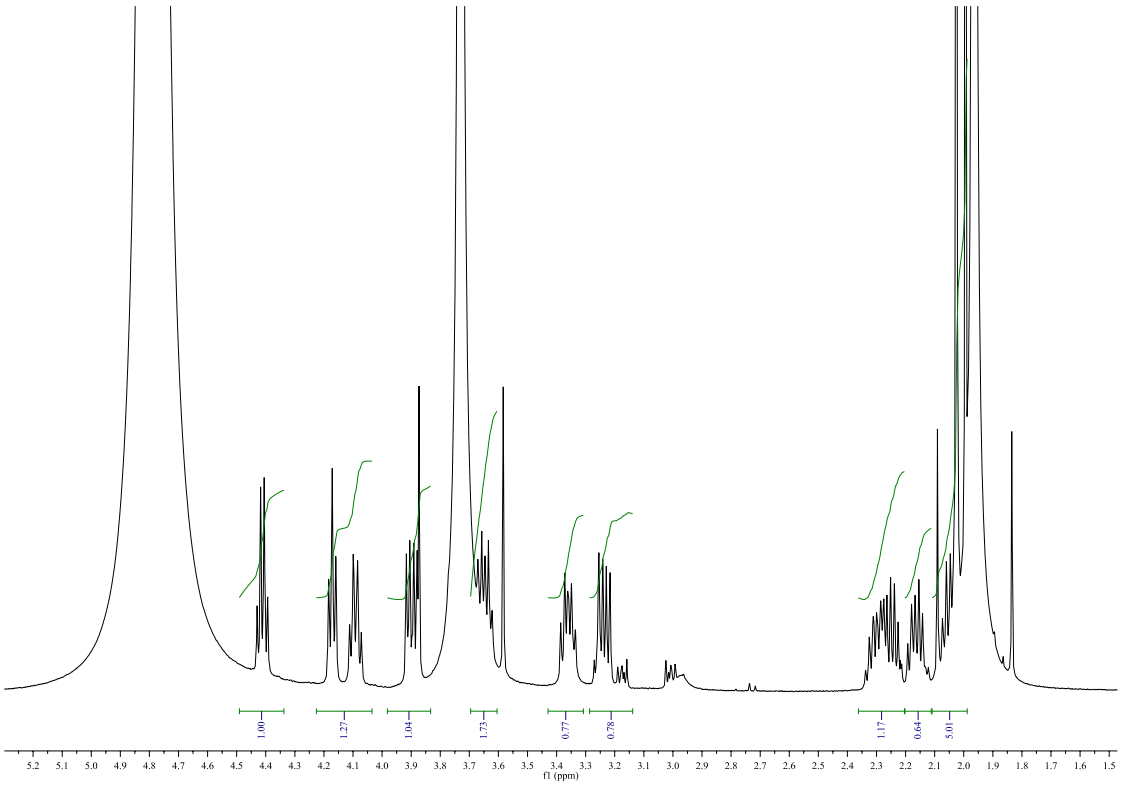

Figure 5.4. 500 MHz ^1H NMR spectrum of the intermediate, 2-hydroxy-AcAP.

Other aspects of the NMR spectra of 2-hydroxy-AcAP were thoroughly consistent with the assigned structure. In the $^{1}H–^{1}H$ COSY spectrum, the doublets of doublets at 3.15 ppm and 3.80 ppm showed strong correlation with one another and with the most downfield resonance, a quartet at 4.41 ppm, which I attributed to the C(2) H atom due to its proximity to the electronegative oxygen in the hydroxyl group. The only methylene C atom near to C(2) is C(3), allowing us to assign the two doublets of doublets to the C(3) H atoms. The other two resonances downfield of 4.0 ppm, those at 4.17 and 4.07 ppm, were likely due to the C(1) and C(8) H atoms. The resonance assigned to C(2) showed strong correlation with the resonance at 4.17 ppm and not with the resonance at 4.07 ppm, suggesting that the former resonance was due to the H atom at C(1) and the latter was due to the H atom at C(8). The strong correlation in the COSY spectrum between the resonances arising from C(2) and C(1) further supported our assignments.

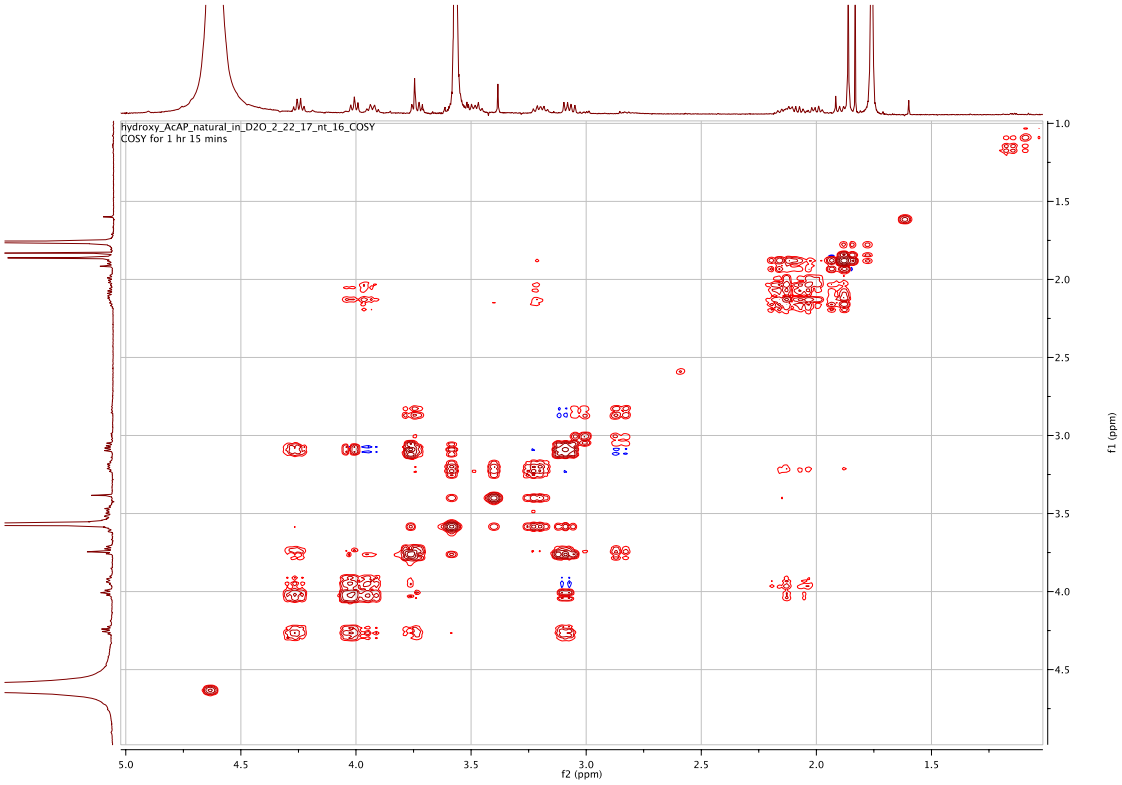

Figure 5.5. 400 MHz ^{1}H–^{1}H COSY NMR spectrum of the intermediate, 2-hydroxy-AcAP.

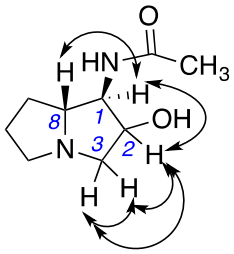

Figure 5.6. COSY correlations between H atoms at C(1), C(2), C(3), and C(8) in 2-hydroxy-AcAP.

There are seven downfield resonances (each integrating to 1H) between 3.5 ppm and 4.5 ppm in the ^{1}H NMR spectrum of 2-hydroxy-AcAP. Out of seven, I already assigned five as C(1), C(2), C(3) and C(8). I assigned the remaining downfield resonances, at 3.65 ppm and 3.36 ppm, to the H atoms at C(5) due to their proximity to the electronegative ring

N atom. The remaining resonances in the region of 1.9 to 2.4 ppm, which integrate to 4H, are likely due to the H atoms at C(6) and C(7).

Furthermore, when I irradiated the resonance attributed to the H atom attached to C2 (quartet at 4.42 ppm), there was strong NOE enhancements of two resonances—one attributed to the H atom attached to C8 (quartet at 4.08 ppm) and one attributed to one of the two H atoms attached to C3 (dd at 3.90 ppm)—but only a very small NOE enhancement of the resonance attributed to the H atom attached to C1 (triplet at 4.18 ppm) (Figure *5.7*). These data were consistent with 2-endo-hydroxy-AcAP, but not 2-exo-hydroxy-AcAP, as I expected because of the endo orientation of the C2–O bond in NANL.

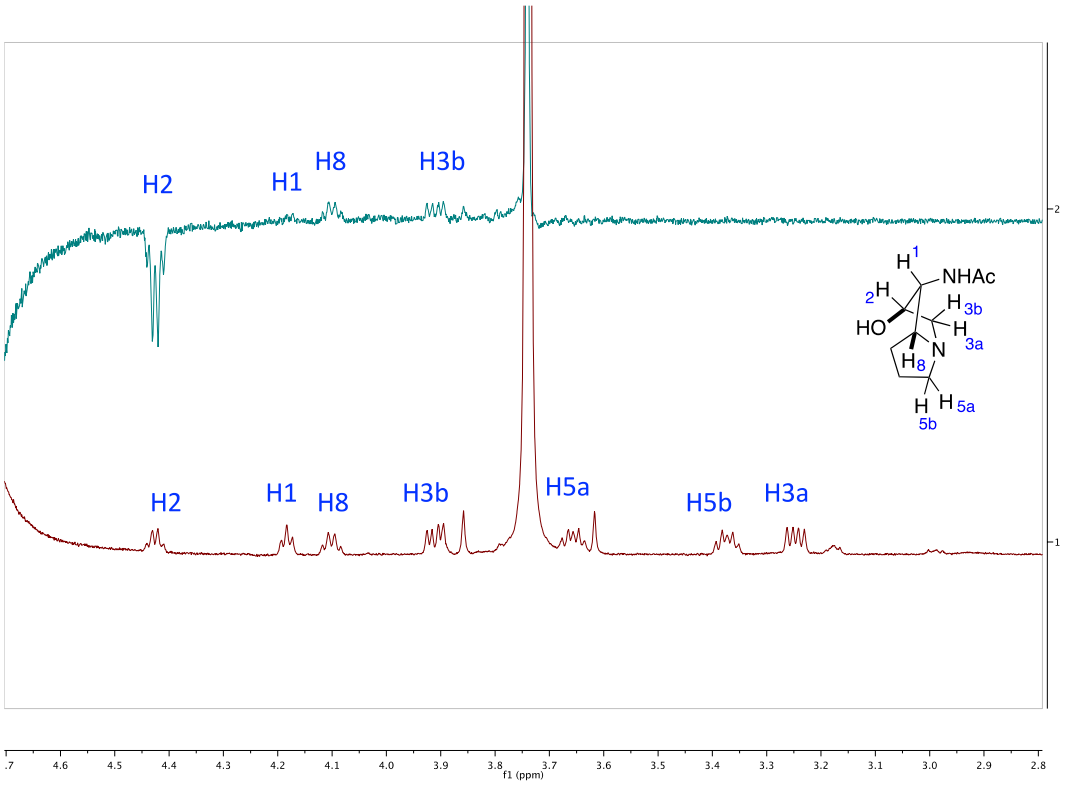

Figure 5.7. 600 MHz NOE difference spectrum of 2-hydroxy-AcAP in D_2O upon irradiation of the resonance at H2 at 4.42 ppm.

5.4. Conclusion

Our results show that LolO begins C–O bond formation in AcAP by C–H activation at C(2), presumably to give a radical intermediate. Hydroxylation then occurs at this position to give 2-*endo*-hydroxy-AcAP. LolO could then catalyze a second C–H activation at C(7), and subsequent addition of the C(2) O atom to the presumed radical at C(7) forms the ether bridge of NANL (Scheme *5.4*).

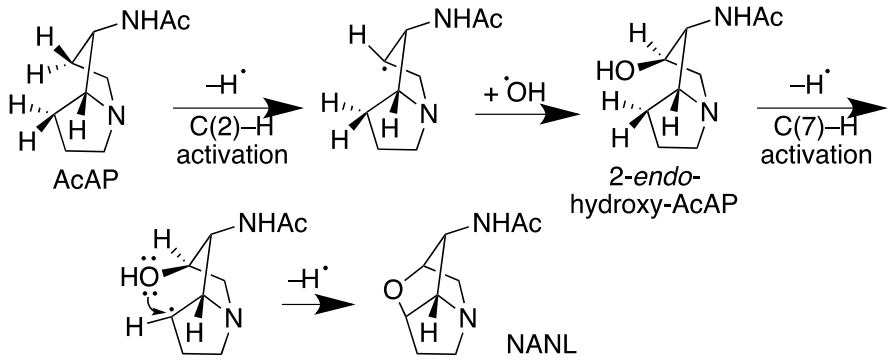

Scheme 5.4. Oxidation occurs first at C(2) and then at C(7) in AcAP to produce NANL.

5.5. Experimental Section

(±)-2,2,8-Trideutero-1-oximinopyrrolizidine ((±)-2,2,8-[$^2H_3$]-10)

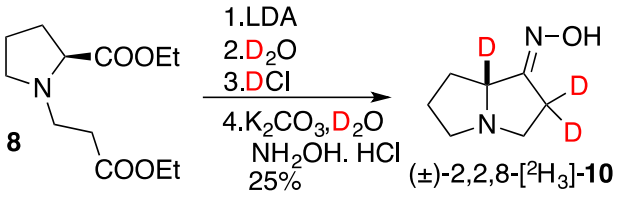

A solution of *n*-BuLi in hexane (2.50 M, 11.1 mL) was added to a solution of diisopropylamine (4.60 mL) in dry THF (100 mL) at –78 °C under nitrogen. After 45 min, a solution of **8** (3.40 g, 13.8 mmol) in THF was added dropwise. The reaction mixture was stirred at –78 °C for 18 h and then brought to RT. D_2O (30.0 mL) was added, and then 7.7

M DCl in D_2O (35.0 mL) was slowly added to the reaction mixture at 0 °C. The mixture was heated to reflux for 1.5 h. The pH of the reaction mixture was adjusted to 9 by dropwise addition of saturated K_2CO_3 in D_2O at 0 °C. $NH_4OH{\cdot}HCl$ (0.96 g, 13.8 mmol) was then added, and the mixture was heated to reflux for 2 h. The mixture was then stirred for 24 h. Solvent and water were evaporated, and the crude mixture was extracted with CH_2Cl_2. The solvent was concentrated and poured onto a silica column and then eluted with CH_2Cl_2:CH_3OH:NH_4OH (8:2:0.2). The solvent was evaporated to yield (±)-2,2,8-[$^2H_3$]-**10** (0.49 g, 3.47 mmol, 25%) as a light brown powder and as an inseparable mixture of diastereomers. ^1H NMR (400 MHz, CD_3OD): δ 3.17-2.50 (m, 4H), 2.33-2.18 (m, 1H, major), 2.17-2.05 (m, 1H, minor), 1.99-1.50 (m, 3H). ^2H NMR (61.5 MHz, $CDCl_3$): δ 4.07 (broad s, minor), 3.82 (broad s, major), 2.88-2.21 (merged broad singlets). ^{13}C NMR (100 MHz, CD_3OD): δ (major) 26.5, 29.0 (m), 31.1, 51.7, 54.5, 66.2 (t, 21.8 Hz), 166.3; δ (minor) 26.2, 30.5, 51.1, 54.3, 64.2 (t, 21.8 Hz), 166.1. IR (ATR): 3195, 2177, 1844, 1675, 1509 cm^{-1}. HRMS: *m/z* calcd for $C_7H_{10}D_3ON_2$ (M + H): 144.1211; found: 144.1210.

(±)-1-*exo*-2,2,8-Trideuteroacetamidopyrrolizidine ((±)-2,2,8-[$^2H_3$]-AcAP)

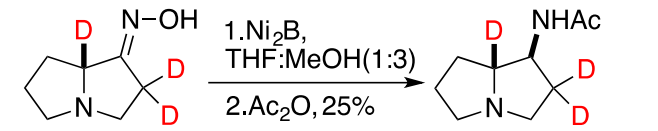

(±)-2,2,8-[$^2H_3$]-**10** (±)-2,2,8-[$^2H_3$]-AcAP

Sodium borohydride (0.24 g, 6.25 mmol) was added in portions to a solution of (±)-2,2,8-[$^2H_3$]-**10** (96 mg, 0.67 mmol) and $NiCl_2$ (0.26 g, 2.01 mmol) in anhydrous MeOH:THF

(3:1, 5.0 mL) at –60 °C over a period of 2 h under nitrogen. (Caution: gas evolution!) After complete addition, the resulting black slurry was allowed to warm up to –30 °C and stirred at this temperature until no more starting material was detected by TLC (18 h). The reaction mixture was warmed to RT, and Ac_2O (in excess) was added with vigorous stirring. The heterogeneous mixture was stirred for a further 4 h. Concentrated ammonium hydroxide (10.0 mL) was added with stirring, and the mixture was filtered through a short pad of Celite. The organic solvent was evaporated, and the aqueous layer was extracted with DCM (3 times). The combined organic layers were washed with brine (2 times), dried over anhydrous $MgSO_4$, and concentrated in vacuum. The crude product was purified by flash chromatography in CH_2Cl_2:CH_3OH:NH_4OH (6:4:0.2) to afford (±)-2,2,8-[$^2H_3$]-AcAP (28 mg, 0.16 mmol, 25% yield) as a gummy yellow solid. ^{1}H NMR (400 MHz, $CDCl_3$): δ 1.60 (dt, J_t = 7.4 Hz, J_d = 12.3 Hz, 1H), 1.74 (dq, J_d = 12.4 Hz, J_t = 6.9 Hz, 1H), 1.83 (ddt, J_d = 18.6 Hz, J_d = 7.4 Hz, J_t = 6.2 Hz, 1H), 1.97 (overlapping s, 4H), 2.61 (dt, J_d = 11.9 Hz, J_t = 6.6 Hz, 2H), 3.00 (dt, J_d = 10.5 Hz, J_t = 6.3 Hz, 1H), 3.18 (d, J_d = 10.6 Hz, 1H), 4.10 (d, J_d = 8.0 Hz, 1H), 5.88 (broad s, 1H). ^{2}H NMR (61.5 MHz, $CDCl_3$): δ 3.20 (broad s, 1H), 2.18 (broad s, 1H), 1.68 (s, 1H). ^{13}C NMR (100 MHz, $CDCl_3$): δ 23.6, 25.6, 30.7, 53.3, 55.3, 55.5, 170.1. IR (ATR): 3257, 2239 (weak), 1652, 1552 cm^{-1}. HRMS: *m/z* calcd for $C_9H_{14}D_3ON_2$ (M + H): 172.2583; found: 172.1524.

1,2-Di-*tert*-butyl-3-hydroxy-3-deuteropyrrolidine-1,2-dicarboxylate (25)

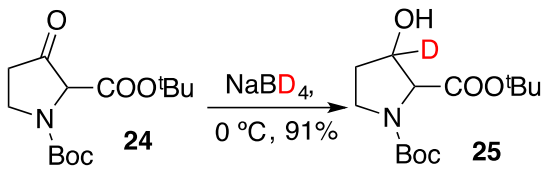

$NaBD_4$ (1.83 g, 43.9 mmol) was added to a solution of **24** (5.01 g, 17.6 mmol) in dry THF (66 mL) at 0 ºC in small portions over a period of 1 h. The reaction mixture was stirred for 3 h at 0 ºC and warmed to RT. The solvent was evaporated, and the residue was dissolved in CH_2Cl_2. The pH of the reaction mixture was adjusted to 2 by the dropwise addition of 1 N HCl with stirring at 0 ºC. The organic layers were washed with brine, dried with $MgSO_4$, and evaporated to give **25** (4.61 g, 15.9 mmol, 91% yield) as a light yellow powder and as a mixture of diastereomers. ^{1}H NMR (400 MHz, $CDCl_3$) δ 1.36 (s, 9H; major), 1.38 (s, 9H; minor), 1.40 (s, 9H; minor), 1.41 (s, 9H; major), 1.88–2.05 (m, 2H), 3.25–3.64 (m, 2 H), 4.12 (s, 1H; major), 4.17 (s, 1H; minor). ^{2}H NMR (61.5 MHz, $CDCl_3$): δ 4.44 (broad s, 1H). ^{13}C NMR (100 MHz, $CDCl_3$) δ (major) =28.1, 28.3, 31.8, 43.8, 64.1, 71.8 (t, 22.3 Hz), 80.0, 81.4, 154.1, 169.6; δ (minor) = 28.0, 28.4, 32.4, 44.2, 63.8, 70.9 (t, 22.0 Hz), 79.7, 81.5, 154.3, 169.7. IR (ATR): 3428, 2165, 1736, 1678 cm^{-1}. HRMS: *m/z* calcd for $C_{14}H_{25}DNO_5$ (M + H): 289.3621: found: 289.1868.

1,2-Di-*tert*-butyl 3,3-dideuteropyrrolidine-1,2-dicarboxylate (27)

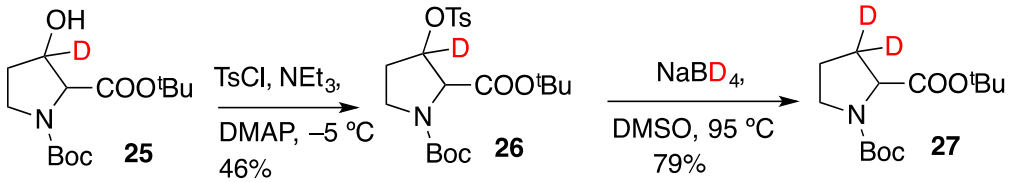

To the mixture of **25** (13.9 g, 48.5 mmol) and DMAP (5.92 g, 48.5 mmol) in dry CH_2Cl_2 (320 mL), triethylamine (49.1 mL, 48.5 mmol) was added. The reaction mixture was cooled to 0 ºC, and TsCl (10.7 g, 56.2 mmol) was added in portions over 1 h. Stirring was continued for a further 54 h at 0 ºC. A saturated solution of NH_4Cl was added to the reaction

mixture at 0 ºC, and the aqueous layer was extracted with CH_2Cl_2. The combined organic extracts were washed with brine, dried with $MgSO_4$, and evaporated. Silica gel chromatography (30% EtOAc in petroleum ether) afforded tosylate **26** (9.83 g, 22.2 mmol, 46% yield). The crude **26** was taken to the next step without purification.

$NaBD_4$ (5,76 g, 13.8 mmol) was added to a solution of crude **26** (10.5 g, 23.8 mmol) in dry DMSO (310 mL), and the mixture was heated to 95 ºC under nitrogen for 8 h. The reaction mixture was cooled and diluted with brine (effervescence) and extracted with ether. The combined organic layers were dried over $MgSO_4$, and the solvent was evaporated. Flash chromatography (40% EtOAc in petroleum ether) afforded **27** (4.83g, 17.7 mmol, 79% yield) as a white gum. ^{1}H NMR (400 MHz, $CDCl_3$) δ 1.44 (s, 9H; major), 1.45 (s, 9H; minor), 1.47 (s, 9H; major), 1.48 (s, 9H; minor), 1.77–1.97 (m, 2H), 3.47 (m, 2H), 4.10 (s, 1 H; major), 4.18 (s, 1 H; minor). ^{2}H NMR (61.5 MHz, $CDCl_3$): δ 1.81 (broad s, 1H), 2.07 (broad s, 1H). ^{13}C NMR (100 MHz, $CDCl_3$) δ (major) =23.3, 28.1, 28.4, 30.3 (p, 20.25 Hz), 46.4, 59.6, 79.6, 80.8. 154.0, 154.4, 172.4; δ (minor) = 24.1, 28.0, 28.5, 29.3 (p, 20.25 Hz), 46.6, 59.6, 79.4, 153.8, 153.8, 172.3. IR (ATR): 2283-2162, 1737, 1697 cm^{-1}. GC-MS (EI): 217 (5%), 203 (2%), 187 (3%), 172 (25%), 144(17%), 116 (100%), 72 (97%), 57 (95%).

(±)-3,3-Dideuteroproline hydrochloride ((±)-3,3-[$^2H_2$]-Pro·HCl)

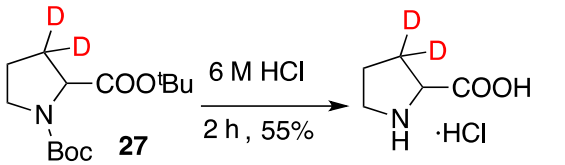

(±)-3,3-[$^2H_2$]-Pro·HCl

Aqueous HCl (6.0 M, 50 mL) was added to a solution of **27** (9.21 g, 33.7 mmol), and the reaction mixture was stirred for 2 h at RT. The water was evaporated to give 3,3-[$^2H_2$]-Pro·HCl (2.82 g, 18.4 mmol, 55%) as a brown gum. ^{1}H NMR (400 MHz, D_2O) δ 2.04 (t, 7.3 Hz, 2H), 3.40 (qt, J_t = 7.3 Hz, J_q = 11.8 Hz, 2H), 4.42 (s, 1H). ^{2}H NMR (61.5 MHz, D_2O): δ 2.14 (broad s, 1H), 2.41 (broad s, 1H), 8.39 (broad s, 1H), 8.92 (broad s, 1H). ^{13}CNMR (100 MHz, D_2O) δ 25.7, 30.2 (p, 20.8 Hz), 48.7, 62.0, 174.3. IR (ATR): 3359, 2032-1926, 1727, 1626 cm^{-1}. EI-MS: Positive ion 117.9 amu, negative ion 173 amu.

(±)-Ethyl 3,3-dideuteroprolinate ((±)-3,3-[$^2H_2$]-7)

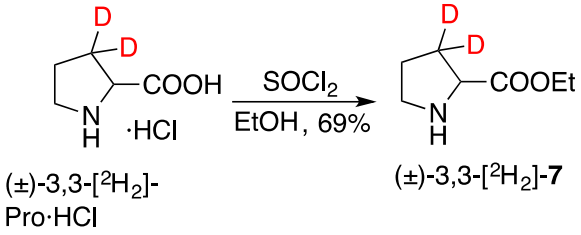

(±)-3,3-[$^2H_2$]-Pro·HCl

(±)-3,3-[$^2H_2$]-**7**

The compound 3,3-[$^2H_2$]-Pro·HCl (3.15 g, 20.5 mmol) was suspended in ethanol (28 mL) and heated to 60 ºC. Thionyl chloride (12.2 g, 102 mmol) was added dropwise to the above suspension, and the resulting solution was refluxed for 4 h. Excess thionyl chloride and ethanol were evaporated, and the resulting solid was dissolved in CH_2Cl_2 (18 mL). Water (3 mL) was added to the reaction mixture, and concentrated ammonia (5 mL) was added to it dropwise. The aqueous layer was extracted with CH_2Cl_2. The combined organic layers were dried over $MgSO_4$, and the solvent was evaporated to afford (2.1 g, 14 mmol, 69%) (±)-3,3-[$^2H_2$]-**7** as a yellow oil. ^{1}H NMR (400 MHz, $CDCl_3$) δ 1.28 (t, 7.1 Hz, 3H), 1.65-1.84 (m, 2 H), 2.92 (dt, J_d = 10.2 Hz, J_t = 6.7 Hz, 1H), 3.08 (dt, J_d = 10.2 Hz, J_t = 6.8 Hz,

1H), 3.75 (s, 1H), 4.18 (q, 7.1 Hz, 2H). ^{2}H NMR (61.5 MHz, $CDCl_3$): δ 1.68 (broad s, 1H), 1.96 (broad s, 1H). ^{13}C NMR (100 MHz, $CDCl_3$) δ 14.1, 25.1, 29.5 (p, 20.3 Hz), 46.9, 59.5, 60.1, 175.1. IR (ATR): 3347, 2230-2125, 1727 cm^{-1}. GC-MS (EI): 145 (5%), 72 (100%), 55 (2%).

(±)-Ethyl (2*S*)-*N*-(3-ethoxy-3-oxopropyl)-3,3-dideuteroprolinate ((±)-3,3-[$^{2}H_2$]-8)

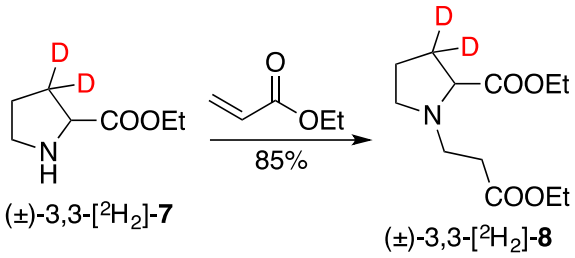

(±)-3,3-[$^{2}H_2$]-**7** (±)-3,3-[$^{2}H_2$]-**8**

The compound (±)-3,3-[$^{2}H_2$]-**7** (2.06 g, 14.7 mmol) and ethyl acrylate (7.09 g, 70.8 mmol) were added to the reaction vessel and refluxed under nitrogen for 24 h. The reaction mixture was allowed to come to RT and concentrated. It was poured onto a silica column, then eluted with 40% EtOAc in petroleum ether. The solvent was evaporated to yield **(±)**-3,3-[$^{2}H_2$]-**8** (2.97 g, 12 mmol, 85%) as a yellow oil. ^{1}H NMR (400 MHz, $CDCl_3$): δ 1.25 (t, 7.1 Hz, 3H), 1.28 (t, 7.1 Hz, 3H), 1.75-1.95 (m, 2H), 2.43 (q, 8.5 Hz, 1H), 2.52 (t, 7.6 Hz, 1H), 2.71-2.81 (m, 1H), 3.04 (dt, J_d = 12.2 Hz, J_t = 7.7 Hz, 1H), 4.15 (td, J_d= 3.4 Hz, J_t = 8.0 Hz, 1H), 3.21 (s, 1H), 4.13 (q, 7.1 Hz, 2H), 4.18 (q, 7.1 Hz, 2H). ^{2}H NMR (61.5 MHz, $CDCl_3$): δ 1.71 (broad s, 1H), 1.88 (broad s, 1H). ^{13}C NMR (100 MHz, $CDCl_3$): δ 13.8, 13.9, 22.8, 28.5 (p, 20.1 Hz), 33.6, 49.5, 52.9, 60.0, 60.2, 65.3, 171.8, 173.6. IR (ATR): 2233-2131, 1728, 1612 cm^{-1}. HRMS: *m/z* calcd for $C_{12}H_{20}D_2O_4N$ (M + H): 246.3227: 246.1669.

(±)-7,7-Dideutero-1-oximinopyrrolizidine ((±)-7,7-[$^2H_2$]-10)

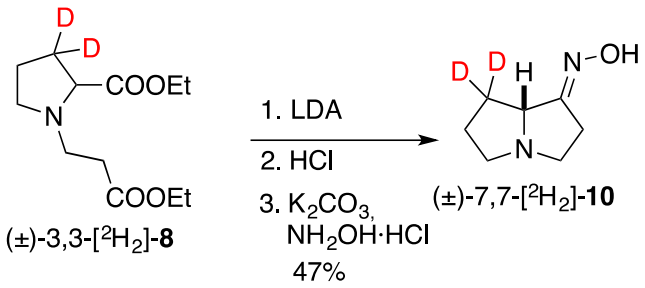

To the solution of diisopropylamine (2.18 mL, 21.5 mmol) in dry THF (85 mL) under nitrogen at –78 °C, n-BuLi (2.4 M in hexane) (7.5 mL) was added. The reaction mixture was allowed to react for 1 h. A solution of (±)-3,3-[$^2H_2$]-**8** (2.21 g, 8.9 mmol) in THF (43 mL) was prepared and added to the above reaction mixture dropwise. The reaction mixture was stirred at –78 °C for 18 h and then brought to RT. H_2O (30 mL) was added to the reaction mixture, and conc. HCl (30 mL) was added to it drop-by-drop at 0 ºC, followed by 1.5 h reflux. The reaction mixture was adjusted to pH 9 by adding saturated solution of K_2CO_3 in H_2O at 0 °C. $NH_4OH{\cdot}HCl$ (0.62 g, 8.9 mmol) was added to the reaction mixture, which was allowed to reflux for 2 h. The mixture was then stirred for 24 h. Solvent and water were evaporated, and the crude compound was extracted with CH_2Cl_2. The solvent was concentrated, and the remainder was poured onto a silica column and then eluted with CH_2Cl_2:CH_3OH:NH_4OH (8:2:0.2). Solvent was evaporated to yield (±)-7,7-[$^2H_2$]-**10** (0.6 g, 4.2 mmol, 47%) as a light brown powder and as an inseparable mixture of diastereomers. ^1H NMR (400 MHz, $CDCl_3$): δ 4.07 (s, 1H), 3.80 (s, 1H), 3.20 – 2.82 (m, 6H), 2.84 – 2.39 (m, 6H), 1.94 – 1.68 (m, 4H). ^2H NMR (61.5 MHz, $CDCl_3$): δ 2.29 (broad s, 1H), 2.21

(broad s, 1H), 1.88 (s, 1H), 1.75 (broad s, 1H). ^{13}C NMR (100 MHz, CD_3OD): δ (major) 26.2, 30.3 (m, 20 Hz), 30.9, 51.7, 54.4, 64.4, 166.2; δ (minor) 25.8, 30.2 (m, 20 Hz), 51.1, 54.2, 62.9, 165.8. IR (ATR): 3202, 2235-2125, 1842, 1675, 1509 cm^{-1}. HRMS: *m/z* calcd for $C_7H_{11}D_2N_2O$ (M + H): 143.1148: 143.1149.

(±)-1-*exo*-7,7-Dideuteroacetamidopyrrolizidine ((±)-7,7-[$^2H_2$]-AcAP)

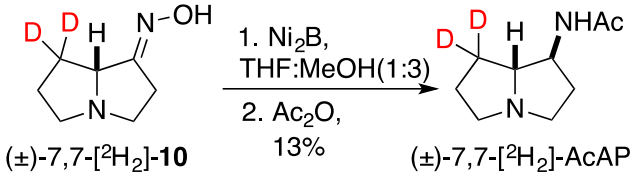

(±)-7,7-[$^2H_2$]-**10** (±)-7,7-[$^2H_2$]-AcAP

$NaBH_4$ (0.19 g, 5.0 mmol) was added portionwise to a solution of (±)-7,7-[$^2H_2$]-**10** (0.08 g, 0.5 mmol) and $NiCl_2$ (0.21 g, 1.6 mmol) in anhydrous MeOH:THF (3:1, 5 mL) at –60 C over a period of 2 h (Caution: gas evolution!). After complete addition, the resulting black slurry was allowed to warmed up to –30 °C and stirred at this temperature until no more starting material was detected by TLC (18 h). Then, the reaction mixture was warmed to room temperature, and Ac_2O (in excess) was added with vigorous stirring. The heterogeneous mixture was stirred for a further 4 h. Concentrated ammonium hydroxide (10 mL) was added with stirring, and the mixture was filtered through a short pad of Celite. The organic solvent was evaporated and extracted with DCM (3 times), and the combined organic layers were washed with brine (2 times), dried over anhydrous $MgSO_4$, and concentrated in vacuo. The crude product was purified by flash chromatography, eluting with CH_2Cl_2:CH_3OH:NH_4OH (6:4:0.2), to afford (±)-7,7-[$^2H_2$]-AcAP (13.2 mg, 0.078 mmol, 13%) as a gummy yellow solid. ^{1}H NMR (400 MHz, $CDCl_3$): δ 1.77 (m, 2H), 1.86

(dq, J_d = 12.1 Hz, J_t = 6.0 Hz, 1H), 1.99 (s, 3H), 2.21 (dp, J_d = 13.0 Hz, J_p= 6.6 Hz, 1H), 2.66 (qd, J_d = 6.7 Hz, J_q = 9.8 Hz, 2H), 3.08 (dt, J_d = 10.7 Hz, J_t = 6.4 Hz, 1H), 3.41-3.22 (m, 2H), 4.15 (dtd, J_d = 6.7 Hz, J_d= 8 Hz, J_t = 5.1 Hz, 1H), 6.3 (broad s, 1H). ^{2}H NMR (61.5 MHz, $CDCl_3$): δ 1.98 (broad s, 1H), 1.62 (broad s, 1H). ^{13}C NMR (100 MHz, $CDCl_3$): δ 23.5, 25.3, 30.0 (m, 20 Hz), 32.8, 53.4, 55.2, 55.37, 70.9, 170.2. IR (ATR): 3233, 2233 (weak), 1659, 1541 cm^{-1}. HRMS: *m/z* calcd for $C_9H_{15}D_2ON_2$ (M + H): 171.1461; found: 171.2597.

Chapter 6. What is the stereochemical course of C-H bond oxidation by LolO?

6.1. Introduction

We have now shown that LolO abstracts an H atom from C(2) of AcAP first and from C(7) second. It remains for us to elucidate the stereochemical course of the C–H bond abstractions. We know, of course, that the new C–O bonds at both C(2) and C(7) form on the endo face, but the C(2) radical that must precede C–O bond formation can be produced by abstraction of *either* the endo or the exo H atom from C(2), and likewise from C(7) (Scheme *6.1*). In this chapter, we describe how we determined the stereochemical course of H atom abstraction by LolO.

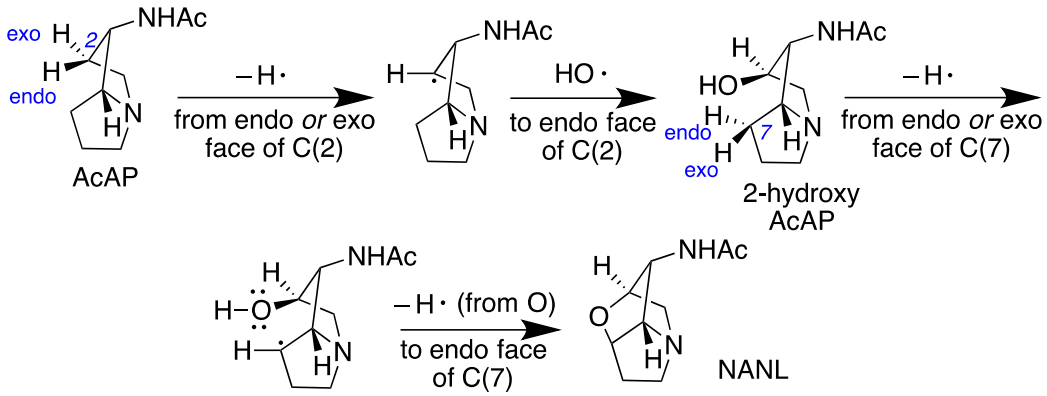

Scheme 6.1. Both exo and endo H atom abstraction in AcAP can allow for an endo bond to the O atom.

We decided to investigate this question by feeding stereospecifically deuterium-labeled precursors to loline-producing culture followed by GC–MS analysis of the extent of deuterium enrichment of the produced NFL. From our groups' previous work, we knew that C(3) of L-proline became C(7) of NFL (Scheme *6.2*).[12] With the reasonable assumption that the C(3) configuration of L-Pro would remain unchanged until the C–H

abstraction event, we expected that feeding *cis*-3-[^{2}H]-Pro would lead to the intermediate 7-*exo*-7-[^{2}H]-AcAP, whereas feeding *trans*-3-[^{2}H]-Pro would lead to the intermediate 7-*endo*-7-[^{2}H]-AcAP. Therefore, if LolO abstracted the endo H atom at C(7) of AcAP, then feeding *cis*-3-[^{2}H]-Pro would give 7-[^{2}H]-NFL, whereas feeding *trans*-3-[^{2}H]-Pro would give NFL with no D atoms incorporated. By contrast, if LolO abstracted the exo H atom at C(7) of AcAP, then feeding *cis*-3-[^{2}H]-Pro would give NFL with no D atoms incorporated, whereas feeding *trans*-3-[^{2}H]-Pro would give 7-[^{2}H]-NFL.

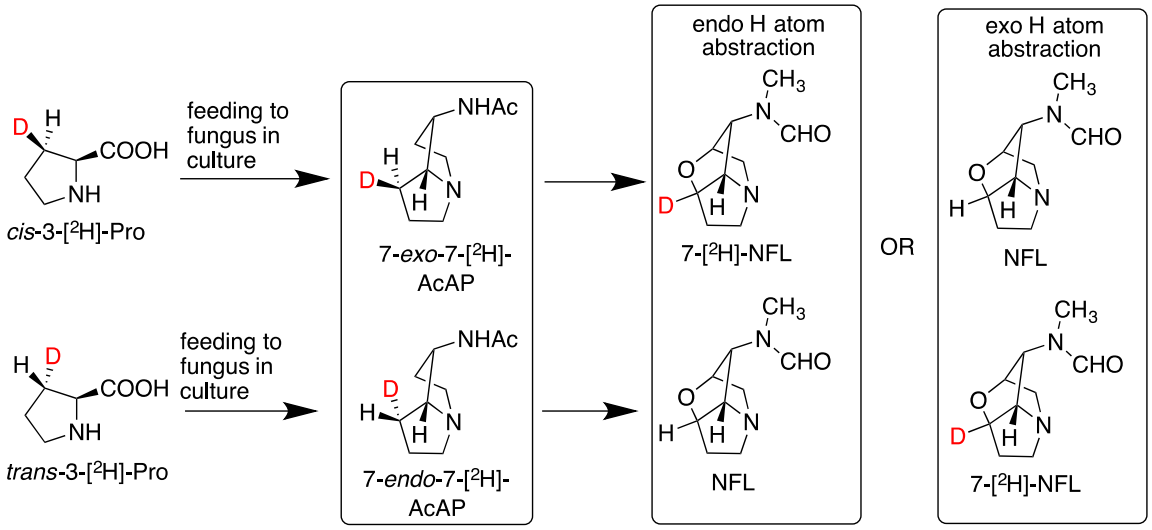

Scheme 6.2. Probing the stereochemistry of H atom abstraction from C(7) of AcAP using deuterium-labeled L-proline.

Similarly, from our groups' previous work, we knew that C(3) of L-Asp became C(2) of NFL (Scheme *6.3*).[12] If we assumed that the C(3) configuration of L-Asp remained unchanged until the C–H abstraction event, we expected that feeding (3*R*)-3-[^{2}H]-Asp would lead to the intermediate 2-*exo*-2-[^{2}H]-AcAP, whereas feeding (3*S*)-3-[^{2}H]-Asp would lead to the intermediate 2-*endo*-2-[^{2}H]-AcAP. Therefore, if LolO abstracted the

endo H atom at C(2) of AcAP, then feeding (3*R*)-3-[^{2}H]-Asp would give 2-[^{2}H]-NFL, whereas feeding (3*S*)-3-[^{2}H]-Asp would give NFL with no D atoms incorporated. By contrast, if LolO abstracted the exo H atom at C(2) of AcAP, then feeding (3*R*)-3-[^{2}H]-Asp would give NFL with no D atoms incorporated, whereas feeding (3*S*)-3-[^{2}H]-Asp would give 2-[^{2}H]-NFL.

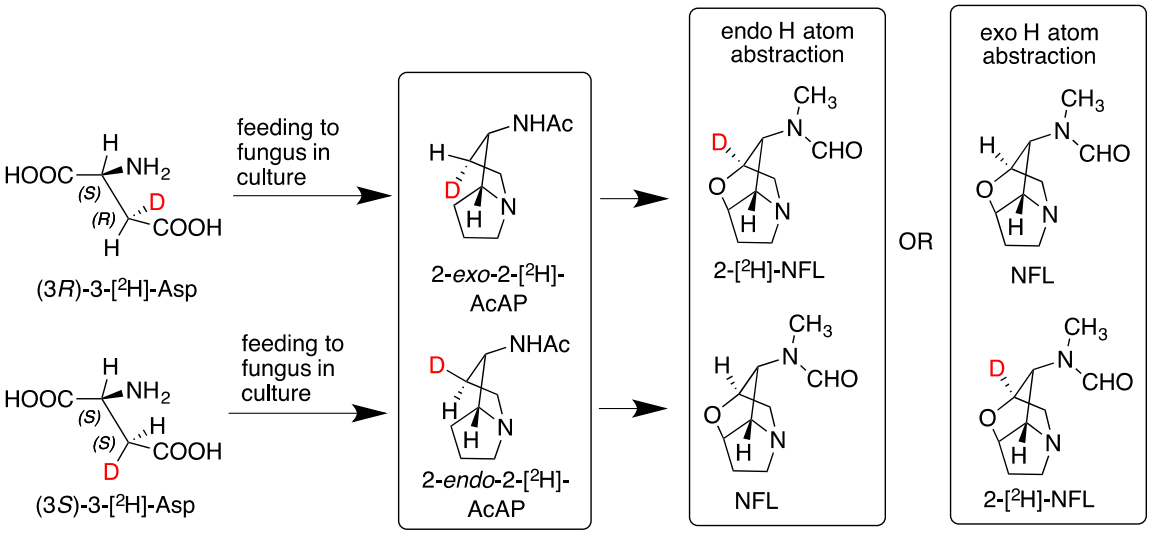

Scheme 6.3. Probing the stereochemistry of H atom abstraction from C(2) of AcAP using deuterium-labeled L-Asp.

We hypothesize that LolO abstracts the endo H atom from both C(2) and C(7). The Fe center in LolO almost certainly delivers the OH group to the endo face of C(2), so it is likely that AcAP coordinates to the Fe center on its endo face. It then seems likely that the abstraction of H atoms from both the C(2) and C(7) positions of AcAP occurs from the endo face due to the proximity of the Fe center to the endo face of AcAP.

6.2. Results and discussion

6.2.1. Synthesis of *cis*- and *trans*-3-[^{2}H]-Pro

In order to study the stereochemistry of H atom abstraction at C(7) of AcAP, I prepared regio- and stereospecifically deuterated prolines from *trans*-3-hydroxy-L-Pro (**28**). Following the literature procedure,[13] the N of proline derivative **28** was protected with a Boc group, and the product was converted to its *t*-butyl ester (Scheme *6.4*). The product **29** was then divided into two portions. One portion was tosylated, reduced with $NaBD_4$, and deprotected with 6 M HCl to give *cis*-3-[^{2}H]-Pro·HCl. The other portion of **29** was subjected to a Mitsunobu reaction to give **31**, which was then tosylated, reduced with $NaBD_4$, and deprotected with 6 M HCl to give *trans*-3-[^{2}H]-Pro·HCl.

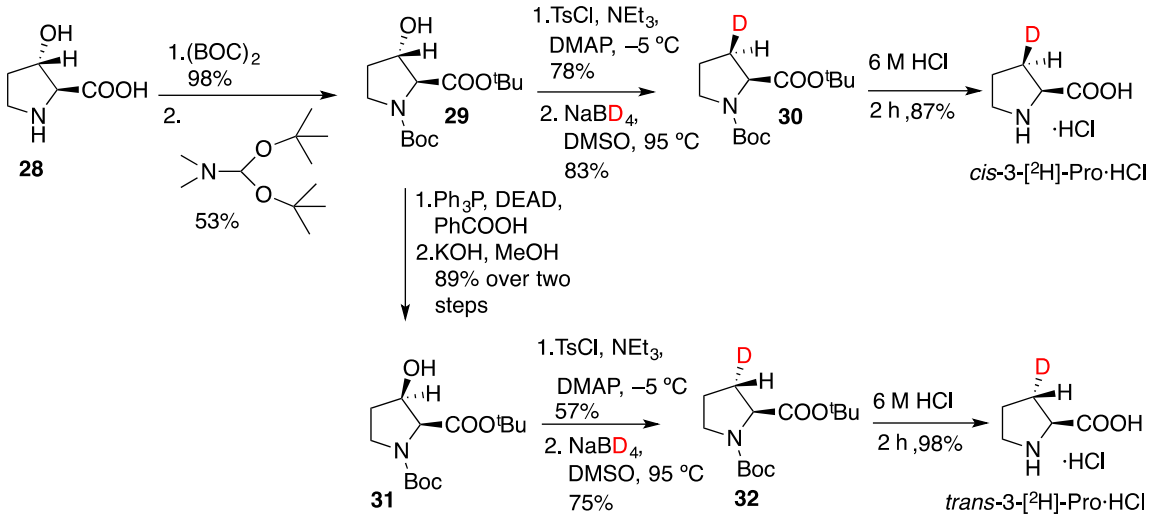

Scheme 6.4. Synthetic routes to *cis*- and *trans*-3-[^{2}H]-Pro·HCl.

6.2.2. Results of feeding experiments with *cis*- and *trans*-3-[2H]-Pro

Dr. Juan Pan fed *cis*-3-[^{2}H]-Pro·HCl and *trans*-3-[^{2}H]-Pro·HCl to cultures of *E. uncinata* at 4 mM final concentrations. I extracted the cultures with $CHCl_3$, and the products were analyzed by GC–MS (Figure *6.1*). The MS of undeuterated NFL has a

prominent peak at 183 amu that is assigned as an [M + H] peak, plus a small peak at 184 amu due to a heavier isotope of C, N, or O. Incorporation of one D atom into NFL results in an increase in the intensity of the peak at 184 amu (+1 amu). I found that NFL isolated from the culture which was fed with *cis*-3-[^{2}H]-Pro·HCl retained one D atom in NFL, as shown by the large increase in the intensity of the 184 amu peak (Figure *6.1*A), whereas the culture fed with *trans*-3-[^{2}H]-Pro·HCl showed only a small increase in the intensity of the 184 amu peak (Figure *6.1*B).

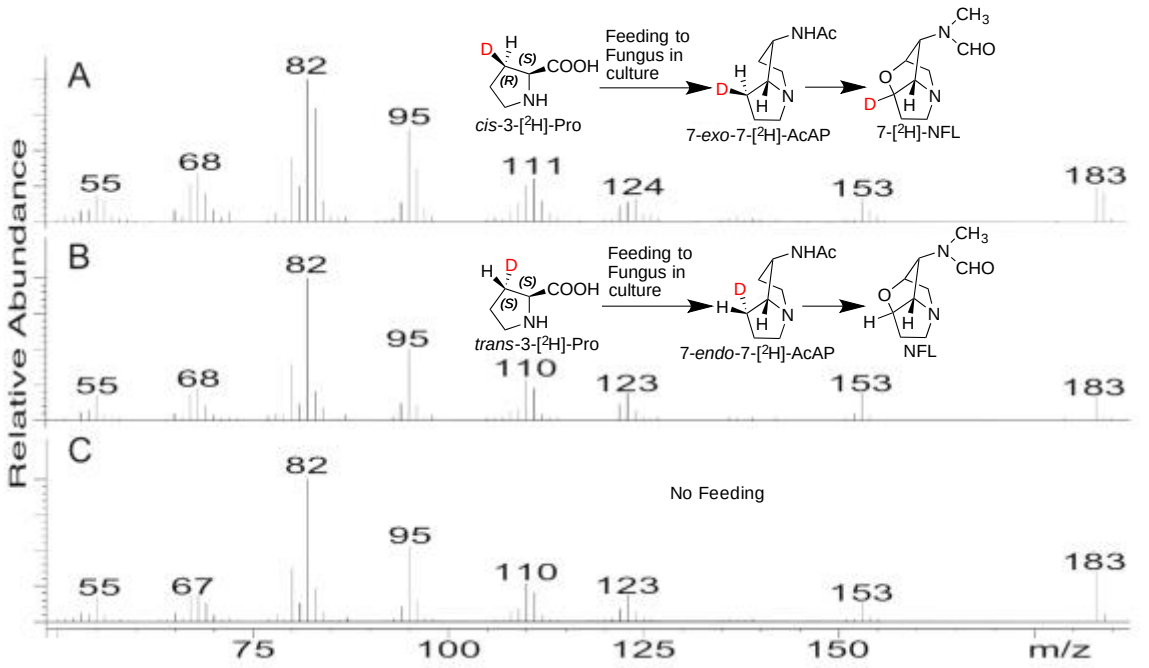

Figure 6.1. Mass spectrum showing NFL production in loline-producing culture from the feeding of, (A) *cis*-3-[2H]-Pro·HCl; (B) *trans*-3-[2H]-Pro·HCl; (C) without any feeding.

I calculated the extent of incorporation of D in the two cases to be 30.5% and 2.9%, respectively (Table *6.1*). In both cases, the incorporation of D was significantly different from control (Figure *6.1*C; p = 0.04 and 0.03, respectively). I attribute the much smaller 2.9% incorporation from the feeding of *trans*-3-[^{2}H]-Pro·HCl to contamination of this

isomer with some *cis*-3-[^{2}H]-Pro·HCl, as evident in the ^{1}H NMR spectrum of *trans*-3-[^{2}H]-Pro·HCl (Figure *6.2*).

Table 6.1. Relative deuterium incorporation from deuterated prolines in NFL. (a) Significantly different from control (p = 0.03); (b) significantly different from controls (p = 0.04).

Compounds	**Conc. (mM)**	**Amu shift (183 + 1)**	**% enrichment of 183 + 1 amu peak (mean ± SD)**
cis-3-[^{2}H]-Pro·HCl	4	+1	30.51 ± 2.26[(a)]
trans-3-[^{2}H]-Pro·HCl	4	+1	2.93 ± 0.27[(b)]

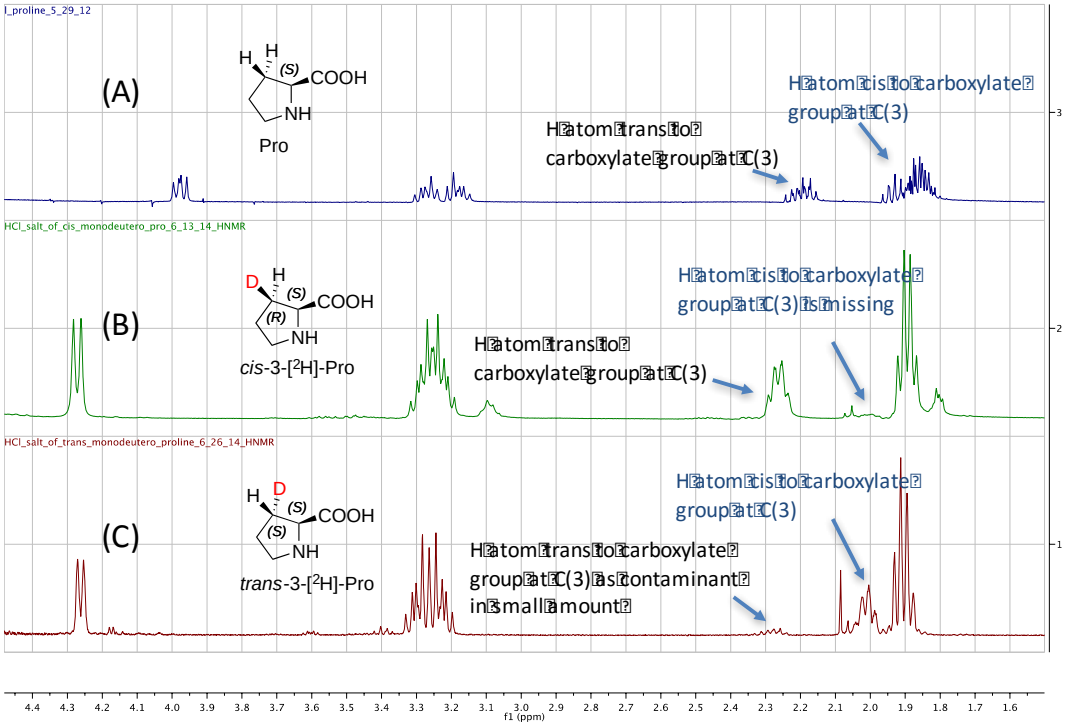

Figure 6.2. ^{1}H NMR spectra showing contamination of *trans*-3-[^{2}H]-Pro·HCl with *cis*-3-[^{2}H]-Pro·HCl. (A) Pro; (B) *cis*-3-[^{2}H]-Pro·HCl; (C) *trans*-3-[^{2}H]-Pro·HCl with small amount of *cis*-3-[^{2}H]-Pro·HCl as contaminant.

The strong incorporation of one D atom into the isolated NFL when fungal cultures were fed with *cis*-3-[^{2}H]-Pro·HCl suggested that LolO abstracted the endo hydrogen at the C(7) position of AcAP during ether bridge formation, a conclusion that was consistent with our original hypothesis (Scheme *6.5*).

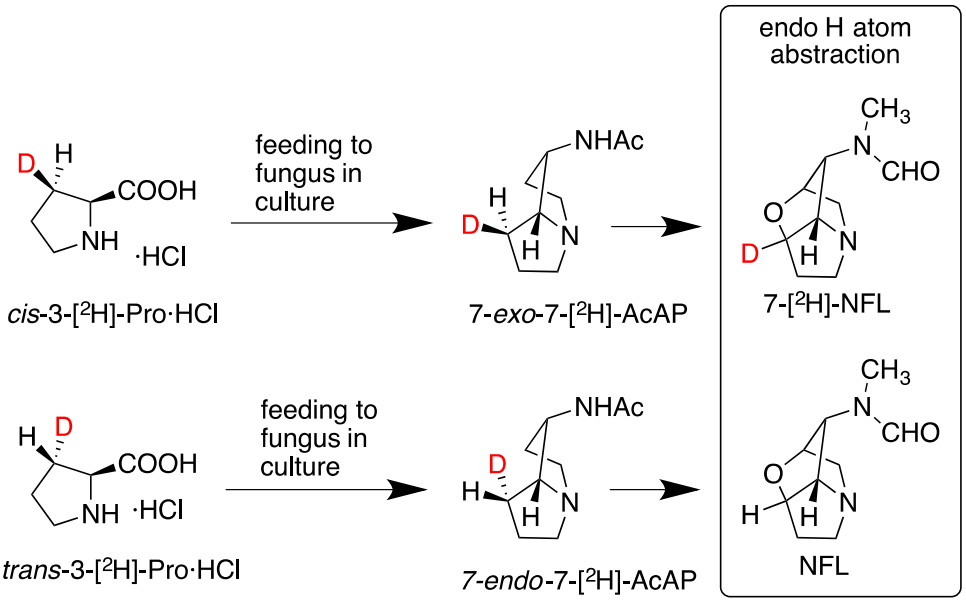

Scheme 6.5. Abstraction of endo H atom by LolO from C(7) of AcAP.

6.2.3. Synthesis of (3*R*)-(3-^{2}H)-Asp and (3*S*)-(2,3-$^{2}H_2$)-Asp

To ascertain whether LolO abstracted the endo or exo H atom at C(2) of AcAP, I prepared stereospecifically deuterium-labeled aspartic acids chemoenzymatically. I first cloned, expressed, and purified the aspartate aminotransferase B (AspB) enzyme by standard molecular biology tools.[47] (an AspB-expression plasmid was kindly contributed by Dr. M. Otzen from University of Groningen, Nijenborgh, Netherlands.) Following the

literature procedure,[48] I then added commercially available 2,3-[$^2H_2$]-fumaric acid to a solution of AspB in aqueous NH_4Cl, obtaining (3*S*)-2,3-[$^2H_2$]-Asp with 88.9% dideuteration as measured by HRMS. Similarly, I added undeuterated fumaric acid to a solution of AspB and ND_4Cl in D_2O, obtaining (3*R*)-3-[^2H]-Asp with 94.5% monodeuteration by HRMS (Scheme *6.6*). (In this latter case, I used AspB that I had purified in D_2O buffer, because AspB purified in H_2O buffer gave a much lower incorporation of D into the final product.)

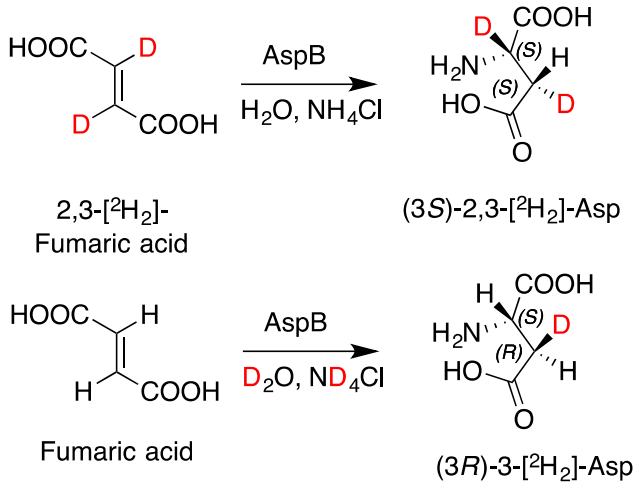

Scheme 6.6. Synthetic route to (3*R*)-3-[^2H]-and (3*S*)-2,3-[$^2H_2$]-Asp.

6.2.4. Possible complications due to deuterium at the C(2) position of (3*S*)-2,3-[$^2H_2$]-Asp

Due to the nature of our synthetic route to the (3*S*)-deuterated isotopomer of Asp, I could not avoid introducing deuterium into its C(2) position. Unfortunately, the incorporation of deuterium into the C(2) position led to complications in our ability to draw conclusions from certain experimental outcomes. Specifically, multiple PLP enzymes in the biosynthetic pathway might or might not exchange the C(2) D atom of (2*S*,3*S*)-2,3-

[$^2H_2$]-Asp for an H atom (Scheme *6.7*). If D–H exchange did not occur, then depending on whether the endo or exo H at C(2) of AcAP was abstracted, I would obtain either [^{2}H]-NFL or [$^2H_2$]-NFL. On the other hand, if D–H exchange did occur, I would obtain either undeuterated NFL or [^{2}H]-NFL. Hence, if I obtained [^{2}H]-NFL, then, without prior knowledge of whether the C(2) D atom of (2*S*,3*S*)-2,3-[$^2H_2$]-Asp was involved in exchange, it would have been difficult for us to determine whether LolO abstracted the endo or exo H atom at C(2) of AcAP. We would revisit this after feeding experiments.

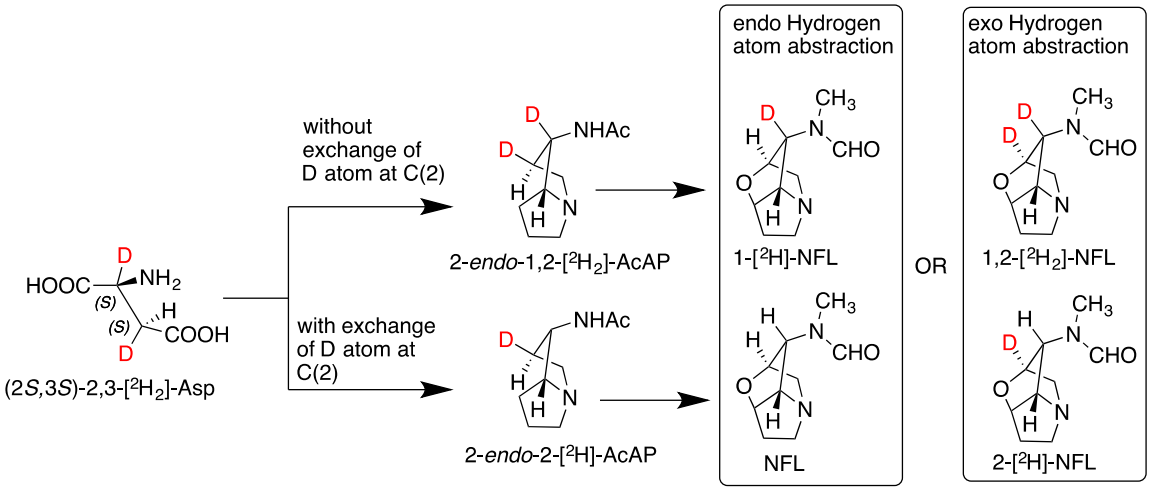

Scheme 6.7. Complications due to deuterium at C(2) position of (3*S*)-2,3-[$^2H_2$]-Asp.

6.2.5. Results of feeding experiments with (2*S*,3*S*)-3-[^{2}H]-Asp and (2*S*,3*S*)-2,3-[$^2H_2$]-Asp.

I fed (3*R*)-3-[^{2}H]- and (3*S*)-2,3-[$^2H_2$]-Asp to loline-producing cultures separately in triplicate. Table *6.2* shows the results of GC-MS analysis of the NFL obtained from the feedings. The feedings of (3*R*)-3-[^{2}H]-Asp gave NFL that was significantly more enriched in one D atom than unfed control. By contrast, the feeding of (3*S*)-2,3-[$^2H_2$]-Asp gave NFL

that was not significantly different from unfed control. The feeding of (3*S*)-2,3-[$^2H_2$]-Asp gave essentially no [$^2H_2$]-NFL. These results led us to conclude that, (1) the C(2) D atom was largely exchanged for H during the pathway leading up to AcAP, and (2) in support of our original hypothesis, the endo H atom at the C(2) position of AcAP was abstracted by LolO during ether bridge formation in the loline biosynthetic pathway (Scheme *6.10*).

Table 6.2. Relative deuterium incorporation from deuterated aspartic acids in NFL (a) Significantly different from control; (b) Not significantly different from control.

Compounds	**Conc. (mM)**	**Amu shift (M + *n*)**	**% enrichment of 183 + Z amu peak (mean ± SD)**	***p* value with respect to control**
(3*R*)-3-[^{2}H]-Asp	4	+1	4.1 ± 0.9	0.0029[(a)]
(3*S*)-2,3-[$^2H_2$]-Asp	4	+1	1.1 ± 0.4	0.9137[(b)]
(3*S*)-2,3-[$^2H_2$]-Asp	4	+2	0.2 ± 0.3	0.8139[(b)]

Earlier, I noted that our interpretation of the deuterated aspartic acids feeding results depended on the reasonable assumption that the C(2) configuration of Asp was not altered in the course of loline biosynthesis. Further reflection on the biosynthetic pathway, however, has revealed to us that this assumption is incorrect. I know that Pro and Hse (probably *O*-Ac-Hse) are the precursors to loline biosynthesis. We have previously shown that Pro and *O*-Ac-Hse combine through a γ-substitution reaction to give the diamino diacid *N*-(3-amino-3-carboxypropyl)proline (NACPP) (Scheme *1.5*), and circumstantial evidence suggests that LolC, a PLP enzyme, catalyzes this step.[15] The mechanism of PLP-catalyzed

γ-substitution reactions is as follows (Scheme *6.8*): temporary conversion of the α-amino acid of *O*-Ac-Hse to an α-imino acid, tautomerization to an enamine, and elimination of $^-$OAc to form an α,β-unsaturated iminium ion. A nucleophile then reacts with the α,β-unsaturated iminium ion to produce a new enamine, which is then restored to the initial α-amino acid. During the formation of first enamine, LolC removes H^+ from C(3) of Hse, the very same position that I was deuterating in Asp in order to probe which H atom (exo or endo) LolO abstracted from C(2) of AcAP.

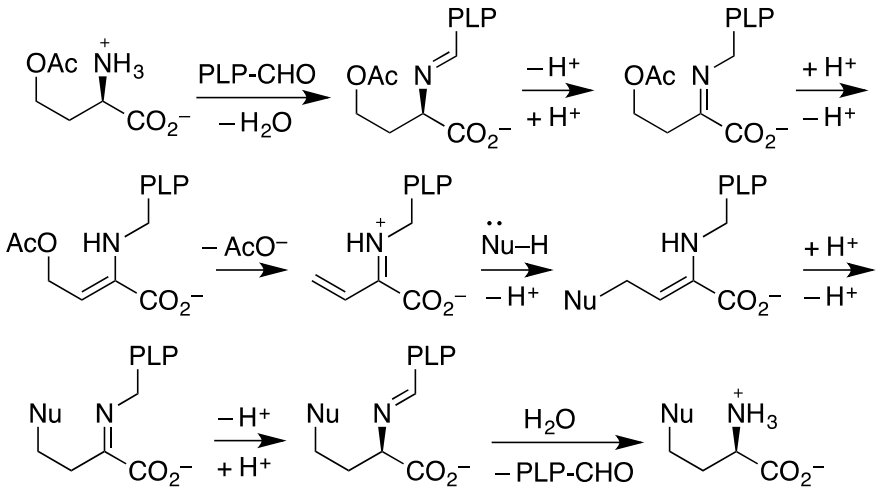

Scheme 6.8. Proposed mechanism by which LolC and O-acetylhomoserine (thiol) lyase catalyze γ-substitution reactions.

If LolC is catalyzing the combination of Pro and *O*-Ac-Hse through the above mechanism, then the stereochemistry and the extent of D labelling installed at C(3) of (3R)- and (3S)-3-[^{2}H]-Asp is prone to change in numerous ways (Scheme *6.9*). LolC showed similarity to the γ-type PLP enzyme cystathionine γ-synthase.[15] The mechanism proposed for the cystathionine γ-synthase on the basis of crystal structure have same amino acid removes and restores the C(3) H^+.[49] If LolC has similar active site as cystathionine γ-synthase, then we can assume that LolC will restore H^+ or D^+ to the same face of C(3)

from which LolC removes it. Another complication though, is that the enzyme might restore the same atom that it removed, or it might restore a different one. If the enzyme removes the pro-R H^+ or D^+ and replaces it with a different H^+ (Scheme *6.9*A), it would convert the R isotopolog to undeuterated, and it would preserve the configuration of the S isotopolog. Similarly, if the enzyme removes the pro-S H^+ or D^+ and replaces it with a different H^+ (Scheme *6.9*B), it would preserve the configuration of the R isotopolog, and it would convert the S isotopolog to undeuterated.

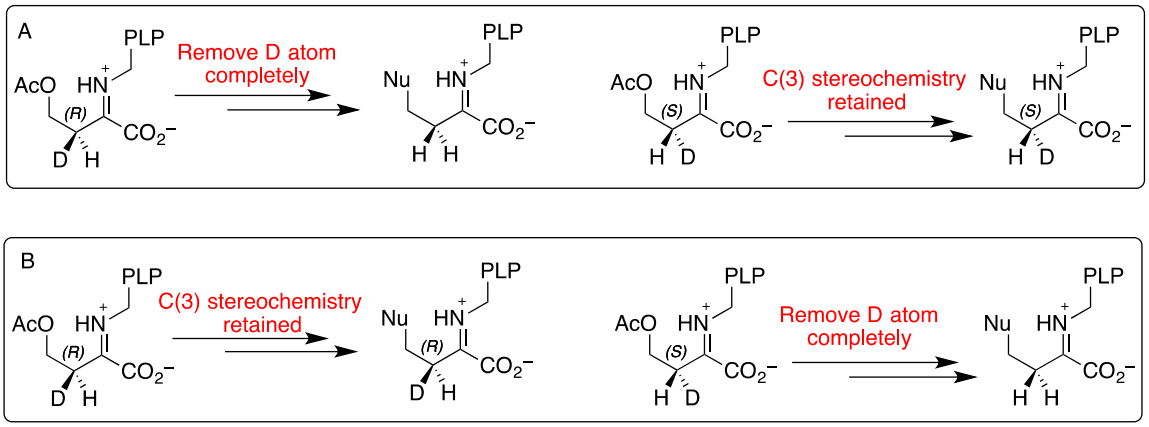

Scheme 6.9. Effect of LolC on D atom content and configuration of Asps deuterated at C(3). (A) LolC removes pro-R H/D, restores a different H^+ to same face.; (B): LolC removes pro-S H/D, restores a different H^+ to same face.

With this analysis, we could predict the effect of six different scenarios on the extent of deuteration of the NFL that we would obtain upon feeding our two Asp isotopologs (Table *6.3*). After matching the predicted results to the actual results from the feeding experiments (Table *6.2*), we hold to our original conclusion that LolO abstracts the endo H atom from C(2) (Scheme *6.10*).

Table 6.3 Possible outcomes of feeding experiments of (3R)- and (3S)-3-[^{2}H]-Asp after LolC and LolO reactions. The first and third cells match the observed feeding results. (d_1 denotes monodeuterated and d_0 denotes undeuterated)

3-[^{2}H]-Asp configuration at C3	H or D that LolC removes from C3	LolC restores on C3	Asp C3 after LolC	NFL from endo H abstraction	NFL from exo H abstraction
R	pro-R or pro-S	same atom	R	d_1	d_0
S	pro-R or pro-S	same atom	S	d_0	d_1
R	pro-R	different H^+	none	d_0	d_0
S	pro-R	different H^+	S	d_0	d_1
R	pro-S	different H^+	R	d_1	d_0
S	pro-S	different H^+	none	d_0	d_0

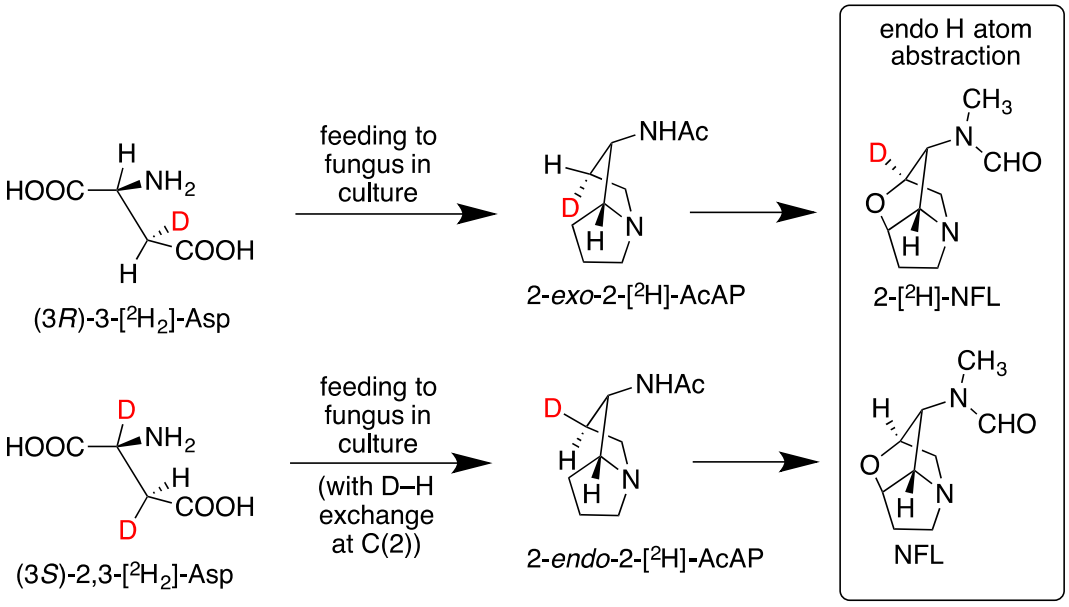

Scheme 6.10. Abstraction of endo hydrogen atom by LolO from C(2) of AcAP.

6.3. Conclusion

Our experiments support the hypotheses that LolO abstracts the endo H atoms from the C(2) and C(7) positions of AcAP. This information is consistent with a mechanism where AcAP binds to LolO in such a way that the catalytic Fe center resides on the endo face of AcAP, and the Fe center is intimately involved in both the C–H abstractions and the C–O bond formations leading to NANL.

6.4. Experimental Section

6.4.1. Synthesis of *cis*- and *trans*-3-[^{2}H]-L-prolines

(2*S*,3*S*)-*N*-*tert*-Butoxycarbonyl-*trans*-3-hydroxyproline (29)

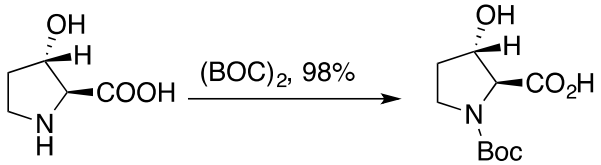

28 **29**

A 10% aqueous solution of NaOH (2.2 mL) was added to alcohol **28** (1.0 g, 7.6 mmol) suspended in a mixture of THF/H_2O (2:1, 10 mL). Di-*tert*-butyl dicarbonate (1.7 g, 7.6 mmol) was added, and the reaction mixture was stirred for 21 h at RT. The organic solvent was evaporated, and the mixture pH was adjusted to 2 by addition of 10% aqueous $KHSO_4$ solution. The mixture was extracted with EtOAc, washed with brine, dried with $MgSO_4$, and evaporated to give crude **29** (1.7 g, 7.5 mmol, 98% yield) as a yellow viscous oil. ^{1}H NMR (400 MHz, $CDCl_3$) δ 1.43 (s, 9H; major), 1.47 (s, 9H; minor), 1.82–1.93 (m, 2H; minor), 1.98–2.10 (m, 2H; major), 3.46–3.62 (m, 4H), 4.10 (br, 1H; major), 4.17 (br, 1H; minor), 4.37-4.41 (m, 1H). ^{13}C NMR (100 MHz, $CDCl_3$) δ (major) 28.7, 33.0, 45.5, 69.6, 76.0, 81.6, 156.2, 174.5; δ (minor) 28.9, 33.6, 45.9, 69.3, 75.2, 81.5, 156.6, 174.2. IR

(ATR): 3283, 1741, 1653 cm^{-1}.

***tert*-Butyl (2*S*,3*S*)-*N*-*tert*-butoxycarbonyl-*trans*-3-hydroxy-L-proline (29)**

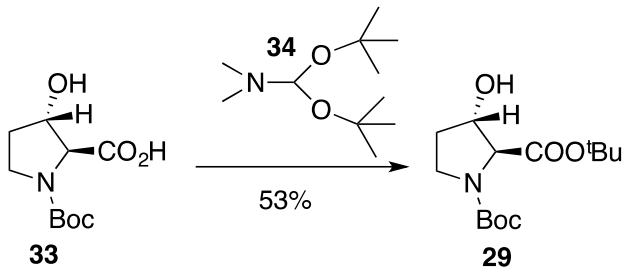

Neat **34** (5.8 mL) was added to **33** (1.54 g, 6.67 mmol), and the mixture was stirred for 12 h at 80 ºC under nitrogen. The solution was cooled to RT, and H_2O (5.8 mL) was added. The mixture was stirred for 22 h at RT. Saturated aqueous $NaHCO_3$ (15 mL) was added, and the mixture was extracted with Et_2O. The organic layer was washed with water and brine and dried with $MgSO_4$. The crude compound was purified by flash chromatography (5% MeOH in CH_2Cl_2) to give **29** (1.02 g, 3.55 mmol, 53% yield) as a yellow viscous oil. ^1H NMR (400 MHz, $CDCl_3$) δ 1.35 (s, 9H; major), 1.37 (s, 9H; minor), 1.38 (s, 9H; minor), 1.39 (s, 9H; major), 1.78–2.04 (m, 2H), 2.8 (br s, 1H; minor), 2.9 (br s, 1H; major), 3.44–3.60 (m, 2 H), 4.02 (br s, 1H; major), 4.08 (br s, 1H; minor), 4.26–4.35 (m, 1H). ^{13}C NMR (100 MHz, $CDCl_3$) δ (major) 27.8, 31.8, 44.2, 68.7, 74.7, 79.7, 81.2, 154.2, 170.3; δ (minor) 28.2, 32.4, 44.5, 68.6, 73.7, 79.5, 81.4, 154.5, 170.2; IR (ATR): 3454, 3357, 1735, 1660 cm^{-1}. HRMS: *m/z* calcd for $C_{14}H_{26}NO_5$ (M + H): 288.3635: 288.1807.

***tert*-Butyl (2*S*,3*R*)-*N*- *tert*-Butoxycarbonyl-*cis*-3-deuteroprolinate (30)**

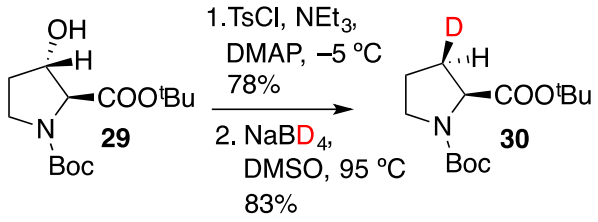

Triethylamine (1.45 mL, 10.4 mmol) was added to a mixture of alcohol **29** (0.3 g, 1 mmol) and DMAP (0.13 g, 1.0 mmol) in dry CH_2Cl_2 (20 mL). TsCl (0.23 g, 1.2 mmol) was added in portions over 1 h at 0 °C, and the reaction mixture was stirred at 0 °C for 54 h. A saturated solution of NH_4Cl was then added at 0 °C, and the aqueous layer was extracted with CH_2Cl_2. The combined organic extracts were washed with brine, dried with $MgSO_4$, and evaporated. Silica gel chromatography (50% EtOAc in petroleum ether) afforded the tosylate (0.36 g, 78% yield). The tosylate (0.36 g, 0.82 mmol) was dissolved in dry DMSO (12 mL), and $NaBD_4$ (0.21 g, 4.9 mmol) was added. The reaction mixture was heated to 95 °C under nitrogen for 8 h. It was cooled and diluted with brine (effervescence), and the aqueous phase was extracted with Et_2O. The combined organic layers were dried over $MgSO_4$, and the solvent was evaporated. Flash chromatography (40% EtOAc in petroleum ether) afforded **30** (0.185 g, 0.68 mmol, 83% yield) as a white gum. ^{1}H NMR (400 MHz, $CDCl_3$) δ 1.38 (s, 9H), 1.40 (s, 9H), 1.68–1.94 (m, 2H), 2.01–2.18 (m, 1H), 3.12-3.55 (m, 2H), 4.04 (d, 8.6 Hz, 1H; major), 4.12 (d, 8.6 Hz, 1H; minor). ^{13}C NMR (100 MHz, $CDCl_3$) δ (major) 23.4, 28.1, 28.5, 30.7 (t, 20.81 Hz), 46.4, 59.8, 79.7, 80.9, 154.1, 172.4; δ (minor) 23.2, 28.1, 28.5, 46.6, 59.7, 79.5, 154.4, 172.3. ^{2}H NMR (61.5 MHz, $CDCl_3$): δ 1.89 (broad s, 1H). IR (neat): 1739, 1701 cm^{-1}. HRMS [M]+: *m/z* calcd for $C_{17}H_{21}D_2NO_4$: 307.1747: 307.1744.

***cis*-3-Deuteroproline·hydrochloride (*cis*-3-[^{2}H]-Pro·HCl)**

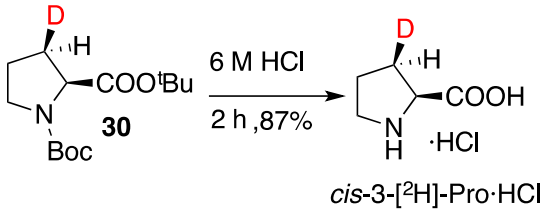

Compound **30** (185 mg, 0.680 mmol) was dissolved in 6 M HCl (7 mL), and the reaction mixture was stirred for 2 h at RT. The water was evaporated to give *cis*-3-[^{2}H]-Pro·HCl (79 mg, 0.52 mmol, 87%) as a brown gum. ^{1}H NMR (400 MHz, D_2O) δ 2.01–2.12 (q, 7.1 Hz, 2H), 2.35-2.49 (m, 1H), 3.42 (qt, J_t = 7.3 Hz, J_q = 11.7 Hz, 2H), 4.43 (d, 8.8 Hz, 1H). ^{13}C NMR (100 MHz, D_2O) δ 25.8, 30.5 (t, 20.4 Hz), 48.8, 62.1, 174.4. ^{2}H NMR (61.5 MHz, D_2O): δ 2.14 (broad s, 1H), 8.38 (broad s, 1H), 8.91 (broad s, 1H). IR (ATR): 3398, 2464, 1915, 1725 cm^{-1}. EI-MS: Positive ion 116.9 amu ([M + H]), negative ion 35.1 amu ([Cl]).

***tert*-Butyl (2*S*,3*R*)-*N*-*tert*-butoxycarbonyl-*cis*-3-hydroxyproline (31)**

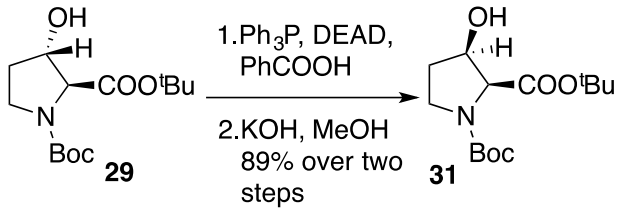

DEAD (848 mg, 4.87 mmol) in dry THF (8 mL) was added to a solution of triphenylphosphine (1.28 g, 4.87 mmol), benzoic acid (0.59 g, 4.9 mmol), and **29** (700 mg, 2.44 mmol) in dry THF (20 mL) at 0 ºC under nitrogen. The reaction mixture was stirred for 5 min at 0 ºC, and then for 22 h at RT. The solvent was evaporated, the residue was suspended in methanolic KOH solution (1.0 M, 43 mL) at 0 ºC, and the mixture was stirred

for 30 min. The solvent was evaporated, and the residue was partitioned between EtOAc and water. The organic layer was washed with brine, dried with $MgSO_4$, and evaporated. Flash chromatography (30% acetone in petroleum ether) afforded **31** (624 mg, 2.17 mmol, 89% over two steps) as a white solid. ^{1}H NMR (400 MHz, $CDCl_3$) δ 1.35 (s, 9H; major), 1.37 (s, 9H; minor), 1.39 (s, 9H; minor), 1.40 (s, 9H; major), 1.86–2.06 (m, 2H), 3.23–3.41 (m, 1H), 3.44–3.61 (m, 1H), 4.12 (d, 7.0 Hz, 1H; major), 4.15 (d, 7.0 Hz, 1H; minor), 4.30–4.40 (p, 6.6 Hz, 1H). ^{13}C NMR (100 MHz, $CDCl_3$) δ (major) 28.0, 28.1, 31.7, 43.6, 64.0, 71.9, 79.7, 81.1, 154.0, 169.5; δ (minor) 27.9, 28.2, 32.2, 44.0, 63.8, 71.0, 79.5, 81.2, 154.2, 169.6. IR (ATR): 3240, 2162, 1740, 1693 cm^{-1}. HRMS: *m/z* calcd for $C_{14}H_{26}NO_5$ (M + H): 288.3635: 288.1807.

tert-Butyl (2_S_,3_S_)-_N_-_tert_-butoxycarbonyl-_trans_-3-deuteroprolinate (32)

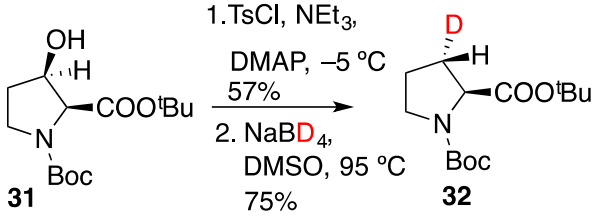

Triethylamine (3.0 mL, 22 mmol) was added to a mixture of alcohol **31** (624 mg, 2.17 mmol) and DMAP (0.265 g, 2.17 mmol) in dry CH_2Cl_2 (40 mL). TsCl (0.50 g, 2.6 mmol) was added in portions over 1 h at 0 ºC, and the reaction mixture was stirred at 0 ºC for 54 h. A saturated solution of NH_4Cl was added at 0 ºC, and the aqueous layer was extracted with CH_2Cl_2. The combined organic extracts were washed with brine, dried with $MgSO_4$, and evaporated. Silica gel chromatography (50% EtOAc in petroleum ether) afforded the tosylate (959 mg, 2.17 mmol, 57% yield). The tosylate (549 mg, 1.24 mmol) was dissolved

in dry DMSO (20 mL), and $NaBD_4$ (260 mg, 6.22 mmol) was added to it. The reaction mixture was heated to 95 ºC under nitrogen for 8 h. It was cooled and diluted with brine (effervescence), and the aqueous phase was extracted with Et_2O. The combined organic layers were dried over $MgSO_4$, and the solvent was evaporated. Flash chromatography (40% EtOAc in petroleum ether) afforded **32** (256 mg, 0.941 mmol 75%) as a white gum. ^{1}H NMR (400 MHz, $CDCl_3$) δ 1.36 (s, 9H), 1.39 (s, 9H), 1.68–1.92 (m, 3H), 2.01–2.18 (m, 1H), 3.19-3.55 (m, 2H), 4.03 (s, 1H; major), 4.11 (s, 1H; minor). ^{13}C NMR (100 MHz, $CDCl_3$) δ (major) 23.4, 28.1, 28.5, 30.7 (t, 20.3 Hz), 46.4, 59.7, 79.7, 80.9, 154.1, 172.4; δ (minor) 24.2, 28.1, 28.5, 29.7 (t, 20.7 Hz), 46.6, 59.7, 79.5, 154.4, 172.4. ^{2}H NMR (61.5 MHz, $CDCl_3$): δ 2.14 (broad s, 1H); IR (neat): 1738, 1689 cm^{-1}. HRMS [M]+: *m/z* calcd for $C_{17}H_{21}D_2NO_4$: 307.1747: 307.1744.

trans-3-Deuteroproline hydrochloride (_trans_-3-[^{2}H]-Pro·HCl)

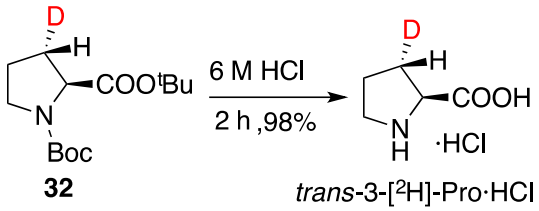

Compound **32** (256 mg, 0.340 mmol) was dissolved in 6 M HCl (7.5 mL), and the reaction mixture was stirred for 2 h at RT. The water was evaporated to give *trans*-3-[^{2}H]-Pro·HCl (107 mg, 0.704 mol, 98%) as a brown gum. ^{1}H NMR (400 MHz, D_2O) δ 2.00–2.25 (m, 3H), 3.36–3.53 (m, 2 H), 4.44 (d, 7.0 Hz, 1H). ^{13}C NMR (100 MHz, D_2O) δ 25.8, 30.6 (t, 22 Hz), 48.7, 62.1, 174.5. ^{2}H NMR (61.5 MHz, D_2O): δ 2.39 (broad s, 1H), 8.35 (broad s, 1H), 8.88 (broad s, 1H). IR (ATR): 3355, 2165-2066, 1736 cm^{-1}. EI-MS: Positive ion 116.9

amu ([M + H]), negative ion 35.1 amu ([Cl]).

6.4.2. Transformation, expression and purification of AspB-His_6 enzyme

The procedure for transformation, expression and purification of AspB-His_6 was performed as reported by B. Feringa, D. B. Janssen, G. J. Poelarends et al. with modification.[47]

6.4.2.1. Transformation and expression

The AspB-His_6 plasmid (with pBAD expression system) was transformed into Top10 cells, plated on a LB plate with ampicillin antibiotics, and incubated overnight at 37 ºC. A colony of Top10 cells containing AspB-His_6 plasmid was collected using a pipette tip and used to inoculate 5 mL LB medium (with ampicillin) in a 14 mL Falcon tube with loose cap. (We used 100 μL of ampicillin (100 mg/ml) for 100 mL LB.) The mixture was incubated in a shaker overnight at 37 ºC at 180 rpm. The tube was removed from incubator and poured into 500 mL LB with ampicillin and incubated at 37 ºC, 180 rpm. Optical density at 600 nm with UV/Vis was measured until it reached 0.7-0.8. Thereafter, the culture was induced with sterile arabinose solution (final concentration 0.08%) and incubated in a shaker overnight at 37 ºC at 180 rpm. The cells were centrifuged at 4000 rpm and 4 ºC for 15 min using a JA-25-50 rotor. The LB was decanted, and the cell pellet was transferred into a 50 mL Falcon tube and suspended in lysis buffer (50 mM NaH_2PO_4, 300 mM NaCl, 10 mM imidazole, pH 8.0) in an ice bath. The cells were disrupted by sonicating in Branson 250 microtip for 3 × 1 min with 3 min rest in between each cycle (60 W output). The lysate was centrifuged for 30 min at 17,000 g at 4 ºC using JA-25-50 rotor to remove cell debris. The protein was in the supernatant, which was collected into a 15 mL tube.

6.4.2.2. Purification with Ni NTA agarose

All the steps in the AspB-His_6 purification were done at 4 °C. The Ni NTA agarose solution (4 fractions of 1 mL) was equilibrated 3 times with lysis buffer. The 1 mL lysate solution was added to each fraction and incubated at 4 °C for 30 min under rotation in an end-over-end rotor. The column was washed three times with buffer A (50 mM NaH_2PO_4, 300 mM NaCl, 20 mM imidazole, pH 8.0; 0.5 mL/column). The AspB-His_6 protein was eluted from the column by using buffer B (50 mM NaH_2PO_4, 300 mM NaCl, 250 mM imidazole, pH 8.0; 0.25 mL/column). The purified protein was passed through PD-10 column using 50 mM equilibrating phosphate buffer (pH 8). The fractions were concentrated in a centrifugal concentrator with 30 kDa molecular weight cut-off (Pall Corporation, Port Washington, NY), and the absorbance of the protein was measured at 280 nm. The protein was diluted with sterile 10% glycerol and stored at –80 ºC until further use.

6.4.3. Synthesis of deuterium-labeled aspartic acids

(2*S*,3*S*)-2,3-Dideutero-L-aspartic acid ((2*S*,3*S*)-2,3-[$^2H_2$]-Asp)

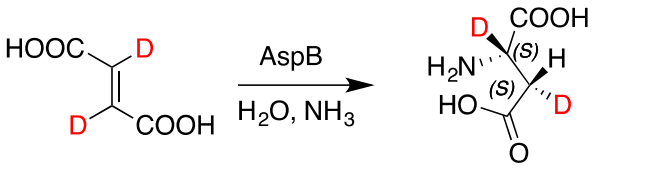

2,3-[$^2H_2$]-Fumaric acid

(2*S*,3*S*)-2,3-[$^2H_2$]-Asp

2,3-Dideuterofumaric acid (0.50 g, 4.2 mmol) was suspended in water (4 mL), the pH was adjusted to 9 with aqueous NH_4OH, and $MgCl_2 \cdot 6H_2O$ (0.516 mg, 2.54 mmol) and KCl

(44 mg, 1.1 mmol) were added. The pH was again adjusted to 9 with aqueous ammonia hydroxide, and AspB enzyme was added. The reaction mixture was incubated at 25 °C for 72 h. The solution was heated at 100 °C for 2 min and then filtered through Celite. The filtrate pH was reduced to 1 with 12 M HCl and extracted with Et_2O (2 times). The aqueous layer was adjusted to pH 4, and EtOH was added to precipitate the aspartic acid. Filtration gave (2*S*,3*S*)-2,3-[$^2H_2$]-Asp as a white solid (0.41 g, 3.0 mmol, 68%). ^{1}H NMR (400 MHz, D_2O) δ 3.10 (s, 1H). ^{2}H NMR (61.5 MHz, D_2O): δ 2.14 (broad s, 1H), 2.41 (broad s, 1H). ^{13}C NMR (100 MHz, D_2O) δ 34.5 (t, 20 Hz), 50.7 (t, 21.4 Hz), 173.0, 174.6. IR (ATR): 2165-2076, 1685, 1639 cm^{-1}. HRMS: *m/z* calcd for $C_4H_6D_2NO_4$ (M + H): 136.1227: 136.0575.

(3*R*)-3-deutero-L-aspartic acid ((3*R*)-3-[^{2}H]-Asp)

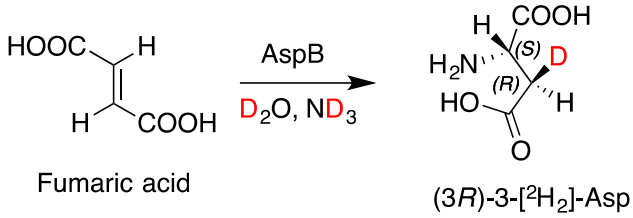

Fumaric acid (3*R*)-3-[$^2H_2$]-Asp

Fumaric acid (0.5.0 g, 4.3 mmol) was suspended in D_2O (20 mL), the pH was adjusted to 9 with ND_4OH in D_2O, and $MgCl_2.6H_2O$ (525 mg, 2.58 mmol) and KCl (44.7 mg, 1.15 mmol) were added. The pH was again adjusted to 9 with ND_4OH in D_2O, and AspB enzyme (purified in D_2O buffer) was added. The reaction mixture was incubated at 25 °C for 72 h. The solution was heated to 100 °C for 2 min and then filtered through Celite. The filtrate pH was reduced to 1 with 12 M HCl and extracted with Et_2O (2 times). The aqueous layer was adjusted to pH 4, and EtOH was added to precipitate the aspartic acid. Filtration

gave (3*R*)-3-[^{2}H]-Asp as white solid (213 mg, 1.59 mmol, 48%). ^{1}H NMR (400 MHz, D_2O) δ 2.94 (d, 7.5 Hz, 1H), 4.06 (d, 7.58 Hz, 1H). ^{2}H NMR (61.5 MHz, D_2O): δ 2.86 (broad s, 1H). ^{13}C NMR (100 MHz, D_2O) δ 34.5 (t, 20.2 Hz), 50.8, 173.0, 174.6. IR (ATR): 2231-2078, 1684, 1639 cm^{-1}. HRMS: *m/z* calcd for $C_4H_7DNO_4$ (M + H): 135.1166: 135.0512.

6.4.4. Fungal isolation from infected plant (e167)

The procedure for fungal (*Neotyphodium uncinatum*) isolation was same as reported in our groups' previous work.[11] Leaf blades from the grasses (number 167 from the plant collection) were collected from the greenhouse. They were cleaned and washed three times with autoclaved water in a 50 mL Falcon tube to remove any soil. They were sterilized by washing with 95% ethanol for 10 sec, followed by rinsing with autoclaved water. They were soaked in 50% bleach for 30 min, with shaking every 10 min. The bleach was slowly poured into the waste container, and each tube was washed three times with autoclaved water. The leaf blades were cut into 2-mm sections and plated on PDA plates with penicillin (350 uL) and streptomycin (350 uL) using sterilized forceps. They were incubated at 22 ºC for two weeks with frequent checking for unknown growth. After 2 weeks, fungal mycelium was removed with a sterile blade, homogenized in sterile water with a sterile stick, and drop-inoculated on an antibiotic-free PDA plate. In order to have fresh fungus, it was subcultured every 7-10 days.

6.4.5. Preparation of minimal media for the culture of fungus

Minimal media was prepared as reported in our groups' previous work.[11] A basal salt solution of pH 5.5 was made by mixing K_2HPO_4 (1.369 g) and KH_2PO_4 (4.083 g) in 100 mL of Milli-Q water. MOPS (5.856 g) was then added, the pH was adjusted to 5.5 with NaOH, and the solution was autoclaved. $MgSO_4$ (2mM, 0.493 g) was dissolved in 100 mL of Milli-Q water and autoclaved separately to prevent precipitation of salts. A solution of thiamine (0.6 mL of 0.6 mM) and a solution of 1 mL of trace elements to give 3.6 mM H_3BO_3, 1 mM $CuSO_4$, 0.7 mM KI, 0.8 mM FeNa- ethylenediaminetetraacetic acid, 1 mM $MnSO_4$, 0.5 mM $NaMoO_4$, and 0.4 mM $ZnSO_4$ was added to 116.7 mL solution of sucrose (20 mM, 6.846 g) and urea (15 mM, 0.900 g) in Milli-Q water. This solution was filtered sterilely. Basal salts at pH 5.5 and $MgSO_4$ were mixed together and added to the sterile solution of thiamine, trace elements, sucrose, and urea. The volume was made to 1 L by adding autoclaved Milli-Q water. The final concentration of the phosphate buffer and MOPS were 30 mM.

6.4.6. Feeding deuterated Asp to fungal culture and sampling from cultures

Fungal culture in minimal media was prepared as reported in our groups' previous work.[13] The fungal mycelium was removed with a sterile blade from the PDA plate and homogenized in sterile water using a sterile stick. The fungal inoculum (250 uL/plate) was added into the 15 mL minimal media in 18 polystyrene petri plates (60 × 15 mm). The cultures were incubated in rotary shaker at 22 ºC at 70 rpm. Sterile solutions of (2*S*,3*S*)-3-[^{2}H]-Asp, (2*S*,3*S*)-2,3-[$^2H_2$]-Asp, and (2*S*)-2,2,3-[$^2H_3$]-Asp were prepared in Milli-Q water and fed to loline-producing cultures separately in triplicate on the 6th day of growth. The cultures (1.7 mL) were harvested on the 16th day and lyophilized. The lyophilized

samples were basified using NaOH (1 M, 100 μL) and diluted using $CHCl_3$ (1 mL). The mixture was vortexed, shaked at room temperature at 130 rpm for 1 h, and centrifuged at 13000 rpm for 15 min. The chloroform layer was separated and filtered into a GC-MS vial. The samples were analyzed through GC-MS to measure deuterium incorporation.

Chapter 7. Conclusions and future directions

My investigation of ether bridge formation in loline alkaloid biosynthesis started when Dr. Juan Pan isolated AcAP, a novel metabolite, from fungi that had a mutated *lolO* gene due to RNAi. I synthesized an authentic sample of (±)-AcAP, demonstrated its structure and stereochemistry, and showed its spectroscopic identity with AcAP isolated from a *lolO* mutant.

In order to determine whether AcAP was an intermediate or a shunt product, I synthesized 2′,2′,2′,3-[$^2H_4$]-AcAP. Through feeding of 2′,2′,2′,3-[$^2H_4$]-AcAP to fungal cultures, Dr. Juan Pan established that AcAP is an intermediate in the loline alkaloid biosynthesis, not a shunt product. This finding let us establish AcAP as the LolO substrate and NANL as the first loline produced in loline alkaloid biosynthesis.

However, this experiment did not explain what was the product of LolO-catalyzed oxidation of AcAP, and whether LolO alone, or in combination with other enzymes, installed the ether bridge in AcAP. Through the feeding of (±)-AcAP to yeast modified with the *lolO* gene, Dr. Juan Pan established that NANL is the product of LolO oxidation of AcAP. This result implied that LolO catalyzed *two* C–H activations of AcAP and *both* C–O bond-forming reactions during the formation of the ether bridge in NANL, a very unusual transformation. In addition, initial work by Dr. Wei-chen Chang further confirmed this finding through the feeding of AcAP to purified LolO enzyme. He also observed a hydroxylated product of AcAP, a previously unknown metabolite.

In order to resolve whether initial hydroxylation of AcAP catalyzed by LolO occurred at C(2) or C(7), I synthesized (±)-7,7-[$^2H_2$]- and (±)-2,2,8-[$^2H_3$]-AcAP. Dr. Juan Pan subjected (±)-AcAP, (±)-7,7-[$^2H_2$]-, and (±)-2,2,8-[$^2H_3$]-AcAP to the LolO oxidation

reaction under single-oxidation conditions. She observed a very large KIE in the case of (±)-2,2,8-[$^2H_3$]-AcAP only, demonstrating that LolO abstracted the C(2) H atom first to produce 2-hydroxy-AcAP. Further support for the structure of 2-hydroxy-AcAP was obtained upon its isolation by Dr. Juan Pan. I used the isolated material to establish the structure and stereochemistry of 2-*endo*-2-hydroxy-AcAP by NMR.

Next, I wanted to investigate the stereochemical course of C–H bond abstraction (exo or endo) by LolO from C(2) and C(7) of AcAP. In order to do this, I synthesized *trans*- and *cis*-3-[^2H]-Pro and (2*S*,3*R*)-3-[^2H]- and (2*S*,3*S*)-2,3-[$^2H_2$]-Asp. Feedings to loline-producing cultures conducted by both Dr. Juan Pan (Pro) and me (Asp) showed that the endo H atom was abstracted from both the C(2) and C(7) positions of AcAP en route to ether bridge formation in loline alkaloid biosynthesis (Scheme *1.4*).

In summary, I was able to investigate the ether bridge formation with the help of our collaborators. There are still many unanswered questions remaining regarding the biosynthesis of the loline alkaloids. Dr. Wei-chen Chang observed that LolO seems to be consuming its unnatural enantiomer (Figure *4.2*), so in a future study, one could study the ability of LolO to oxidize a range of substrates. To better understand the structure of LolO, X-ray crystallization of LolO with AcAP would be helpful.

To understand the kinetics and mechanism of the second C–H activation event catalyzed by LolO, one could isolate more 7,7-[$^2H_2$]-2-hydroxy-AcAP and subject it to LolO oxidation again. Alternatively, one could synthesize 7,7-[$^2H_2$]-2-*endo*-2-hydroxy-AcAP to accomplish the same goal. One could also study the crystal structure of (±)-AcAP and try to understand why the crystal I was able to grow had such an unusual structure (Figure *2.18*).

With all my heart, I wish very well for all future researchers and graduate students who would be working to answer all the above questions and any other questions which may arise.

Appendix

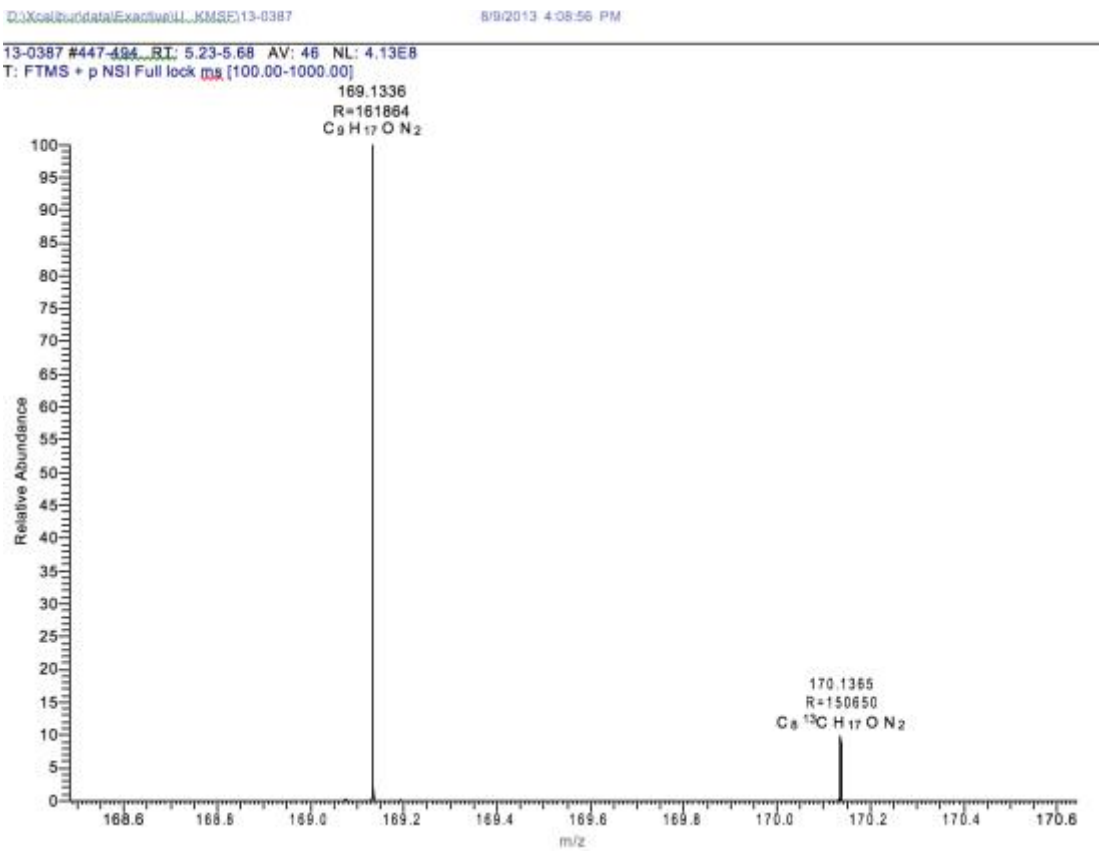

Figure A.1. HRMS of (±)-AcAP

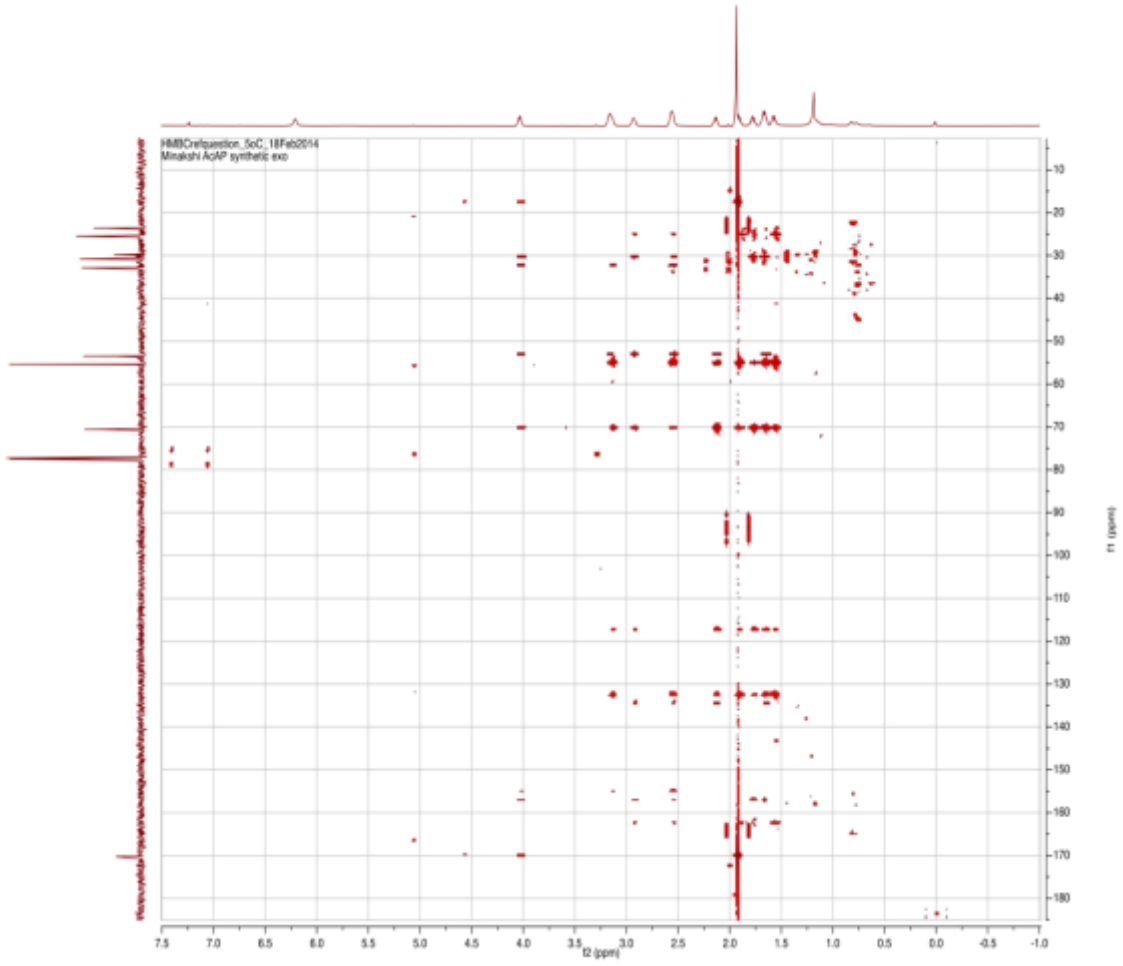

Figure A.2. $^{1}H–^{13}C$ HMBC of (±)-AcAP

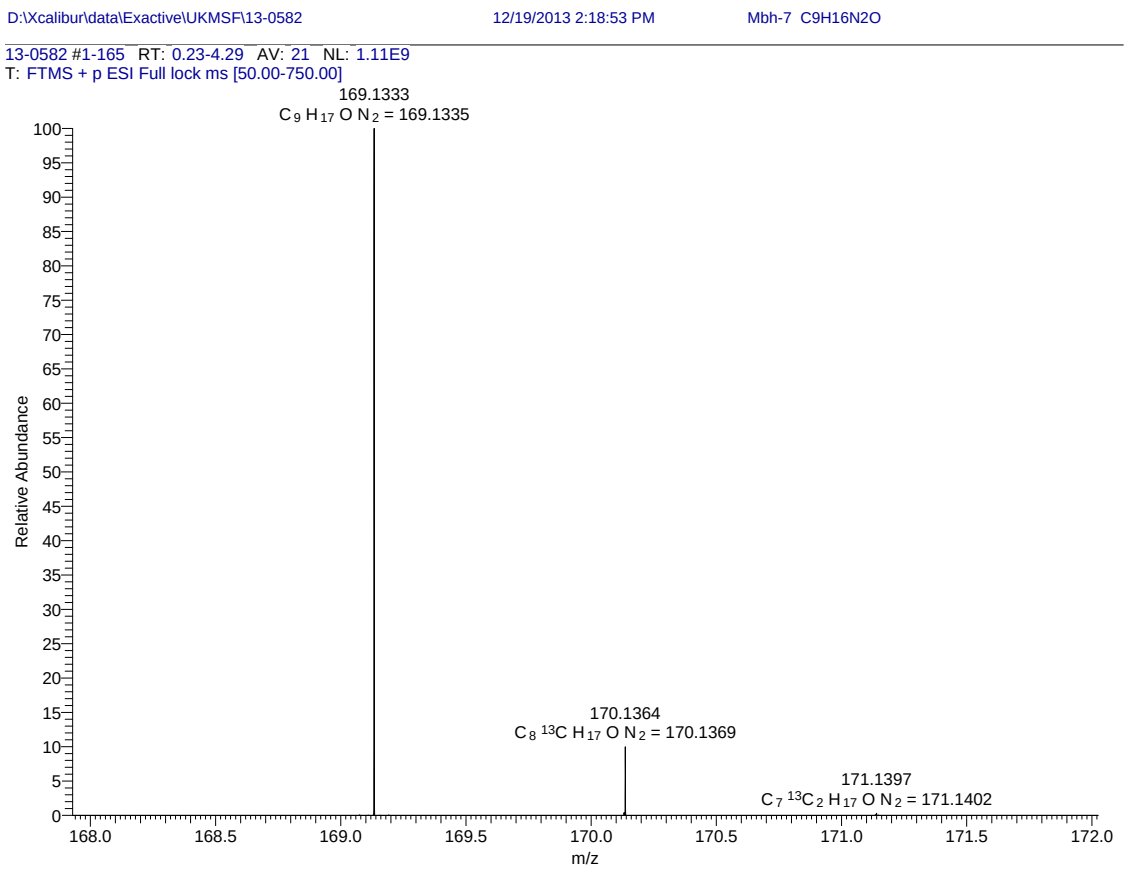

Figure A.3. HRMS of (±)1-*epi*-AcAP

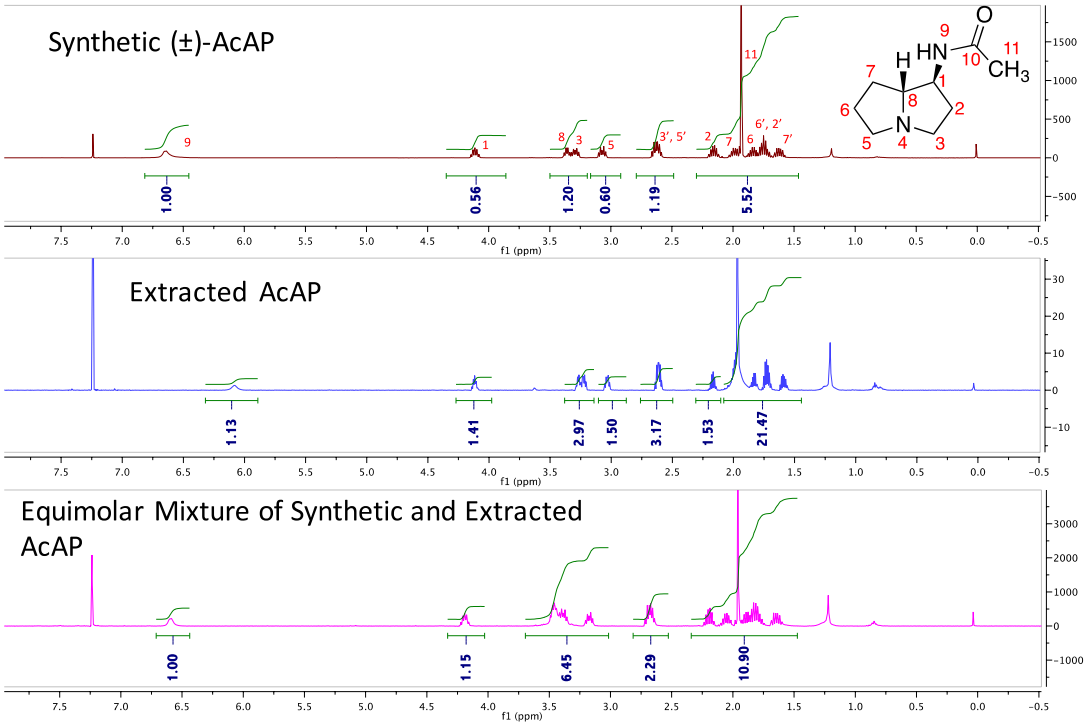

Figure A.4. ^{1}HNMR of equimolar mixture of synthetic and isolated AcAP.

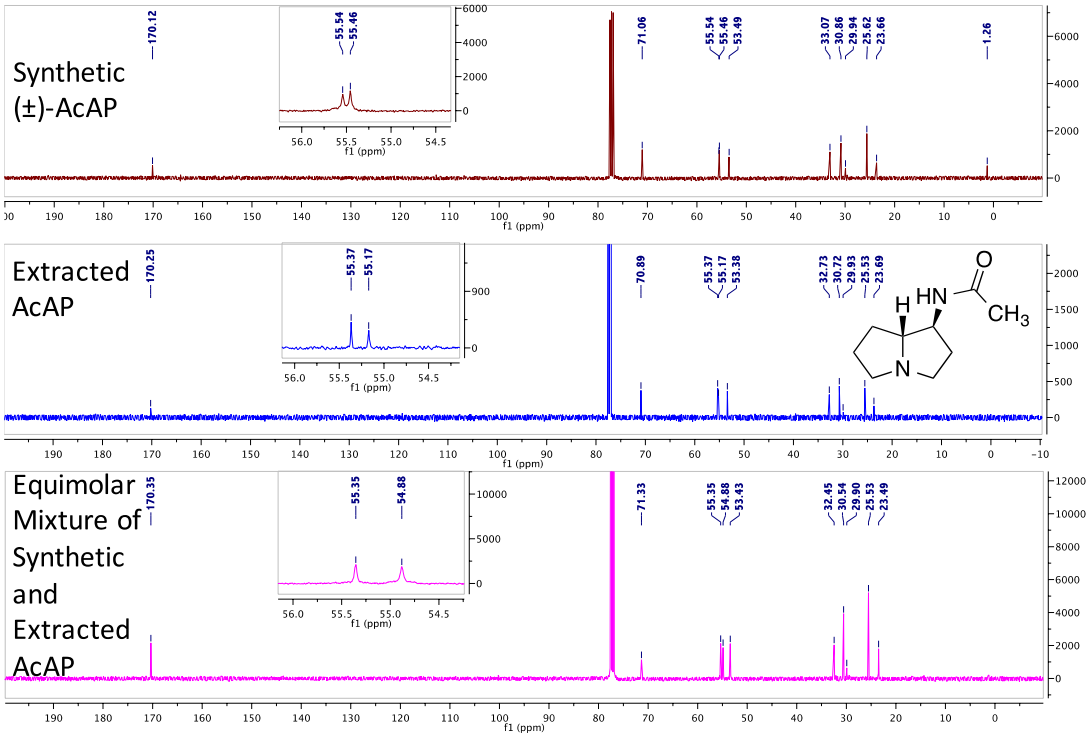

Figure A.5. ^{13}C NMR of equimolar mixture of synthetic and isolated AcAP.

Extracted AcAP

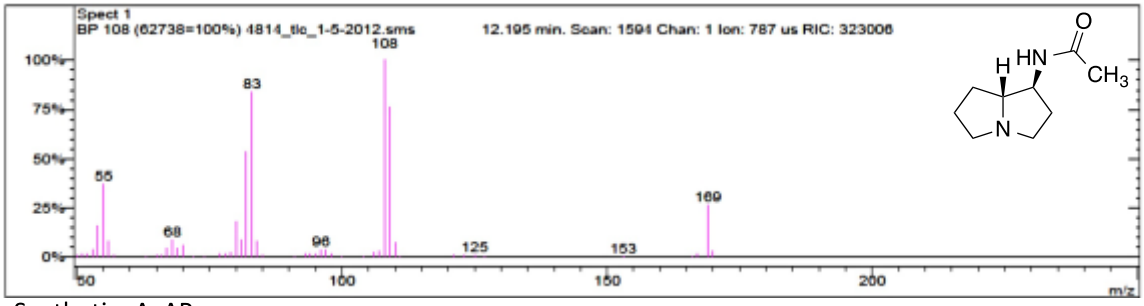

Synthetic AcAP

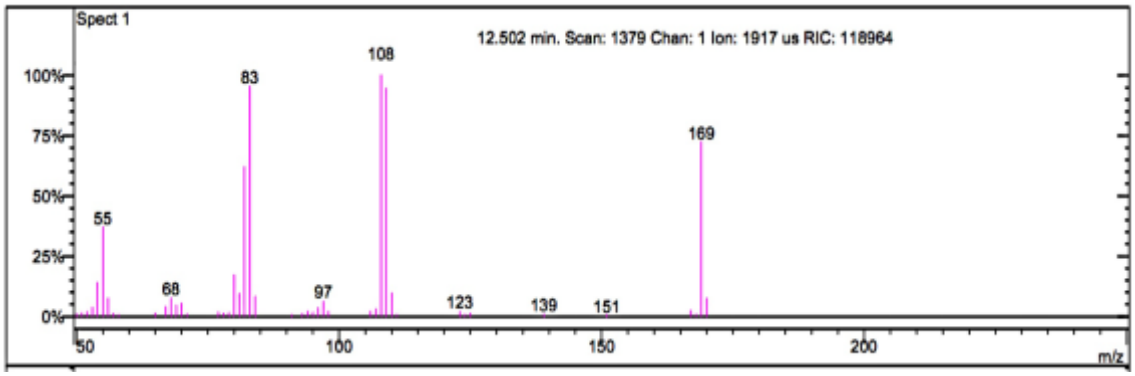

Figure A.6. GC-MS of equimolar mixture of synthetic and isolated AcAP.

Table A.1: Crystal data and structure refinement for (±)-AcAP

Empirical formula	$C_{18}\ H_{33}\ Cl\ N_4\ O_2$
Formula weight	372.93
Temperature	90.0(2) K
Wavelength (Å)	1.54178 A
Crystal system, space group	Monoclinic,
space group	C2/c
Unit cell dimensions	
A (Å)	20.2461(7)
α (°)	90
B (Å)	9.7027(4)
β (°)	100.562(2)
c (Å)	10.1617(4)
γ (°)	90
Volume ($Å^3$)	1962.36(13)
Z	4
Calculated density (Mg/m^3)	1.262
Absorption coefficient (mm^{-1})	1.871
F (000)	808
Crystal size (mm)	0.230 x 0.060 x 0.020
Θ range for data collection (°)	4.443 to 68.364
Limiting indices	-23<=h<=24,

	-11<=k<=11
	-12<=l<=5
Reflections collected / unique	12509 / 1788
	[R(int) = 0.0481]
Completeness to Θ = 67.679	99.4 %
Absorption correction	Semi-empirical from equivalents
Max. transmission	0.971
Min. transmission	0.754
Refinement method	Full-matrix least-squares on F^2
Data/restraints/parameters	1788 / 36 / 129
Goodness-of-fit on F^2	1.068
Final R indices [I>2sigma(I)]	R1 = 0.0486,
	ωR2 = 0.1416
R indices (all data)	R1 = 0.0500,
	ωR2 = 0.1429
Extinction coefficient	0.0010(3)
Largest diff. peak and hole $e.A^{-3}$	0.823 and -0.207

Table A.2: Atomic coordinates (x 10^4) and equivalent isotropic displacement parameters ($Å^2$ x 10^3) for (±)-AcAP. U(eq) is defined as one third of the trace of the orthogonalized U_{ij} tensor.

	x	y	z	U(eq)
N (1)	5656(1)	7822(2)	2630(2)	30 (1)
N (2)	6412(1)	4380(2)	2918(2)	29 (1)
O (1)	7544(1)	4168(2)	3213(2)	38 (1)
C (2)	6379(1)	5838(2)	2612(2)	29 (1)
C (3)	6025(1)	6176(2)	1188(2)	35 (1)
C (4)	5866(1)	7688(2)	1289(2)	35 (1)
C (5)	5893(1)	9118(2)	3362(2)	39 (1)
C (6)	6528(1)	8708(3)	4313(2)	35 (1)
C (7)	6349(2)	7273(3)	4772(3)	32 (1)
C (1)	5966(1)	6628(2)	3485(2)	29 (1)
C (5´)	5893(1)	9118(2)	3362(2)	39 (1)
C (6´)	6152(12)	8737(18)	4740(16)	35 (1)
C (7´)	6506(11)	7370(20)	4530(30)	32 (1)
C (1´)	5966(1)	6628(2)	3485(2)	29 (1)
C (8)	6984(1)	3651(2)	3160(2)	28 (1)
C (9)	6890(1)	2136(2)	3372(2)	34 (1)
C (1)	5000	2720(1)	2500	31 (1)

Table A.3: Bond lengths [Å] and angles [°] for (±)-AcAP.

N(1)-C(5')	1.494(3)
N(1)-C(5)	1.494(3)
N(1)-C(4)	1.505(3)
N(1)-C(1')	1.512(3)
N(1)-C(1)	1.512(3)
N(1)-H(1N)	1.3114(19)
N(2)-C(8)	1.341(3)
N(2)-C(2)	1.447(3)
N(2)-H(2N)	0.95(3)
O(1)-C(8)	1.233(3)
C(2)-C(3)	1.528(3)
C(2)-C(1')	1.532(3)
C(2)-C(1)	1.532(3)
C(2)-H(2)	1.0000
C(3)-C(4)	1.510(3)
C(3)-H(3A)	0.9900
C(3)-H(3B)	0.9900
C(4)-H(4A)	0.9900
C(4)-H(4B)	0.9900
C(5)-C(6)	1.513(3)
C(5)-H(5A)	0.9900

C(5)-H(5B)	0.9900
C(6)-C(7)	1.532(3)
C(6)-H(6A)	0.9900
C(6)-H(6B)	0.9900
C(7)-C(1)	1.528(3)
C(7)-H(7A)	0.9900
C(7)-H(7B)	0.9900
C(1)-H(1)	1.0000
C(5')-C(6')	1.450(15)
C(5')-H(5'1)	0.9900
C(5')-H(5'2)	0.9900
C(6')-C(7')	1.543(18)
C(6')-H(6'1)	0.9900
C(6')-H(6'2)	0.9900
C(7')-C(1')	1.554(17)
C(7')-H(7'1)	0.9900
C(7')-H(7'2)	0.9900
C(1')-H(1')	1.0000
C(8)-C(9)	1.503(3)
C(9)-H(9A)	0.9800
C(9)-H(9B)	0.9800
C(9)-H(9C)	0.9800

C(5')-N(1)-C(4)	113.95(18)
C(5)-N(1)-C(4)	113.95(18)
C(5')-N(1)-C(1')	107.33(16)
C(4)-N(1)-C(1')	107.33(16)
C(5)-N(1)-C(1)	107.33(16)
C(4)-N(1)-C(1)	107.33(16)
C(5')-N(1)-H(1N)	105.8(17)
C(5)-N(1)-H(1N)	105.8(17)
C(4)-N(1)-H(1N)	110.9(2)
C(1')-N(1)-H(1N)	111.5(16)
C(1)-N(1)-H(1N)	111.5(16)
C(8)-N(2)-C(2)	123.97(18)
C(8)-N(2)-H(2N)	117.8(18)
C(2)-N(2)-H(2N)	118.1(18)
N(2)-C(2)-C(3)	114.07(18)
N(2)-C(2)-C(1')	111.90(16)
C(3)-C(2)-C(1')	103.25(17)
N(2)-C(2)-C(1)	111.90(16)
C(3)-C(2)-C(1)	103.25(17)
N(2)-C(2)-H(2)	109.1
C(3)-C(2)-H(2)	109.1
C(1)-C(2)-H(2)	109.1
C(4)-C(3)-C(2)	102.31(17)

C(4)-C(3)-H(3A)	111.3
C(2)-C(3)-H(3A)	111.3
C(4)-C(3)-H(3B)	111.3
C(2)-C(3)-H(3B)	111.3
H(3A)-C(3)-H(3B)	109.2
N(1)-C(4)-C(3)	104.14(17)
N(1)-C(4)-H(4A)	110.9
C(3)-C(4)-H(4A)	110.9
N(1)-C(4)-H(4B)	110.9
C(3)-C(4)-H(4B)	110.9
H(4A)-C(4)-H(4B)	108.9
N(1)-C(5)-C(6)	104.66(18)
N(1)-C(5)-H(5A)	110.8
C(6)-C(5)-H(5A)	110.8
N(1)-C(5)-H(5B)	110.8
C(6)-C(5)-H(5B)	110.8
H(5A)-C(5)-H(5B)	108.9
C(5)-C(6)-C(7)	102.3(2)
C(5)-C(6)-H(6A)	111.3
C(7)-C(6)-H(6A)	111.3
C(5)-C(6)-H(6B)	111.3
C(7)-C(6)-H(6B)	111.3
H(6A)-C(6)-H(6B)	109.2

C(1)-C(7)-C(6)	102.86(19)
C(1)-C(7)-H(7A)	111.2
C(6)-C(7)-H(7A)	111.2
C(1)-C(7)-H(7B)	111.2
C(6)-C(7)-H(7B)	111.2
H(7A)-C(7)-H(7B)	109.1
N(1)-C(1)-C(7)	105.65(17)
N(1)-C(1)-C(2)	105.27(16)
C(7)-C(1)-C(2)	117.05(19)
N(1)-C(1)-H(1)	109.5
C(7)-C(1)-H(1)	109.5
C(2)-C(1)-H(1)	109.5
C(6')-C(5')-N(1)	107.0(7)
C(6')-C(5')-H(5'1)	110.3
N(1)-C(5')-H(5'1)	110.3
C(6')-C(5')-H(5'2)	110.3
N(1)-C(5')-H(5'2)	110.3
H(5'1)-C(5')-H(5'2)	108.6
C(5')-C(6')-C(7')	100.4(14)
C(5')-C(6')-H(6'1)	111.7
C(7')-C(6')-H(6'1)	111.7
C(5')-C(6')-H(6'2)	111.7
C(7')-C(6')-H(6'2)	111.7

H(6'1)-C(6')-H(6'2)	109.5
C(6')-C(7')-C(1')	101.8(13)
C(6')-C(7')-H(7'1)	111.4
C(1')-C(7')-H(7'1)	111.4
C(6')-C(7')-H(7'2)	111.4
C(1')-C(7')-H(7'2)	111.4
H(7'1)-C(7')-H(7'2)	109.3
N(1)-C(1')-C(2)	105.27(16)
N(1)-C(1')-C(7')	101.8(9)
C(2)-C(1')-C(7')	103.6(10)
N(1)-C(1')-H(1')	114.9
C(2)-C(1')-H(1')	114.9
C(7')-C(1')-H(1')	114.9
O(1)-C(8)-N(2)	123.4(2)
O(1)-C(8)-C(9)	122.1(2)
N(2)-C(8)-C(9)	114.51(19)
C(8)-C(9)-H(9A)	109.5
C(8)-C(9)-H(9B)	109.5
H(9A)-C(9)-H(9B)	109.5
C(8)-C(9)-H(9C)	109.5
H(9A)-C(9)-H(9C)	109.5
H(9B)-C(9)-H(9C)	109.5

Table A.4: Anisotropic displacement parameters ($Å^2$ x 10^3) for (±)-AcAP. The anisotropic displacement factor exponent takes the form: $-2\pi^2 [h^2 a^{*2} U11 + ... + 2 h k a^* b^* U12]$

	U11	U22	U33	U23	U13	U12
N (1)	34 (1)	25 (1)	30 (1)	1 (1)	2 (1)	–2 (1)
N (2)	29 (1)	27 (1)	32 (1)	0 (1)	7 (1)	–2 (1)
O (1)	31 (1)	38 (1)	44 (1)	5 (1)	4 (1)	–1 (1)
C (2)	30 (1)	28 (1)	30 (1)	2 (1)	6 (1)	–2 (1)
C (3)	40 (1)	38 (1)	27 (1)	2 (1)	9 (1)	–2 (1)
C (4)	38 (1)	37 (1)	30 (1)	6 (1)	5 (1)	–2 (1)
C (5)	43 (1)	27 (1)	42 (1)	–2 (1)	– 3 (1)	–4 (1)
C (6)	38 (2)	34 (1)	31 (1)	–3 (1)	0 (1)	–7 (1)
C (7)	35 (2)	34 (1)	26 (1)	–1 (1)	4 (1)	0 (1)
C (1)	30 (1)	29 (1)	26 (1)	1 (1)	2 (1)	0 (1)
C (5´)	43 (1)	27 (1)	42 (1)	– 2 (1)	–3 (1)	–4 (1)
C (6´)	38 (2)	34 (1)	31 (1)	–3 (1)	0 (1)	–7 (1)
C (7´)	35 (2)	34 (1)	26 (1)	–1 (1)	4 (1)	0 (1)
C (1´)	30 (1)	29 (1)	26 (1)	1 (1)	2 (1)	0 (1)
C (8)	31 (1)	32 (1)	21 (1)	–2 (1)	5 (1)	–1 (1)
C (9)	39 (1)	29 (1)	31 (1)	–1 (1)	3 (1)	1 (1)
C (1)	18 (1)	29 (1)	44 (1)	0	1 (1)	0

Table A.5: Hydrogen coordinates (x 10^4) and isotropic displacement parameters ($Å^2$ x 10^3) for (±)-AcAP.

	x	y	z	U (eq)
H (1N)	5000	7830(50)	2500	64(13)
H (2N)	6000 (15)	3900(30)	2880(30)	51(8)
H (2)	6845	6223	2759	35
H (3A)	6324	6015	534	42
H (3B)	5611	5623	929	42
H (4A)	6266	8262	1249	42
H (4B)	5497	7968	558	42
H (5A)	5551	9470	3861	47
H (5B)	5988	9839	2733	47
H (6A)	6629	9355	5077	42
H (6B)	6917	8669	3850	42
H (7A)	6758	6737	5133	38
H (7B)	6063	7336	5464	38
H (1)	5601	6019	3700	34
H (5´1)	6249	9558	2959	47
H (5´2)	5516	9777	3319	47
H (6´1)	5786	8600	5253	42
H (6´2)	6472	9431	5197	42

H (7´1)	6613	6834	5372	38
H (7´2)	6923	7528	4175	38
H (1´)	5639	6053	3874	34
H (9A)	7025	1617	2636	50
H (9B)	6417	1950	3396	50
H (9C)	7169	1853	4222	50

Table A 6: Torsion angles [°] for (±)-AcAP.

C(8)-N(2)-C(2)-C(3)	113.2(2)
C(8)-N(2)-C(2)-C(1')	-130.07(19)
C(8)-N(2)-C(2)-C(1)	-130.07(19)
N(2)-C(2)-C(3)-C(4)	162.39(18)
C(1')-C(2)-C(3)-C(4)	40.7(2)
C(1)-C(2)-C(3)-C(4)	40.7(2)
C(5')-N(1)-C(4)-C(3)	142.14(19)
C(5)-N(1)-C(4)-C(3)	142.14(19)
C(1')-N(1)-C(4)-C(3)	23.4(2)
C(1)-N(1)-C(4)-C(3)	23.4(2)
C(2)-C(3)-C(4)-N(1)	-39.6(2)
C(4)-N(1)-C(5)-C(6)	-96.9(2)
C(1)-N(1)-C(5)-C(6)	21.9(2)
N(1)-C(5)-C(6)-C(7)	-38.6(2)
C(5)-C(6)-C(7)-C(1)	40.4(3)
C(5)-N(1)-C(1)-C(7)	3.7(2)
C(4)-N(1)-C(1)-C(7)	126.6(2)
C(5)-N(1)-C(1)-C(2)	-120.81(19)
C(4)-N(1)-C(1)-C(2)	2.1(2)
C(6)-C(7)-C(1)-N(1)	-27.3(3)
C(6)-C(7)-C(1)-C(2)	89.5(2)
N(2)-C(2)-C(1)-N(1)	-149.51(17)

C(3)-C(2)-C(1)-N(1)	-26.4(2)
N(2)-C(2)-C(1)-C(7)	93.5(2)
C(3)-C(2)-C(1)-C(7)	-143.4(2)
C(4)-N(1)-C(5')-C(6')	-135.3(10)
C(1')-N(1)-C(5')-C(6')	-16.6(10)
N(1)-C(5')-C(6')-C(7')	38.9(17)
C(5')-C(6')-C(7')-C(1')	-46(2)
C(5')-N(1)-C(1')-C(2)	-120.81(19)
C(4)-N(1)-C(1')-C(2)	2.1(2)
C(5')-N(1)-C(1')-C(7')	-13.0(11)
C(4)-N(1)-C(1')-C(7')	109.9(11)
N(2)-C(2)-C(1')-N(1)	-149.51(17)
C(3)-C(2)-C(1')-N(1)	-26.4(2)
N(2)-C(2)-C(1')-C(7')	104.0(10)
C(3)-C(2)-C(1')-C(7')	-132.9(10)
C(6')-C(7')-C(1')-N(1)	35.9(18)
C(6')-C(7')-C(1')-C(2)	145.1(15)
C(2)-N(2)-C(8)-O(1)	3.9(3)
C(2)-N(2)-C(8)-C(9)	-176.46(18)

Symmetry transformations used to generate equivalent atoms:

Table A.7: Hydrogen bonds for (±)-AcAP [Å and °].

D-H...A	d(D-H)	d(H...A)	d(D...A)	<(DHA)

References

1. Clay, K., *Annu. Rev. Ecol. Syst.* **1990,** *21*, 275-297.
2. Strobel, G.; Daisy, B.; Castillo, U.; Harper, J., *J Nat Prod* **2004,** *67*, 257-268.
3. Kogel, K. H.; Franken, P.; Huckelhoven, R., *Curr Opin Plant Biol* **2006,** *9*, 358-363.
4. Schulz, B.; Boyle, C., *Mycol. Res.* **2005,** *109*, 661–686.
5. Cheplick, G. P.; Clay, K., *Oikos* **1988,** *52*, 309-318.
6. G. Kuldau, C. B., *Biological Control* **2008,** *46*, 57–71.
7. Wink, M.; Ashour, M. L.; El-Readi, M. Z., *Front Microbiol* **2012,** *3*, 130.
8. Hofmeister, F., *Arch. Exp. Pathol. Pharmakol.* **1892,** *30*, 203–230.
9. Schardl, C. L.; Grossman, R. B.; Nagabhyru, P.; Faulkner, J. R.; Mallik, U. P., *Phytochemistry* **2007,** *68*, 980-996.
10. Dannhardt, G.; Steindl, L., *Planta Med* **1985,** *51*, 212-214.
11. Blankenship, J. D.; Spiering, M. J.; Wilkinson, H. H.; Fannin, F. F.; Bush, L. P.; Schardl, C. L., *Phytochemistry* **2001,** *58*, 395-401.
12. Blankenship, J. D.; Houseknecht, J. B.; Pal, S.; Bush, L. P.; Grossman, R. B.; Schardl, C. L., *Chembiochem* **2005,** *6*, 1016-1022.
13. Faulkner, J. R.; Hussaini, S. R.; Blankenship, J. D.; Pal, S.; Branan, B. M.; Grossman, R. B.; Schardl, C. L., *Chembiochem* **2006,** *7*, 1078-1088.
14. Spiering, M. J.; Wilkinson, H. H.; Blankenship, J. D.; Schardl, C. L., *Fungal Genetics and Biology* **2002,** *36*, 242-254.
15. Spiering, M. J.; Moon, C. D.; Wilkinson, H. H.; Schardl, C. L., *Genetics* **2005,** *169*, 1403-1414.
16. Faulkner, J. R., *University of Kentucky Doctoral Dissertations. Paper 209.* **2011**.
17. Griffin, M.; Trudgill, P. W., *Biochemistry Journal* **1972,** *129*, 595-603.
18. Hamed, R. B.; Gomez-Castellanos, J. R.; Henry, L.; Ducho, C.; McDonough, M. A.; Schofield, C. J., *Nat Prod Rep* **2013,** *30*, 21-107.
19. Christine, C.; Ikhiri, K.; Ahond, A.; Al Mourabit, A.; Poupat, C.; Potier, P., *Tetrahedron* **2000,** *56*, 1837–1850.
20. Giri, N.; Petrini, M.; Profeta, R., *J Org Chem* **2004,** *69*, 7303-7308.
21. Tang, T.; Ruan, Y.-P.; Ye, J.-L.; Huang, P.-Q., *SYNLETT* **2005,** *2005*, 231–234.
22. Eklund, E. J.; Pike, R. D.; Scheerer, J. R., *Tetrahedron Lett* **2012,** *53*, 4644–4647.
23. Pan, J.; Bhardwaj, M.; Faulkner, J. R.; Nagabhyru, P.; Charlton, N. D.; Higashi, R. M.; Miller, A.-F.; Young, C. A.; Grossman, R. B.; Schardl, C. L., *Phytochemistry* **2014,** *98*, 60-68.
24. Steiner, T., *Angew Chem Int Ed* **2002,** *41*, 48-76.
25. Etter, M. C.; MacDonald, J. C., *Acta Crystallogr F Struct Biol Commun* **1990,** *B46*, 256-262.
26. Staab, H. A.; Saupe, T., *Angew Chem. Inr. Ed. Engl.* **1988,** *27*, 865-879.
27. Pan, J.; Bhardwaj, M.; Nagabhyru, P.; Grossman, R. B.; Schardl, C. L., *PLoS One* **2014,** *9*, e115590.
28. Schofield, C. J.; Zhang, Z., *Current Opinion in Structural Biology* **1999,** *9*, 722–731.
29. Koehntop, K. D.; Emerson, J. P.; Que, L., Jr., *J Biol Inorg Chem* **2005,** *10*, 87-93.

30. Krebs, C.; Dassama, L. M.; Matthews, M. L.; Jiang, W.; Price, J. C.; Korboukh, V.; Li, N.; Bollinger, J. M., Jr., *Coord Chem Rev* **2013,** *257*.
31. Borowski, T.; de Marothy, S.; Broclawik, E.; Schofield, C. J.; Siegbahn, P. E. M., *Biochemistry* **2007,** *46*, 3682-3691.
32. Martinez, S.; Hausinger, R. P., *J Biol Chem* **2015,** *290*, 20702-20711.
33. Wang, X.; Chen, M.; Yang, C.; Liu, X.; Zhang, L.; Lan, X.; Tang, K.; Liao, Z., *Physiol Plant* **2011,** *143*, 309-315.
34. Zocher, G.; Richter, M. E.; Mueller, U.; Hertweck, C., *J Am Chem Soc* **2011,** *133*, 2292-2302.
35. Muller, M.; He, J.; Hertweck, C., *Chembiochem* **2006,** *7*, 37-39.
36. Richter, M. E. A.; Traitcheva, N.; Knüpfer, U.; Hertweck, C., *Angew Chem Int Ed* **2008,** *47*, 8872-8875.
37. Pan, J., *Theses and Dissertations--Plant Pathology* **2014**.
38. Que, L., Jr., *nature structural biology* **2000,** *7*, 182-184.
39. Sinnecker, S.; Svensen, N.; Barr, E. W.; Ye, S.; Bollinger, J. M., Jr.; Neese, F.; Krebs, C., *J Am Chem Soc* **2007,** *129*, 6168-6179.
40. Gorres, K. L.; Pua, K. H.; Raines, R. T., *PLoS ONE* **2009,** *4*.
41. Costas, M.; Mehn, M. P.; Jensen, M. P.; Que, L., Jr., *Chem Rev* **2004,** *104*, 939-986.
42. Tamanaha, E.; Zhang, B.; Guo, Y.; Chang, W. C.; Barr, E. W.; Xing, G.; St Clair, J.; Ye, S.; Neese, F.; Bollinger, J. M., Jr.; Krebs, C., *J Am Chem Soc* **2016,** *138*, 8862-8874.
43. Grzyska, P. K.; Appelman, E. H.; Hausinger, R. P.; Proshlyakov, D. A., *J Am Chem Soc* **2010,** *107*, 3982-3987.
44. Harvey, D., *Modern Analytical Chemistry, 1st ed, McGraw-Hill: Boston* **2000**, 634-636.
45. Ooi, T.; Miki, T.; Maruoka, K., *Org Lett* **2005,** *7*, 191-183.
46. Back, T. G.; Birss, V. I.; Edwards, M.; Krishna, M. V., *The Journal of Organic Chemistry* **1988,** *53*, 3815-3822.
47. Weiner, B.; Poelarends, G. J.; Janssen, D. B.; Feringa, B. L., *Chemistry* **2008,** *14*, 10094-10100.
48. Barclay, F.; Chrystal, E.; Gani, D., *J. Chem. Soc., Perkin Trans. I* **1996**, 683-689
49. Steegborn, C.; Messerschmidt, A.; Laber, B.; Streber, W.; Huber, R.; Clausen, T., *J Mol Biol* **1999,** *290*, 983-996.

Vita

Minakshi Bhardwaj

Education

University of Kentucky, Lexington, KY — Expected May 2017
- Research focus on characterization of intermediates of Loline Biosynthesis
- Advisor: Prof. Robert B. Grossman

University of Delhi, New Delhi, India — July 2008- May 2010
- Master of Science, Organic Chemistry, St. Stephen's College

University of Delhi, New Delhi, India — June - August 2007
- Bachelor of Science, Chemistry (Honors), Gargi College

Awards

- ACS Division of Organic Chemistry Travel Award (August 2016)
- Research Challenge Trust Fund Assistantship (2016-2017)
- Max Steckler Fellowship (2015-2016)
- Research Challenge Trust Fund Assistantship (2014-2015)
- Shri Ravi Khullar Memorial Award (2008**)**

Research Experience

PhD candidate, University of Kentucky, Lexington, KY (August 2011 – present)
- Synthesized isotopically labeled proposed intermediates to elucidate natural product biosynthesis
- Purified organic compounds using recrystallization and column chromatography
- Feeding substrates to the fungus culture
- Protein purification
- Schleck and glovebox techniques
- Low temperature reaction handling
- Molecular characterization using NMR, GCMS, HRMS, FTIR, UV/Vis
- pH-metric Acid- Base Titration
- Detailed knowledge of Mnova NMR software, Chem Draw and MS office

Leadership Experience

University of Kentucky, Department of Chemistry

– Teaching Assistant, Organic Chemistry Laboratory	Fall, 2011 – Spring ,2013; Fall, 2014
– Teaching Assistant, General Chemistry Laboratory	Fall, 2013, Spring, 2014 –Fall, 2015

Research Mentor, University of Kentucky, Lexington, KY

– Trained undergraduate students in Organic synthesis laboratory techniques

Selected Presentations at Professional Meetings

– "Deuterium labeling and characterization of intermediates of loline biosynthesis. (Poster Presentation), **Minakshi Bhardwaj**, Juan Pan, Robert B. Grossman, Christopher L. Schardl, 252nd ACS National Meeting & Exposition, Philadelphia, PA, United States, August 21-25, 2016

– "Preparation and Deuterium Labeling of Intermediates of Loline Biosynthesis Route" (Poster Presentation), **Minakshi Bhardwaj**, Robert B. Grossman, Christopher L. Schardl, Juan Pan, 44th National Organic Chemistry Symposium, University of Maryland, The Clarice Smith Performing Arts Center, College Park, MD, United States, June 28 - July 2, 2015

– "Synthesis of Intermediates of Loline Biosynthesis Pathway" (**Oral Presentation**), **Minakshi Bhardwaj**, Robert B. Grossman, Christopher L. Schardl, Juan Pan, 249th ACS National Meeting & Exposition, Denver, CO, United States, March 22-26, 2015

– "Synthesis of Intermediates of Loline Biosynthesis Pathway" (Poster Presentation), **Minakshi Bhardwaj**, Robert B. Grossman, Christopher L. Schardl, Juan Pan, 25th Naff Symposium, Lexington, KY, United States, April 25, 2014

– "Synthesis of Intermediates of Loline Biosynthesis Pathway" (Poster Presentation), **Minakshi Bhardwaj**, Robert B. Grossman, Christopher L. Schardl, Juan Pan, 247th ACS National Meeting & Exposition, Dallas, TX, United States, March 16-20, 2014

Publications

- "Ether bridge formation in loline alkaloid biosynthesis" Juan Pan, **Minakshi Bhardwaj**, Jerome R. Faulkner, Padmaja Nagabhyru, Nikki D. Charlton, Richard M. Higashi, Anne-Francis Miller, Robert B. Grossman, Carolyn A. Young, and Christopher L. Schardl, Phytochemistry 2014, 98, 60-68.
- "Enzymes from fungal and plant origin required for chemical diversification of insecticidal loline alkaloids in grass-Epichloë symbiota" Juan Pan, **Minakshi Bhardwaj**, Padmaja Nagabhyru, Robert B. Grossman, Christopher L. Schardl, PLOS One 2014, 9(12), e115590, doi:10.1371/journal.pone.0115590.
- "Stereochemical course of the ether bridge formation in N-acetylnorloline catalyzed by LolO, an iron- and α-ketoglutarate-dependent oxygenase". Juan Pan, **Minakshi Bhardwaj**, Bo Zhang, Wei-chen Chang, Christopher L. Schardl, Carsten Krebs, Robert B. Grossman, J. Martin Bollinger Jr. (experiments complete, writing in progress)

Professional Memberships

- Member, American Chemical Society, 2013-present
- Member, Kentucky Academy of Science, 2013-present
- Member, ACS, Division of Organic Chenistry, 2014-present